1-1-2015

Innate Immune Cell Regulation of Metabolic Homeostasis

Jonathan Brestoff
University of Pennsylvania, brestoff@mail.med.upenn.edu

Innate Immune Cell Regulation of Metabolic Homeostasis

Abstract
Obesity is an increasingly prevalent disease regulated by genetic and environmental factors. Emerging studies indicate that immune cells, including monocytes, granulocytes and lymphocytes, regulate metabolic homeostasis and are dysregulated in obesity. Group 2 innate lymphoid cells (ILC2s) can regulate adaptive immunity and eosinophil and alternatively-activated macrophage responses, and were recently identified in murine white adipose tissue (WAT) where they may act to limit the development of obesity. However, ILC2s have not been identified in human adipose tissue, and the mechanisms by which ILC2s regulate metabolic homeostasis remain unknown. Here, we identify ILC2s in human WAT and demonstrate that decreased ILC2 responses in WAT are a conserved characteristic of obesity in humans and mice. Interleukin (IL)-33 was found to be critical for the maintenance of ILC2s in WAT and in limiting adiposity in mice by increasing caloric expenditure. This was associated with recruitment of uncoupling protein 1 (UCP1)+ beige adipocytes in WAT, a process known as beiging or browning that regulates caloric expenditure. IL-33-induced beiging was dependent on ILC2s, and IL-33 treatment or transfer of IL-33-elicited ILC2s was sufficient to drive beiging independently of the adaptive immune system, eosinophils or IL-4 receptor signaling. We found that ILC2s produce methionine-enkephalin peptides that can act directly on adipocytes to upregulate Ucp1 expression in vitro and that promote beiging in vivo. Collectively, these studies indicate that in addition to responding to infection or tissue damage, ILC2s can regulate adipose function and metabolic homeostasis in part via production of enkephalin peptides that elicit beiging.

Degree Type
Dissertation

Degree Name
Doctor of Philosophy (PhD)

Graduate Group
Cell & Molecular Biology

First Advisor
David Artis

Keywords
Adipose, Diabetes, IL-33, Immunometabolism, Metabolic rate, Obesity

Subject Categories
Allergy and Immunology | Endocrinology | Endocrinology, Diabetes, and Metabolism | Human and Clinical Nutrition | Immunology and Infectious Disease | Medical Immunology | Nutrition

INNATE IMMUNE CELL REGULATION OF METABOLIC HOMEOSTASIS

Jonathan R. Brestoff

A DISSERTATION

in

Cell & Molecular Biology

Presented to the Faculties of the University of Pennsylvania

in

Partial Fulfillment of the Requirements for the

Degree of Doctor of Philosophy

2015

Supervisor of Dissertation

_____

David Artis, Ph.D., Professor of Microbiology, Perelman School of Medicine, University of Pennsylvania and Michael Kors Professor of Immunology, Weill Cornell Medical College, Cornell University

Graduate Group Chairperson

_____

Daniel S. Kessler, Ph.D., Associate Professor of Cell and Developmental Biology
Cell and Molecular Biology Graduate Group Chairperson

Dissertation Committee:
Mitchell A. Lazar, M.D./Ph.D., Sylvan H. Eisman Professor of Medicine
Avinash Bhandoola, M.B.B.S., Ph.D., Professor of Pathology and Laboratory Medicine
Terri M. Laufer, M.D., Associate Professor of Medicine
Igor Brodsky, Ph.D., Assistant Professor of Microbiology
Patrick Seale, Ph.D., Assistant Professor of Cell and Developmental Biology
Christopher Hunter, Ph.D., Professor of Pathobiology

INNATE IMMUNE CELL REGULATION OF METABOLIC HOMEOSTASIS

Acknowledgements

I would first like to thank all of scientific collaborators that provided reagents, mice, expertise, advice and support throughout my thesis research. In particular I would like to thank Drs. Patrick Seale, Donna Farber and Kabir Lutfy.

I'd also like to acknowledge and thank my Thesis Committee for being thoughtful and supportive and for providing important scientific advice and mentorship: Drs. Mitch Lazar, Terri Laufer, Avinash Bhandoola, Igor Brodsky and Gary Koretzky. I'd also link to thank Drs. Patrick Seale and Chris Hunter for serving as Ad hoc members.

Thank you to my thesis advisor, Dr. Artis, for providing me the intellectual freedom and resources to pursue my research interests. Your guidance, support and teachings along the way have been more impactful than you probably know.

I would also like to acknowledge all the members of the Artis Lab who made work a fun, supportive environment: Theresa Alenghat, John Attanasio, Thomas Fung, Matthew Hepworth, Brian Kim, Tanel Mahlkoiv, Laurel Monticelli, Mario Noti, Lisa Osborne, Greg Rak, Steven Saenz, Mark Siracusa, Frederike Schmitz, Elia Tait Wojno, Sara Tran. I'd also like to thank Gregory Sonnenberg and members of his lab, as well as Rachel Stine from the Seale Lab.

Last but not least, I would like to thank all my friends and family for their love and support. I can't express in words how grateful and lucky I am to have such caring, supportive people in my life. Mom, Dad, Daniel, Rosa, Anthony. You are amazing – I love you. And most importantly, I'd like to thank my loving wife, Allison. You're the best!

Work in this dissertation is published in part or in whole in the following article:

Brestoff, J.R., Kim, B.S., Saenz, S.A., Stine, R.R., Monticelli, L.A., Sonnenberg, G.F., Thome, J.J., Farber, D.L., Lutfy, K., Seale, P., Artis, D. Group 2 innate lymphoid cells promote beiging of white adipose tissue and limit obesity. *Nature* 519: 242-246, 2015. Epub 22 Dec 2014. doi: 10.1038/nature14115

ABSTRACT

INNATE IMMUNE CELL REGULATION OF METABOLIC HOMEOSTASIS

Jonathan R. Brestoff

David Artis

Obesity is an increasingly prevalent disease regulated by genetic and environmental factors. Emerging studies indicate that immune cells, including monocytes, granulocytes and lymphocytes, regulate metabolic homeostasis and are dysregulated in obesity. Group 2 innate lymphoid cells (ILC2s) can regulate adaptive immunity and eosinophil and alternatively-activated macrophage responses, and were recently identified in murine white adipose tissue (WAT) where they may act to limit the development of obesity. However, ILC2s have not been identified in human adipose tissue, and the mechanisms by which ILC2s regulate metabolic homeostasis remain unknown. Here, we identify ILC2s in human WAT and demonstrate that decreased ILC2 responses in WAT are a conserved characteristic of obesity in humans and mice. Interleukin (IL)-33 was found to be critical for the maintenance of ILC2s in WAT and in limiting adiposity in mice by increasing caloric expenditure. This was associated with recruitment of uncoupling protein 1 $(UCP1)^{+}$ beige adipocytes in WAT, a process known as beiging or browning that regulates caloric expenditure. IL-33-induced beiging was dependent on ILC2s, and IL-33 treatment or transfer of IL-33-elicited ILC2s was sufficient to drive beiging independently of the adaptive immune system, eosinophils or IL-4 receptor signaling. We found that ILC2s produce methionine-enkephalin peptides that can act directly on adipocytes to upregulate *Ucp1*

expression *in vitro* and that promote beiging *in vivo*. Collectively, these studies indicate that in addition to responding to infection or tissue damage, ILC2s can regulate adipose function and metabolic homeostasis in part via production of enkephalin peptides that elicit beiging.

Table of Contents

List of Tables

List of Figures

Chapter 1: Immune cell regulation of metabolic homeostasis

1.1 Obesity is a global public health problem regulated by genetic and environmental factors

Obesity is in an increasingly prevalent metabolic disease characterized by excess accumulation of adipose tissue. Obesity increases the risk of developing a wide variety of diseases including type 2 diabetes, cardiovascular diseases and multiple forms of cancer, and has been strongly associated with increased mortality(Collaboration, 2009; Flegal et al., 2013; Oliveros and Villamor, 2008; Pi-Sunyer, 1999; Pontiroli and Morabito, 2011; Reilly and Kelly, 2011; Rodriguez et al., 2001). In the past few decades, the prevalence of obesity has risen dramatically in both developed and developing nations across all continents (Kelly et al., 2008; Ng et al., 2014), and this has been associated with high

healthcare expenditures (Withrow and Alter, 2011). For example, in the United States, where the prevalence of obesity among adults was 36% in 2010 (Flegal et al., 2012; Ogden et al., 2012, 2014), obesity accounts for approximately $190 billion annually or 20% of total national health care expenditures (Cawley and Meyerhoefer, 2012; Finkelstein et al., 2009). Therefore, obesity is a critical problem with major health and economic consequences. Increasing our understanding of the pathways involved in the development of obesity will be critical for the development of new intervention strategies to prevent or treat this disease and its associated comorbidities.

Genetic and environmental factors are important for the development of obesity and associated diseases (Bouchard, 2008; Brestoff and Artis, 2013; McCarthy, 2010; Walley et al., 2009). In addition, emerging studies have implicated various cell types in the immune system as critical regulators of metabolic homeostasis (Jin et al., 2013; Lumeng and Saltiel, 2011; Odegaard and Chawla, 2011, 2013b; Osborn and Olefsky, 2012). In white adipose tissue (WAT), which regulates metabolism at distant tissues such as the brain, liver and muscle, there is a diverse set of immune cells at steady state (Exley et al., 2014; Ibrahim, 2010; McNelis and Olefsky, 2014; Mraz and Haluzik, 2014). This network of immune cells appears to be poised to recognize, integrate and respond to environmental signals including bacterial products, endogenous lipid species and hormones in order to coordinate metabolism (Odegaard and Chawla, 2013a). Changes in

immune cell composition and function in WAT have been closely associated with obesity and the regulation of metabolic homeostasis, and disruption of this network of immune cells can have either detrimental or beneficial effects on mammalian health (Exley et al., 2014; Lumeng and Saltiel, 2011; Mraz and Haluzik, 2014; Odegaard and Chawla, 2013b; Osborn and Olefsky, 2012). This implies that dissecting the complex interactions between immune and metabolic systems will be important for understanding the biology underlying obesity and have implications for understanding how current and future therapeutics might influence metabolism.

The purpose of this Chapter is to describe our current understanding of how immune cells in white adipose tissue regulate metabolism. First, we will summarize recent advances in the roles of white, beige and brown adipose tissues in the regulation of weight gain. Second, we will describe the immune cell composition of adipose tissue at steady state and discuss how these immune cell pathways interact and contribute to the maintenance of metabolic homeostasis. Third, we will characterize immunologic changes that occur in adipose in the setting of obesity and discuss how these changes contribute to metabolic dysfunction. Finally, we will discuss potential therapeutic implications of targeting the immune system to treat obesity and its associated diseases.

1.2 Roles of adipose tissues in the regulation of obesity

Mammals possess multiple types of adipose tissues including white, brown and beige adipose. These tissues are found in distinct anatomic locations and are comprised of different adipocyte cell types – white, beige and/or brown – that have unique developmental and functional properties that are critical for host metabolism (Fig. 1) (Bartelt and Heeren, 2014; Cannon and Nedergaard, 2004; Harms and Seale, 2013; Ibrahim, 2010; Peirce et al., 2014; Pfeifer and Hoffmann, 2014; Wu et al., 2013). This section describes white, brown and beige adipocyte cell types and summarizes their roles in regulating weight gain.

1.2.1 White adipocytes

White adipose tissue (WAT) is distributed in subcutaneous depots and in association with organs, where it has important roles in insulation and physical protection of the viscera, and is comprised predominantly of white adipocytes (Peirce et al., 2014; Pfeifer and Hoffmann, 2014). These specialized cell types arise from a $Myf5^-$ pre-adipocyte lineage and store large amounts of triglycerides in a single large lipid droplet (Pfeifer and Hoffmann, 2014; Sanchez-Gurmaches and Guertin, 2014). In addition to their ability to store triglycerides, white adipocytes respond to hormonal signals to induce lipolysis and release free fatty acids (FFA) into the circulation for oxidation or storage by other cell types (Arner et al., 2011; Bartness et al., 2010). Therefore, white adipocytes are critical for regulating both fat storage and release. Beyond this function, white adipocytes

produce various adipocyte-specific hormones (also known as adipokines) such as leptin, resistin, retinol binding protein 4 (RBP4) and adiponectin among other adipokines that regulate metabolic homeostasis by acting on distant organs such as the brain, kidney, liver and skeletal muscle (Allison and Myers, 2014; Kadowaki et al., 2006; Kershaw and Flier, 2004; Kotnik et al., 2011; Lazar, 2007; Ouchi et al., 2011).

In the context of obesity, mature white adipocytes become hypertrophic through accumulation of triglycerides (Kubota et al., 1999), and adipocytes proliferate to increase adipocyte numbers in WAT (Foster and Bartness, 2006; Hausman et al., 2001; Spalding et al., 2008). As WAT expands, adipocytes increase production of leptin to suppress food intake and therefore limit the rate of triglyceride accumulation and adipocyte expansion (Allison and Myers, 2014). Leptin also has pro-inflammatory effects by eliciting type 1 effector cytokine production by immune cells (Attie and Scherer, 2009; Gregor and Hotamisligil, 2011; Mraz and Haluzik, 2014; Ouchi et al., 2011). In addition to leptin, RBP4 and resistin production by white adipocytes are increased in obesity, and both of these factors promote insulin resistance in mice (Kotnik et al., 2011; Lazar, 2007; Moraes-Vieira et al., 2014; Norseen et al., 2012; Steppan et al., 2001; Yang et al., 2005). Upregulation of RBP4 expression has been linked to inappropriate sensing of low glucose levels by adipocytes (Yang et al., 2005), whereas resistin levels are regulated by insulin and TNF-α among other factors (Lazar, 2007;

Song et al., 2002). Both of these factors appear to promote insulin resistance in mice, at least in part, through elicitation of a type 1 immune responses in WAT (Jung and Choi, 2014; Ouchi et al., 2011). In contrast to leptin, resistin and RBP4, adiponectin production by white adipocytes is decreased in the context of obesity (Ouchi et al., 2011). In addition, adiponectin has insulin-sensitizing and anti-inflammatory effects (Gregor and Hotamisligil, 2011; Kadowaki et al., 2006; Lumeng and Saltiel, 2011), and loss of this anti-inflammatory signal may be one factor that contributes to the development of inflammation in WAT in obesity. Therefore white adipocytes appear to link metabolic status of mammals to immune responses in WAT.

1.2.2 Brown adipocytes

Although brown adipocytes can also produce adipokines, these cells differ from white adipocytes developmentally, functionally and anatomically. In mice, brown adipocytes arise from a $Myf5^{+}$ lineage and are developmentally more closely related to skeletal muscle cells than to white adipocytes (Kajimura et al., 2009; Seale et al., 2008). The primary function of brown adipocytes in both mice and humans is to convert chemical energy into heat via Uncoupling protein 1 (UCP1) (Cannon and Nedergaard, 2004). UCP1 is a long chain fatty acid/proton symporter that dissipates the mitochondrial electrochemical gradient, thereby uncoupling energy substrate oxidation from ATP synthesis and resulting in the generation of heat (Fedorenko et al., 2012; Matthias et al., 2000). This process

is critical for maintaining core body and in the regulation of weight gain by regulating whole body energy expenditure. In the latter case, for example, mice that lack UCP1 develop obesity when housed at thermoneutrality (30°C) as compared to UCP1-sufficient controls (Feldmann et al., 2009). Although global deletion of UCP1 impairs thermogenesis in both brown and beige adipocytes, interscapular BAT is believed to be an important regulator of metabolic rate and obesity susceptibility in mice.

Brown adipocytes are found in discrete brown adipose tissue (BAT) depots. In mice, the largest BAT depot is present in the interscapular space and smaller depots are present in the axilla and along the cervical column (Bartelt and Heeren, 2014). In humans, brown adipocytes are abundant in newborns including the interscapular space (Hondares et al., 2014), whereas in lean adult humans brown adipocytes are reported to be present in the supraclavicular space of the neck and adjacent to the cervical column and heart (van Marken Lichtenbelt et al., 2009; Virtanen et al., 2009). Subsequent studies have determined that in healthy adults supraclavicular neck BAT exhibits a gene expression profile and has morphologic characteristics consistent with beige adipocytes (Lee et al., 2014; Sharp et al., 2012; Wu et al., 2012).

1.3.3 Beige adipocytes

Like brown adipocytes, beige adipocytes (also known as brown-like or brite adipocytes) express high levels of UCP1 and store triglyceride in one or more lipid droplets, giving rise to a paucilocular or multilocular cell morphology. However, beige and brown adipocytes differ from each other in their developmental and anatomic characteristics. Brown adipocytes arise from a $Myf5^{+}$ precursor and are developmentally related to skeletal muscle cells (Kajimura et al., 2009; Seale et al., 2008), whereas beige adipocytes arise from $Myf5^{-}$ precursors within WAT and are developmentally related to smooth muscle cells (Long et al., 2014) and/or white adipocytes (Sanchez-Gurmaches and Guertin, 2014). Beige adipocytes are believed to arise from multiple developmental pathways, including differentiation from committed beige pre-adipocytes as well as white-to-beige transdifferentiation in which mature white adipocytes are converted into a beige adipocyte (Fig. 1) (Barbatelli et al., 2010; Harms and Seale, 2013; Moisan et al., 2014; Sanchez-Gurmaches and Guertin, 2014; Wang et al., 2013b; Wu et al., 2012). This suggests that there is a close developmental relationship between white and beige adipocytes and that there may be distinct developmental pathways resulting in a heterogeneous population of beige adipocytes. In mice, beige adipocytes are enriched in subcutaneous WAT compared to visceral fat, however beige adipocytes are elicited in both subcutaneous and visceral WAT (Qiu et al., 2014). Whether beige adipocytes in

subcutaneous and visceral fat differ from each other developmentally or functionally remains unclear.

Beige adipocytes are elicited in response to environmental stimuli including exposure to cold environmental temperatures and are activated or induced to differentiate in response to a range of small molecules and hormones, including norepinephrine (Qiu et al., 2014; Rao et al., 2014), adenosine (Gnad et al., 2014), lactate (Carriere et al., 2014), β-aminoisobutyric acid (BAIBA) (Roberts et al., 2014), prostaglandin E_2 (PGE_2) (Madsen et al., 2010), parathyroid hormone-related protein (PTHrp) (Fisher et al., 2012), bone morphogenetic protein 4 (BMP4) (Qian et al., 2013), BMP7 (Schulz et al., 2011), fibroblast growth factor 21 (FGF21) (Fisher et al., 2012), irisin (Wu et al., 2012) and meteorin-like (Rao et al., 2014). Although many factors are known to promote beige adipocyte differentiation or function, it remains unknown whether these factors act on different subsets of beige adipocytes or whether they elicit developmentally or functionally distinct subsets of beige adipocytes. In addition, it is unclear whether these factors coordinately regulate beige adipocyte function.

Nonetheless, recent studies indicate that selective deletion of beige but not brown adipocytes results in impaired glucose homeostasis and increased susceptibility to weight gain in response to high fat diet feeding (Cohen et al.,

2014). Conversely, deletion of LGR4 results in enhanced beige adipocyte development and function and is associated with increased metabolic rate and decreased obesity (Wang et al., 2013a). Further, 129Sv mice that are resistant to diet-induced obesity exhibit increased beiging of WAT compared to C57BL/6 mice that are susceptible to diet-induced obesity (Shabalina et al., 2013). Feeding 129Sv mice a HFD supplemented with indomethacin blunted the PGE2/beige adipocyte pathway and resulted in increased accumulation of WAT compared to controls fed a HFD without indomethacin (Madsen et al., 2010). In the context of human obesity, the incidence of brown/beige adipose tissue (Sharp et al., 2012) is significantly decreased in obese patients compared to lean patients (Saito et al., 2009), and ephedrine-induced activation of this tissue is impaired in human obesity (Carey et al., 2013). In addition, UCP1 expression was found to be higher in cultured beige adipocytes from lean patients as compared to obese patients, suggesting that beige adipocyte differentiation or activation is impaired in human obesity (Carey et al., 2014). These studies indicate that beige adipocytes confer beneficial metabolic properties and that loss of beige fat function may have deleterious metabolic effects including increased susceptibility to weight gain.

1.3 Immune cell composition and function in lean white adipose tissue

White adipose is a heterogeneous tissue comprised of multiple cell types including a diverse array of immune cells. In the steady state, these immune cells tend to be associated with the type 2 immune axis and include alternatively activated macrophages (AAMacs), eosinophils, group 2 innate lymphoid cells (ILC2s), invariant natural killer T (iNKT) cells, T helper type 2 (Th2) cells, regulatory T (T_{reg}) cells and other immune cell populations that communicate with each other and participate in cross-talk with adipocytes. As discussed below, the interface between immune cells and adipocytes contributes to the regulation of lipid storage, glucose utilization, redox balance and energy expenditure (Fig. 2). However, in the context of obesity, type 2 immune cells in WAT become dysregulated and, in some cases, acquire a pro-inflammatory phenotype that exacerbates adipose tissue inflammation with deleterious effects on metabolism. In this section, we discuss emerging concepts in the composition of function of immune cells in WAT at steady state and how changes in these immune cells in obesity contribute to metabolic dysfunction.

1.3.1 The IL-4/Alternatively activated macrophage pathway

Alternatively activated macrophages (AAMac) are IL-4- and IL-13-dependent cells that require Signal transducer and activator of transcription 6 (STAT6) to maintain an alternative activation state that is distinct from the classical activation

state induced by interferon-γ (IFNγ) (Gordon and Martinez, 2010; Hill et al., 2014; Martinez et al., 2009; Odegaard and Chawla, 2011; Olefsky and Glass, 2010). AAMacs are critical for protective immunity against helminth pathogens and are associated with pathologic allergic inflammation in the lung (Gordon and Martinez, 2010; Martinez et al., 2009), and recent studies have implicated AAMacs in the regulation of metabolic homeostasis (Hill et al., 2014; Odegaard and Chawla, 2011; Olefsky and Glass, 2010). Early studies linking AAMacs to metabolism demonstrated that macrophage-specific deletion of Peroxisome proliferator-associated receptor (PPAR)-γ results in decreased AAMacs in WAT in association with increased weight gain, elevated fat accumulation, impaired glucose uptake and insulin resistance following HFD feeding (Odegaard et al., 2007). In addition, deletion of PPAR-δ in leukocytes also impaired AAMac responses and was associated with increased adiposity and insulin resistance (Odegaard et al., 2008). These loss of function studies are complemented by gain-of-function approaches indicating that administration of exogenous IL-4 to mice to boost AAMac responses protected mice from HFD-induced obesity and insulin resistance (Chang et al., 2012; Ricardo-Gonzalez et al., 2010). Together, these studies identified a critical role for the IL-4/AAMac axis in the regulation of metabolic homeostasis.

Emerging work has revealed that AAMacs employ a diverse functional repertoire to regulate metabolism. For example, a subset of AAMacs in WAT expresses

genes involved in iron handling and has the capacity to store large amounts of iron in lean mice (Orr et al., 2014). The capacity of these specialized AAMacs to store iron is diminished in the setting of obesity, leading to accumulation of iron in adipocytes (Orr et al., 2014) and iron-initiated production of highly toxic lipid aldehydes that damage cellular proteins, impair adipocyte insulin sensitivity and lead to mitochondrial dysfunction (Curtis et al., 2010; Curtis et al., 2012). Therefore it appears that specialized iron-storing AAMacs have an essential role in regulating iron homeostasis in WAT to maintain optimal glucose metabolism and mitochondrial function at steady state, and that dysregulation of these cells in obesity may have deleterious effects on glucose and energy homeostasis. Consistent with this, treatment of obese mice with the iron chelator deferoxamine is associated with improved glucose tolerance, decreased body weight and fat mass, and less inflammation in fat compared to obese controls that received vehicle (Tajima et al., 2012).

In addition, AAMacs from adipose are capable of producing catecholamines such as norepinephrine that act on adipocytes via adrenergic receptors to stimulate lipolysis, activate mitochondrial biogenesis and upregulate expression of Uncoupling protein 1 (UCP1) (Fig. 2 and Fig. 3) (Liu et al., 2014; Nguyen et al., 2011; Qiu et al., 2014; Rao et al., 2014). Recent studies suggest that AAMacs are critical for optimal brown and beige adipocyte responses (Nguyen et al., 2011; Qiu et al., 2014; Rao et al., 2014). Mice that lack IL-4 and IL-13 (*Il4/13*$^{-/-}$);

the shared receptor for these cytokines, IL-4Rα (*Il4ra*$^{-/-}$); or STAT6, a transcription downstream of IL-4Rα signaling (Stat6$^{-/-}$) have defective AAMac responses (Martinez et al., 2009) and exhibit decreased upregulation of UCP1 expression in BAT and impaired defense of core body temperature following acute exposure to cold environmental temperatures (Nguyen et al., 2011). IL-4 was shown to activate AAMacs to produce catecholamines such as norepinephrine (NE) that act on the β_3 adrenergic receptor (β_3AR) to stimulate lipolysis, elicit mitochondrial biogenesis and activate UCP1 in BAT (Nguyen et al., 2011).

However IL-4/IL-4Rα interactions do not appear to be required for BAT responses in the context of chronic exposure to severe cold environmental temperatures over a period of 3 days (Qui et al., 2014). In this context, AAMacs in WAT produce NE to promote beiging of WAT (Fig. 3) (Qiu et al., 2014; Rao et al., 2014). Mice lacking IL4/13, STAT6 or IL-4Rα failed to undergo optimal beiging of WAT and had decreased metabolic rate compared to wildtype controls in the setting of chronic cold exposure (Qiu et al., 2014; Rao et al., 2014). This phenotype appears to be mediated by macrophage-intrinsic production of norepinephrine, as mice that lack the rate-limiting step of catecholamine synthesis, tyrosine hydroxylase (Th), in LysM-Cre-expressing cells such as macrophages exhibit impaired beige fat development and exhibit a 10-15% decrease in whole body oxygen consumption in the setting of chronic exposure

to mild (room temperature) or severe (5°C) cold environmental temperatures (Qiu et al., 2014). This defect in metabolic rate suggests that AAMac-derived catecholamines might also be important for limiting weight gain. Consistent with this, mice that lack Receptor interacting protein 140 (RIP140) had increased AAMac responses in WAT and elicitation of beiging that was associated with protection from diet-induced obesity (Liu et al., 2014). In addition, treatment of mice with exogenous IL-4 elicits beiging and increases oxygen consumption levels in an UCP1-dependent manner, effects that are associated with protection from diet-induced obesity (Chang et al., 2012; Qiu et al., 2014; Ricardo-Gonzalez et al., 2010).

1.3.2 Sources of IL-4 in WAT: eosinophils and invariant natural killer T (iNKT) cells

The importance of AAMacs in regulation of metabolic homeostasis led to studies of the sources of IL-4 in WAT. Using the *4get* mouse, a reporter strain that identifies IL-4-competent cells, it was determined that eosinophils are an abundant immune cell population in WAT and are an important source IL-4 in this compartment at steady state (Wu et al., 2011). Eosinophils are recruited to WAT in the setting of chronic exposure to cold environmental temperatures, and *ΔDblGata1* mice that lack eosinophils exhibit defective beiging of WAT (Qiu et al., 2014; Rao et al., 2014). In addition, eosinophils are decreased in WAT of HFD-fed and genetically obese *ob/ob* mice (Wu et al., 2011). Mice lacking

eosinophils or IL-5, which is required for eosinophil homeostasis (Rosenberg et al., 2013; Rothenberg and Hogan, 2006), develop more severe obesity and insulin resistance than wildtype controls in association with dysregulated AAMac responses (Wu et al., 2011). Further, transgenic mice that constitutively overexpress IL-5 or that were infected with helminth pathogens had increased eosinophil accumulation in WAT and were protected from diet-induced obesity and insulin resistance (Wu et al., 2011; Yang et al., 2013b). This indicates that eosinophils are important regulators of metabolic homeostasis in WAT. Although eosinophils appear to promote AAMac responses in WAT through production of IL-4 (Wu et al., 2011; Qiu et al., 2014), whether eosinophils have other functions in WAT such as tissue remodeling remains unknown.

In addition to eosinophils, invariant natural killer T (iNKT) cells that express lipid antigen-specific T cell receptor variants appear to be an important source of IL-4 and IL-13 in WAT (Hams et al., 2013; Lynch et al., 2012). iNKT cells in WAT produce more IL-4 and IL-10 and less IFN-g than do iNKT cells in the liver and spleen (Lynch et al., 2012), suggesting that iNKT cells in WAT are in an “alternative activation” state. Consistent with this, recent work has shown that mammals produce endogenous αGalCer and that these endogenous lipid antigens promote production of type 2 cytokines by iNKT cells (Kain et al., 2014), and that adipocytes can present lipid antigen to iNKT cells (Huh et al., 2013). iNKT cells are decreased in murine and human obesity, and surgical or dietary

treatment of obesity restores iNKT cells in WAT (Lynch et al., 2012). Jα18-deficient mice that lack iNKT cells exhibit increased body weight and adiposity when fed a HFD compared to wildtype controls, and CD1d-deficient mice that cannot present lipid antigen to iNKT cells develop spontaneous obesity on a low fat diet (Lynch et al., 2012). In addition, mice lacking iNKT cells had more severe glucose intolerance and increased pro-inflammatory macrophages in WAT (Lynch et al., 2012), suggesting that iNKT cells are essential for limiting inflammatory responses in the setting of obesity. Adoptive transfer of iNKT cells induces weight loss and decreases adipocyte size while improving insulin resistance in HFD-fed mice (Hams et al., 2013; Lynch et al., 2012), and treatment of HFD mice with αGalCer recapitulates these effects in an iNKT-dependent manner by increasing IL-4 and IL-10 production by iNKT cells (Lynch et al., 2012). Therefore, eosinophils and iNKT cells may be important sources of IL-4 or other factors that support AAMac function or that directly regulate metabolic homeostasis to limit obesity and insulin resistance.

1.3.3 The IL-33/Group 2 innate lymphoid cell pathway

Group 2 innate lymphoid cells (ILC2s) are a recently described immune cell type (Moro et al., 2009; Price et al., 2010; Neill et al. 2010) that controls eosinophil and AAMac responses (Molofsky et al., 2013; Nussbaum et al., 2013). ILC2s are members of a broader family of ILCs that comprise T-bet-dependent Group 1 ILCs that produce IFN-γ; GATA-3-dependent ILC3s that produce IL-5, IL-13 and

amphiregulin; and RORγt-dependent ILC3s that produce IL-17A and IL-22 (Kim, 2014; Monticelli et al., 2012; Sonnenberg et al., 2013; Spits et al., 2013; Spits and Cupedo, 2012). In barrier surfaces such as the gut and lung, ILC2s respond to epithelial-derived cytokines IL-33, IL-25 and thymic stromal lymphopoietin (TSLP) to initiate type 2 immune responses that protect against helminth infection or that promote pathologic allergic inflammation (Kim, 2014; Monticelli et al., 2012; Sonnenberg et al., 2013; Spits et al., 2013; Spits and Cupedo, 2012). ILC2s were recently shown to be present in murine WAT, where these cells constitutively produce the effector cytokines IL-5 and IL-13 to maintain eosinophil and AAMac responses, respectively, in WAT (Molofsky et al., 2013). Strikingly, IL-5-deficient mice exhibit decreased energy expenditure and increased obesity compared to IL-5-sufficient controls (Molofksy et al., 2013; Wu et al., 2011). Recent studies showed that antibody-mediated depletion of ILC2s is associated with increased weight gain and more severe insulin resistance in mice fed a high fat diet (Hams et al., 2013), and transferring IL-25-elicted ILC2s is sufficient to promote weight loss in diet-induced obese mice (Hams et al., 2013). This suggests that ILC2s negatively regulate the development of obesity, although the mechanisms of this remain poorly understood. One possibility is that ILC2s limit adiposity via regulation of the eosinophil/IL-4/AAMac pathway to elicit beiging. Future studies will be required to investigate the mechanisms by which ILC2s regulate metabolic homeostasis.

The cytokine IL-33 is critical for stimulating proliferation and activation of ILC2s (Kim et al., 2014; Molofsky et al., 2013; Monticelli et al., 2011; Moro et al., 2010; Neill et al., 2010; Price et al., 2010) and is expressed at higher levels in WAT of obese mice and humans compared to non-obese controls (Zeyda et al., 2013). Given that ILC2s are decreased in murine obesity (Molofsky et al., 2013), this suggests that in the obese state ILC2s may be hypo-responsive to IL-33 or have altered cell death, proliferation or migration. IL-33 was recently shown to be critical for protecting mice from obesity (Miller et al., 2010). Mice lacking the IL-33R exhibit increased obesity and exacerbated impairments in glucose homeostasis following HFD feeding, and treatment of genetically obese *ob/ob* mice with recombinant IL-33 limits adiposity and improves glucose metabolism in association with enhanced AAMac responses in WAT (Miller et al., 2010).

1.3.4 $CD4^+$ T helper cells and regulatory T cells

In addition to regulating the ILC2/eosinophil/AAMac pathway, IL-33 also acts on adaptive immune cells such as Th2 cells (Molofsky et al., 2013) and regulatory T cells (Tregs) (Schiering et al., 2014). Although Th2 cells are relatively rare in WAT (Molofsky et al 2013) and remain poorly understood in the context of obesity, T_{regs} in WAT have been shown to be unique members of the T_{reg} pool exhibiting uniquely elevated expression of PPARγ, Foxp3 and IL-10 and are dysregulated in obese mice and humans (Cipolletta et al., 2012; Deiuliis et al., 2011; Feuerer et al., 2009). T_{regs} in WAT contribute to the maintenance of insulin

sensitivity in WAT by limiting inflammation and producing insulin-sensitizing factors such as IL-10 (Cipolletta et al., 2012; Feuerer et al., 2009; Ilan et al., 2010). In obesity, T_{regs} are decreased in both mice and humans (Cipolletta et al., 2012; Feuerer et al., 2009; Wagner et al., 2013), and this decrease in T_{regs} may be due to aberrant WAT iNKT cell responses in obese WAT (Lynch et al., 2014). iNKT cells in WAT produce IL-2 to sustain T_{regs} and are an additional source of IL-10 (Lynch et al., 2014; Lynch et al., 2012). IL-10 suppresses Monocyte chemotactic protein-1 (MCP-1) expression by adipocytes to limit inflammatory macrophage infiltration of WAT and inhibits the ability of tumor necrosis factor-α (TNF-α) to downregulate GLUT-4 expression and impair insulin action in adipocytes (Lumeng et al., 2007). Interestingly, recent studies indicate that the anti-diabetic class of drugs known as thiazoladinediones (TZD), which are PPAR-gamma agonists, ameliorate insulin resistance in obese mice via their effects on T_{regs} (Cipolletta et al., 2012). Therefore promoting T_{reg} responses may be a useful strategy to treat or prevent type 2 diabetes.

1.4 Immune cell responses in white adipose tissue in obesity

In obesity, white adipose tissue undergoes metabolic and inflammatory changes. As white adipocytes accumulate triglycerides and become hypertrophic, the vasculature in WAT becomes rarified leading to hypoxia and oxidative stress (Curtis et al., 2010; Pasarica et al., 2009). These changes are associated with increased adipocyte cell death and elevated production of adipocyte-derived

inflammatory mediators, including the adipokines leptin, resistin and RBP4 (Attie and Scherer, 2009; Greenberg and Obin, 2006; Lazar, 2007; McNelis and Olefsky, 2014; Osborn and Olefsky, 2012; Ouchi et al., 2011). As discussed below, these and other pro-inflammatory factors initiate a type 1 immune response in obese WAT that is characterized by increased accumulation of $CD4^+$ Th1 cells, $CD8^+$ cytotoxic T cells, pro-inflammatory classically activated macrophages (Fig. 4). These changes are discussed in this section.

1.4.1 Adipocytes, macrophages and type 1 cytokine-associated T cells participate in a proinflammatory positive-feedback loop in obesity

In obesity adipocyte-derived inflammatory mediators such as monocyte chemotactic protein (MCP-1), CXCL12, prostaglandins, leukotrienes and other factors are increased and promote classically activated monocyte/macrophage activation, proliferation and infiltration of white adipose tissue (Amano et al., 2014; Nomiyama et al., 2007; Oh et al., 2012; Weisberg et al., 2003). These cells engulf dying or dead adipocytes, forming crown-like structures (CLS) that are characterized morphologically as a ring of macrophages and other immune cells surrounding an adipocyte (Murano et al., 2008; Ouchi et al., 2011). The formation of CLS may be an adaptive mechanism to scavenge cellular debris or to limit the release of toxic lipid species when adipocytes undergo cell death, via phagocytosis. However, in addition to their phagocytic roles in CLS, classically activated macrophages in WAT of obese mice produce IL-1β, TNF-α, IFN-γ and

IL-6 among other factors that potentiate the type 1 inflammatory response (Lumeng et al., 2007; Nguyen et al., 2007; Zeyda et al., 2010). These cytokines act directly on adipocytes and other cell types in distant tissues such as skeletal muscle and liver to inhibit insulin-dependent glucose uptake (Exley et al., 2014; Gregor and Hotamisligil, 2011; Jin et al., 2013; Osborn and Olefsky, 2012). This pro-inflammatory process is therefore associated with the development of insulin resistance by promoting chronic low-grade type 1 inflammation.

The accumulation of macrophages in obese WAT also appears to be regulated by $CD8^+$ T cells (Rausch et al., 2008). These adaptive immune cells are recruited to WAT before infiltration by pro-inflammatory macrophages in the setting of high fat diet feeding (Nishimura et al., 2009). Deletion of $CD8^+$ T cells decreases macrophage accumulation in WAT of obese mice and ameliorates obesity-associated insulin resistance, and adoptive transfer of $CD8^+$ T cells to mice fed a HFD is sufficient to promote macrophage infiltration of WAT and exacerbate insulin resistance (Nishimura et al., 2009). In the setting of HFD feeding, $CD8^+$ T cells produce IFN-γ that has multiple effects on immune cells in WAT (Revelo et al., 2014). IFN-γ acts on macrophages to upregulate expression of pro-inflammatory effector cytokines and to increase expression of Major histocompatibility complex class II (MHC II) (Schroder et al., 2004). This promotes macrophage antigen presentation to $CD4^+$ T cells and incudes Th1 polarization and proliferation (Cho et al., 2014; Morris et al., 2013). T-bet-

dependent Th1 cells produce TNF-α and IFN-γ further potentiate insulin resistance in WAT (Cho et al., 2014; Morris et al., 2013; Stolarczyk et al., 2013). Thus, the $CD8^+$ T cell/classically activated macrophage pathway in WAT appears to be critical for downstream T helper type 1 (Th1) cell responses.

Adipocytes also appear to directly contribute to Th1 cell responses in obesity. With increased triglyceride deposition, adipocytes upregulate their expression of leptin, a hormone that limits food intake, as a compensatory mechanism to guard against overly rapid weight gain (Allison and Myers, 2014). While this is a beneficial response to maintain energy homeostasis, in WAT leptin acts on $CD4^+$ T cells to induce Th1 polarization and IFN-γ expression to drive a pro-inflammatory immune response that limits insulin sensitivity (Deng et al., 2013). In turn, IFN-γ upregulates CIITA and MHC-II expression in adipocytes (Deng et al., 2013) and macrophages (Cho et al., 2014; Morris et al., 2013) to adipocyte antigen presentation to Th1 cells. These MHC-II-mediated inflammatory changes in obesity are critical drivers of insulin resistance (Cho et al., 2014; Deng et al., 2013). Therefore it appears that adipocytes, macrophages, $CD8^+$ T cells and $CD4^+$ Th1 cells participate in a pro-inflammatory positive-feedback loop with deleterious consequences for WAT inflammation and glucose metabolism.

1.4.2 Alternatively activated macrophages acquire a classical activate state in obesity and potentiate type 1 inflammation in WAT

As discussed above, AAMacs have critical roles for regulating metabolic homeostasis in WAT at steady state. In obesity, however, AAMacs appear to acquire a pro-inflammatory M1-like phenotype that contributes to the development in type 1 inflammatory responses in WAT. For example, in obesity, AAMacs decrease their expression of IL-10 and upregulate expression of TNF-α, IFN-γ, IL-6 and IL-1β (Han et al., 2013; Lumeng et al., 2007; Moraes-Vieira et al., 2014). This phenotypic switch in AAMacs appears to be driven, at least in part, by retinol binding protein 4 (RBP4) that is upregulated in obesity and that impairs glucose homeostasis (Graham et al., 2006; Norseen et al., 2012). AAMacs from transgenic mice that overexpress RBP4 exhibit upregulated expression of antigen presentation machinery, TNF-α and IL-1β, and polarize $CD4^+$ T cells in WAT towards a Th1 phenotype characterized by increased expression of T-bet and IFN-γ (Moraes-Vieira et al., 2014). Interestingly, this effect was not observed in the liver, suggesting a tissue-specific effect of RBP4 on antigen presenting cells and T cell activation (Moraes-Vieira et al., 2014). In addition, transfer of RBP4-activated bone marrow-derived DCs (BMDCs) to lean recipient mice was sufficient to promote Th1 cell polarization in WAT and insulin resistance compared to unactivated BMDCs (Moraes-Vieira et al., 2014). This suggests that AAMacs in WAT become dysregulated in the setting of obesity and acquire a

pro-inflammatory classical activation state that supports Th1 cell polarization and the development of insulin resistance.

1.5 Perspectives and Conclusions

Adipose tissues are diverse in their structure and function and have multiple roles in the regulation of energy balance and weight gain (Fig. 1). WAT is essential for triglyceride storage and regulation of glucose homeostasis, and white adipocytes appear to link mammalian metabolic status to immune cell responses in WAT. In addition, WAT contains beige adipocytes that have been shown to be key regulators of energy expenditure and the development of obesity. In the lean state WAT is populated by type 2 cytokine-associated immune cells including AAMacs, eosinophils, ILC2s, Th2 and iNKT cells as well as anti-inflammatory cells such as T_{regs}. These immune cells participate in a complex dialog to maintain optimal immune and adipocyte function (Fig. 2). Although the precise mechanisms by which type 2 immune cells in WAT regulate each other, it appears that elicitation of these cell pathways is associated with increased insulin sensitivity, optimal adipocyte mitochondrial function and in some cases elicitation of beige adipocytes within WAT (Fig. 3). Conversely, disruption of these immunologic pathways results in impaired adipocyte function characterized by insulin resistance, oxidative stress, impaired respiratory capacity and triglyceride deposition resulting in adipocyte hypertrophy and weight gain. Therefore, type 2 immune pathways in white adipose tissue appear to have protective roles that

support maintenance of metabolic homeostasis and limit the development of obesity. This implies that eliciting type 2 immune cell pathways may be a useful strategy to treat or prevent obesity.

However in the context of obesity, the immunologic milieu of WAT undergoes a dramatic shift from a type 2 to type 1 cytokine-associated inflammatory environment (Fig. 4). Type 2 immune cells are decreased or dysregulated, and in some cases acquire a pro-inflammatory phenotype (e.g. iNKT cells and AAMacs). As type 2 immune cells tend to be associated with protection against obesity, these alterations in type 2 cytokine-associated immunologic pathways may contribute to the development of obesity and associated metabolic dysfunction, and therefore subsequent type 1 inflammatory responses. In addition, in obesity there is recruitment of various granulocytes, monocytes and lymphocytes to WAT. These cell types produce cytokines such as TNF-α, IFN-γ and IL-1β among others that potentiate type 1 immune responses and enhance antigen presentation to CD4+ T cells, polarizing these cells towards a Th1 cell phenotype. In turn, Th1 cells produce additional TNF-α and IFN-γ, establishing a positive-feedback loop resulting in chronic low-grade type 1 inflammation and dysregulated glucose homeostasis. The precipitating factors that initiate type 1 immune responses in WAT are not well understood but may be related to adipocyte cell death (Spalding et al., 2008), hypoxia (Sun et al., 2011), the generation of toxic lipid species (Muoio and Newgard, 2006), direct effects of

dietary lipids or carbohydrates (Calder, 2002), and translocation of commensal bacteria to WAT (Amar et al., 2011; Cani et al., 2007) among other factors. The apparent multifactorial nature of the type 1 immune response in WAT suggests that targeting downstream inflammatory mediators such as IFN-γ, TNF-α or IL-1β might have beneficial therapeutic effects in obesity-associated insulin resistance.

Finally, emerging studies have revealed complex immunomodulatory cross-talk between the type 1 and type 2 immune systems, where type 2 inflammation impairs type 1 responses and vice versa (Osborne et al., 2014; Reese et al., 2014). Given the dramatic shift in the immunologic landscape within obese WAT from a type 2 to type 1 cytokine-associated response, the effectiveness of "two-factor" immunomodulatory therapies (e.g., neutralizing TNF-α antibody plus recombinant IL-4) should be explored as potential anti-obesity regimens.

1.6 Figures

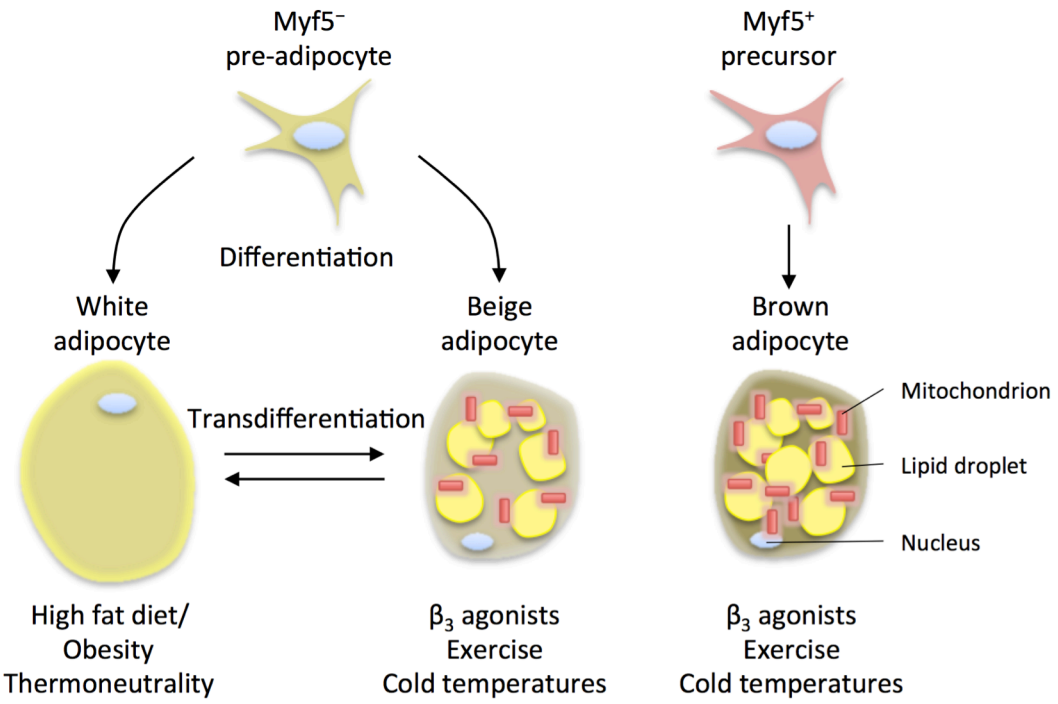

Figure 1. White, beige and brown adipocytes are developmentally and functionally distinct cell populations. White and beige adipocytes arise from a Myf5$^-$ precursor cell population that is bipotent. These pre-adipocytes give rise to white or beige adipocytes depending on the stimulus and physiologic setting. White adipocytes are promoted by high fat diet feeding or obesity and by thermoneutrality (30°C in mice). Beige adipocytes are elicited by β_3 adrenergic receptor agonists such as norepinephrine or epinephrine, and are recruited within WAT in the settings of chronic exercise or exposure to cold environmental temperatures. Although white and beige adipocytes emerge from pre-adipocytes via cell differentiation, mature white and beige adipocytes may undergo a process called transdifferentiation, in which one cell type acquires phenotypic characteristics of the other. In contrast, brown adipocytes arise from a Myf5$^+$ precursor cell population and are present in discrete brown adipose tissue (BAT) depots. Despite being developmentally distinct cell populations, beige and brown adipocytes are activated by similar physiologic stimuli, including exercise- and cold temperature-induced hormones and metabolites.

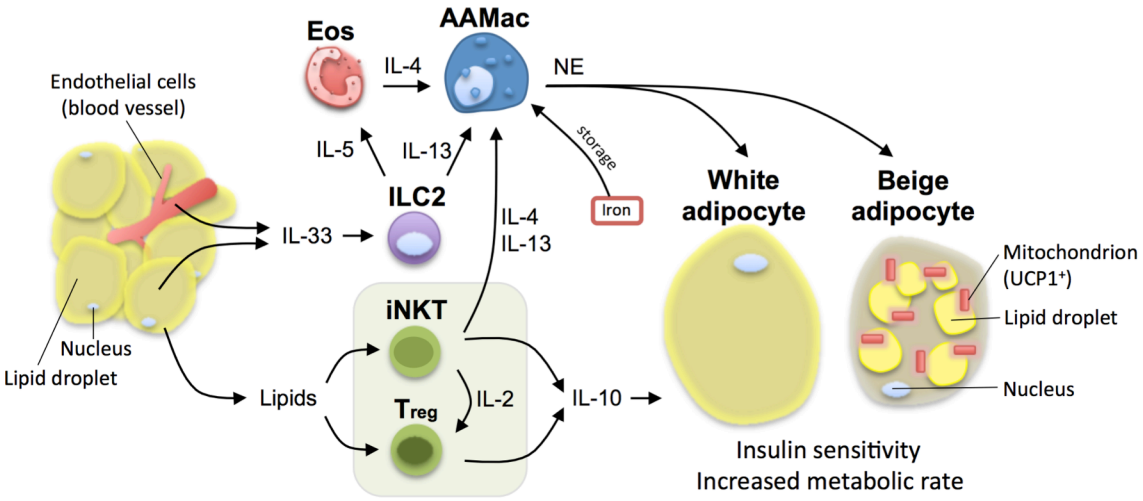

Figure 2. Healthy white adipose tissue (WAT) is enriched in type 2 cytokine-associated immune cells. In the lean state, adipocytes and endothelial cells in WAT constitutively produces interleukin (IL)-33 that can act on Group 2 innate lymphoid cells (ILC2s) to induce production of IL-5 and IL-13 that sustain eosinophil (Eos) and alternatively activated macrophage (AAMac) responses, respectively, in WAT. In addition, eosinophils produce IL-4 that is necessary to maintain AAMac responses in WAT. AAMacs have multiple functions to maintain metabolic homeostasis, including storing large amounts of iron, leading to sequestration of this pro-oxidative metal cation from adipocytes to prevent lipid peroxidation, oxidative damage to proteins and mitochondrial dysfunction. In addition, AAMacs produce norepinephrine (NE) that acts on both white and beige adipocytes via the β_3 adrenergic receptor to stimulate lipolysis and elicit beige adipocytes that increase metabolic rate. In addition, adipocytes present antigen to invariant natural killer T (iNKT) cells to elicit a unique tissue-specific anti-inflammatory phenotype characterized by increased production of IL-4 and IL-13, which may act on AAMacs, and IL-10. In addition, lipids from adipocytes are believed to promote regulatory T (T_{reg}) responses in WAT to induce production of IL-10. iNKT cells are critical sources of IL-2 and are necessary to sustain T_{regs} in WAT. IL-10 production by iNKT cells and T_{regs} promotes insulin action in white adipocytes to facilitate maintenance of an insulin-sensitive state. Together, these pathways contribute to metabolically healthy WAT.

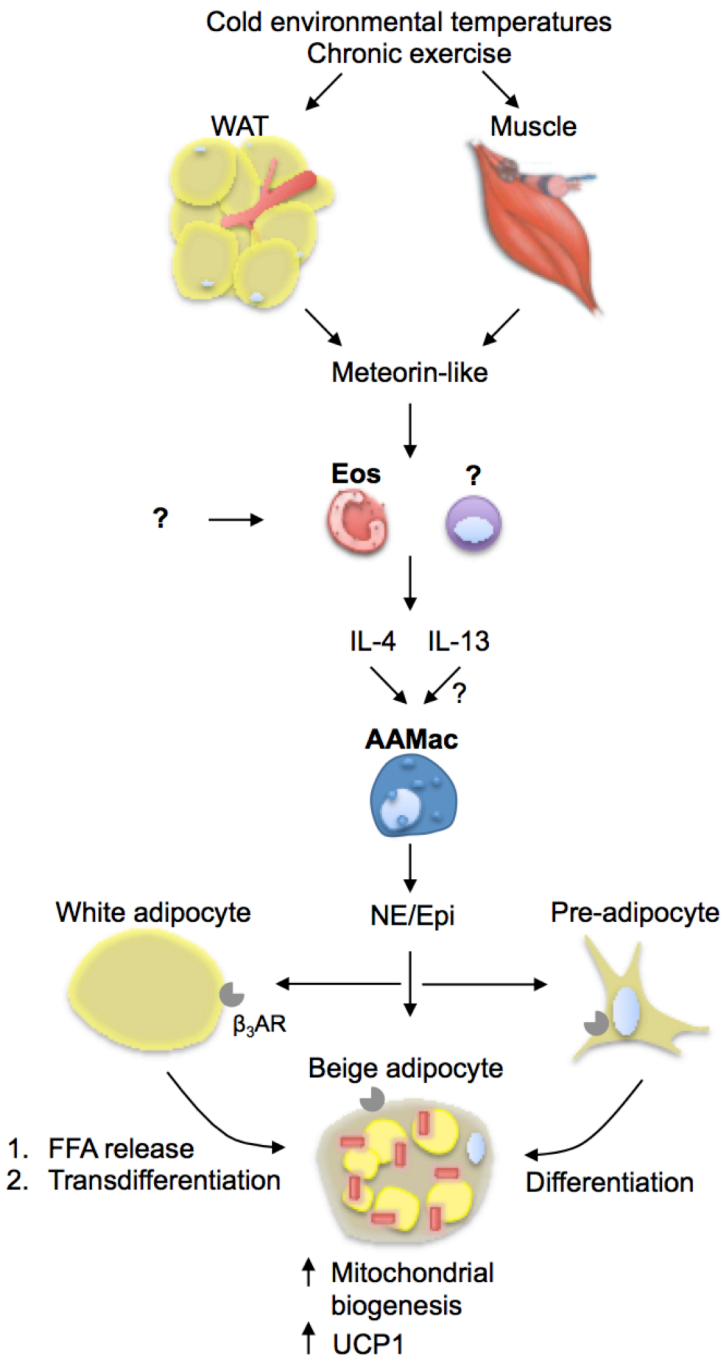

Figure 3. Immunologic mechanisms that regulate beiging. In the context of chronic exposure to cold environmental temperatures or chronic exercise, white adipose tissue (WAT) and muscle produce the adipokine/myokine meteorin-like. This hormone promotes eosinophil (Eos) accumulation in WAT. Whether other factors contribute to increased Eos in WAT to promote beiging remains unknown. Meteorin-like induces IL-4 and IL-13 production by Eos and possibly other cell types. IL-4 and perhaps IL-13 act on AAMacs to stimulate norepinephrine (NE)/ epinephrine (Epi) production. NE/Epi act on the β_3 adrenergic receptor (β_3AR) to stimulate beiging via differentiation and/or transdifferentiation pathways and to activate existing beige adipocytes, resulting in mitochondrial biogenesis, Uncoupling protein 1 (UCP1) upregulation and UCP1-dependent increases in energy expenditure.

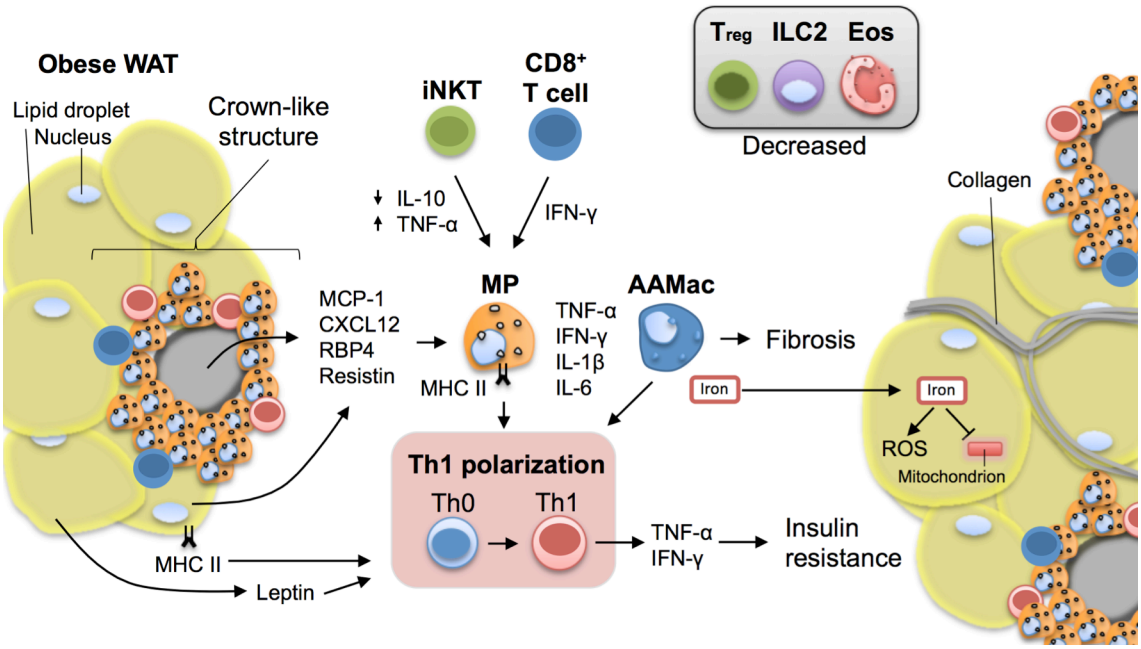

Figure 4. Obese white adipose tissue (WAT) is characterized by type 1 cytokine-associated immune responses. In obese WAT, adipocyte hypertrophy is associated with hypoxia and adipocyte cell death. Dead and neighboring adipocytes produce pro-inflammatory signals such as Monocyte chemotractant protein 1 (MCP1), C-X-C motif chemokine 12 (CXCL12), Retinol binding protein 4 (RBP4) and Resistin that are associated with the recruitment of classically activated macrophages (MP) into WAT and MP activation. MP accumulation in WAT is also mediated by pro-inflammatory invariant natural killer T (iNKT) cells that exhibit impaired production of interleukin (IL)-10 and upregulated production of Tumor necrosis factor-α (TNF-α), and by $CD8^+$ cytotoxic T cells that produce Interferon (IFN)-γ. These factors also promote MP activation and upregulate Major histocompatibility complex class II (MHC II) on MP and adipocytes. MHC II-mediated antigen presentation by MP and adipocytes stimulates polarization of $CD4^+$ T cells towards a T helper type 1 (Th1) phenotype. Supporting this process are TNF-α, IFN-γ, IL-1β and IL-6 produced by MP cells, dysregulated alternatively activated macrophages (AAMacs), iNKT cells and $CD8^+$ T cells. In addition, leptin is upregulated in obese WAT, and this factor also promotes Th1 cell polarization. MP cells, $CD8^+$ T cells and Th1 cells collectively interact to form crown-like structures (CLS) to facilitate phagocytosis of dead adipocytes. This process further promotes antigen presentation and type 1 immune responses, establishing a vicious cycle. Type 1 cytokines such as TNF-α and IFN-γ act directly on adipocytes to impair insulin action, leading to insulin resistance. Dysregulated AAMacs also produce type 1 cytokines in the setting of obesity to contribute to insulin resistance. AAMacs also lose their capacity to store iron, resulting in redistribution of iron to adipocytes. This results in iron-initiated lipid peroxidation that causes reactive oxygen species (ROS) production, insulin resistance and mitochondrial dysfunction. In addition, AAMacs in obese WAT promote collagen deposition in WAT and fibrosis, leading ultimately to exacerbated hypoxia and inflammation and potentiation of the type 1 immune response. These processes occur in the setting of decreased abundance of regulatory T cell (T_{reg}), Group 2 innate lymphoid cell (ILC2) and eosinophils (Eos) that promote insulin sensitivity and metabolic homeostasis in WAT in the steady state.

Chapter 2: Group 2 innate lymphoid cells are dysregulated in human and murine obesity and are regulated by IL-33

2.1 Abstract

In obesity there is a shift from type 2 to type 1 cytokine-associated immune responses in white adipose tissue (WAT) that promote insulin resistance. In addition, emerging studies indicate that type 2 immune cells such as eosinophils and alternatively activated macrophages that limit weight gain become dysregulated in obese WAT, suggesting that decreased type 2 immune responses in WAT may contribute to the development of obesity. Group 2 innate lymphoid cells (ILC2s) were recently identified in murine white adipose tissue (WAT), where they produce interleukin (IL)-5 and IL-13 to maintain eosinophil and AAMac responses in WAT and limit the development of obesity. However, ILC2s have not been identified in human adipose tissue, and the

factors that control ILC2 responses in WAT remain poorly characterized. Here, we identify IL-33 receptor^{+} ILC2s in human WAT and demonstrate that decreased ILC2 populations in WAT are a conserved characteristic of obesity in humans and mice. Employing loss-of-function studies in mice, we demonstrate that endogenous IL-33 is necessary to maintain normal ILC2 frequencies, numbers and effector cytokine production. IL-33-deficient mice exhibited increased adiposity and impaired glucose homeostasis compared to IL-33-sufficient controls. In gain-of-function studies, administering recombinant murine (rm)IL-33 to mice resulted in increased ILC2 accumulation in WAT and ameliorated obesity and glucose intolerance in mice fed a HFD. rmIL-33 treatment was associated with increased caloric expenditure without affecting food intake, suggesting that IL-33 treatment influences body weight by regulating metabolic rate. Collectively, these data indicate that IL-33 is critical for regulating ILC2 responses in WAT and for limiting adiposity, and suggest that the IL-33/ILC2 pathway may be dysregulated in the context of human and murine obesity.

2.2 Introduction

Obesity is an increasingly prevalent metabolic disease characterized by accumulation of excess adipose tissue and insulin resistance (Ogden et al., 2012; Pi-Sunyer, 1999). Genetic and environmental factors contribute to the development of obesity, and emerging studies indicate that the immune system

also regulates weight gain and insulin resistance (Bouchard, 2008; Gregor and Hotamisligil, 2011; Lumeng and Saltiel, 2011; Odegaard and Chawla, 2013b; Osborn and Olefsky, 2012). This implies that dissecting the complex interactions between immune and metabolic systems will be important for understanding the biology underlying obesity and how current and future therapeutics might influence metabolism.

Recent studies indicate that type 2 cytokine-associated immune cells such as alternatively activated macrophages (AAMacs) and eosinophils can regulate metabolic homeostasis. For example, mice with impaired AAMac responses are more susceptible to diet-induced obesity than mice with normal AAMac responses (Odegaard et al., 2007; Odegaard et al., 2008; Ricardo-Gonzalez et al., 2010). In addition, treatment of mice with recombinant IL-4, which induces and maintains AAMac polarization (Martinez et al., 2009), protects mice from the development of obesity (Chang et al., 2012; Ricardo-Gonzalez et al., 2010). Eosinophils are the dominant IL-4-producing cell type in white adipose issue (WAT) (Wu et al., 2011). These innate immune cells are dependent on IL-5 and are traditionally viewed as being end-stage effector cells with critical roles in protective immunity to parasitic helminth infection and pathologic roles in allergic lung inflammation (Rosenberg et al., 2013; Rothenberg and Hogan, 2006). However in WAT, eosinophils are abundant immune cells with homeostatic functions that control weight gain (Wu et al., 2011). For example, mice lacking

eosinophils or IL-5 develop more severe obesity than wildtype controls, and IL-5-transgenic hypereosinophilic mice are protected from diet-induced obesity (Molofsky et al., 2013; Wu et al., 2011). Further, parasitic helminth infection with the hookworm *Nippostrongylus brasiliensis* results in eosinophil accumulation in WAT and decreases obesity in mice fed a high fat diet (HFD) (Wu et al., 2011; Yang et al., 2013b). These studies indicate that eosinophils, a terminal type 2 effector cell population, are important for regulation of weight gain in mice.

Group 2 innate lymphoid cells (ILC2s) are recently described innate immune cells that initiate type 2 immune responses by producing large amounts of the type 2 cytokines IL-5 and IL-13 to control eosinophil and AAMac responses (Molofsky et al., 2013; Moro et al., 2010; Neill et al., 2010; Nussbaum et al., 2013; Price et al., 2010). ILC2s are dependent on the transcription factors Inhibitor of DNA binding 2 (Id2) and T cell factor 1 (TCF1, also known as TCF7) as well as the common gamma chain (γc, also known as IL-2Rγ) among other factors (Monticelli et al., 2011; Moro et al., 2010; Neill et al., 2010; Yang et al., 2013a). In addition, ILC2s are developmentally and functionally dependent on GATA binding protein 3 (GATA-3), which is essential for IL-5 and IL-13 production by ILC2s (Furusawa et al., 2013; Klein Wolterink et al., 2013; Mjosberg et al., 2012). ILC2s are activated by the epithelial cell-derived cytokines IL-33, IL-25 and thymic stromal lymphopoietin (TLSP) to elicit type 2 immune responses important for helminth parasite expulsion and allergic inflammation (Hong et al., 2014; Kim et al., 2013;

Kim et al., 2014; McSorley et al., 2014; Moro et al., 2010; Neill et al., 2010; Price et al., 2010; Roediger et al., 2013; Yang et al., 2013a).

Recent studies have also implicated ILC2s in the regulation of obesity (Hams et al., 2013; Molofsky et al., 2013). Mice fed a HFD for 12 weeks are reported to have decreased frequencies and numbers of ILC2s in association with impaired eosinophil and AAMac responses in WAT (Molofsky et al., 2013). In addition, treatment of HFD-fed lymphocyte-deficient mice with anti-CD90.2 monoclonal antibody was associated with decreased ILC2s in WAT as well as increased weight gain and worsened insulin resistance compared to mice receiving control immunoglobulin (Hams et al., 2013). Gain-of-function studies also indicate that adoptive transfer of IL-25-elicited ILC2s sort-purified from peritoneal exudate cells (PECs) is associated with weight loss in HFD-fed mice (Hams et al., 2013). Collectively, these studies indicate that ILC2s may be dysregulated in obese mice and that ILC2s may act to limit the development of obesity. However, ILC2s have not been identified in human WAT, and whether ILC2s are dysregulated in human obesity remains unknown. In addition, the upstream factors that regulate ILC2 responses in WAT remain poorly understood.

Data presented in this Chapter identify IL-33 receptor $(IL\text{-}33R)^{+}$ ILC2s in human and murine WAT and demonstrate that ILC2 populations are decreased in both human and murine obesity. It is also shown that IL-33 critically regulates ILC2

responses in WAT and the development of obesity in mice. IL-33-deficient mice had decreased frequencies and numbers of ILC2s in epididymal (E)-WAT and inguinal i(WAT) and exhibited impaired ILC2-derived IL-5 and IL-13 expression. When fed a normal low fat diet, IL-33-deficient mice developed spontaneous weight gain and accumulation of fat mass and were insulin resistant. Additionally, treatment of HFD-fed mice with recombinant IL-33 increased ILC2 accumulation in WAT and abrogated HFD-induced increases in fat mass and glucose intolerance. IL-33 treatment decreased whole body adiposity in lean mice, and this was associated with increased caloric expenditure. Collectively, results presented in this Chapter indicate that decreased ILC2 populations in WAT is a conserved characteristic of obesity in mice and humans and implicate the IL-33/ILC2 axis in the regulation of metabolic rate to limit the development of obesity in mice.

2.3 Methods

2.3.1 Mice

C57BL/6 and *Rag1*$^{-/-}$ mice were obtained from Jackson Labs. *Il33*$^{+/+}$ mice were obtained from Taconic, and *Il33*$^{-/-}$ mice were obtained from Amgen Inc via Taconic. *Id2*$^{-/-}$ bone marrow chimeras (Monticelli et al., 2011) and *Tcf7*$^{-/-}$ mice (Yang et al., 2013a) were generated as described previously. For Id2-deficient bone marrow chimeras, 10-20 x 10^6 bone marrow cells from congenically marked

Id2$^{+/+}$ (CD45.1^{+} CD45.2^{-}) or *Id2*$^{-/-}$ (CD45.1^{-} CD45.2^{+}) fetal liver chimeras were transferred by intravenous injection into lethally irradiated wildtype hosts (900 RAD) of a unique congenic marker combination (CD45.1^{+} CD45.2^{+}) (Monticelli et al., 2011). All mice were males and had *ad libitum* access to food and water and were maintained in a specific pathogen free facility with a 12h:12h light:dark cycle (lights on at 7:00 AM, lights off at 7:00 PM). Animals were randomly assigned to groups of n=3-5 mice per group per experiment, and at least two independent experiments were performed throughout. In all *in vivo* experiments, a single technical replicate per mouse was performed except in glucose homeostasis tests described below, in which 2-4 technical replicates were performed per mouse for each time point. For all *in vitro* experiments, 2-3 technical replicates were performed in each independent experiment. Sample sizes in each independent experiment were selected to have power of at least 90% using published sample size/power formulas (Brestoff and Van den Broeck, 2013). All experiments were carried out under the guidelines of the Institutional Animal Care and Use Committee at the University of Pennsylvania.

2.3.2 Human samples

Subcutaneous white adipose tissue (S-WAT) from the abdominal region was obtained from human donors via the New York Human Organ Donor Network (NYODN) and via the Cooperative Human Tissue Network (CHTN) Eastern Division, University of Pennsylvania. NOYDN samples were from recently

deceased organ donors at the time of organ acquisition for clinical transplantation through an approved research protocol and MTA with the NYODN. All NYODN donors were free of cancer and were Hepatitis B-, Hepatitis C-, and HIV-negative. Tissues were collected after the donor organs were flushed with cold preservation solution and clinical procurement process was completed. Samples from CHTN were collected from non-deceased adults undergoing surgery for other purposes (e.g. elective panniculectomies), and were harvested from discarded connective tissue by CHTN staff. All human samples from NYODN and CHTN were stored in DMEM on ice or at 4°C for 24-48 hours before processing.

Donors were defined as non-obese if their body mass index (BMI) was < 30.0 kg/m^2 (n=7) or obese if their BMI was ≥ 30.0 kg/m^2 (n=7). Sample sizes per group were selected to have power >95% using published sample size/power formulas (Brestoff and Van den Broeck, 2013). There were no differences in the proportion of donors from NYODN or CHTN between non-obese and obese groups (Table 1). ILC2 frequencies were also compared for all characteristics shown in Table 1, and those characteristics that had a P-value < 0.10 were interrogated to test whether they could explain the differences in ILC2 frequencies observed between non-obese *vs* obese donors. The human samples from NYODN do not qualify as “human subjects” research, as confirmed by the Columbia University IRB, and the human samples from CHTN were de-identified

and were not obtained for the specific purpose of these studies and therefore are not considered “human subjects” research.

2.3.3 Rodent chow and diet-induced obesity

In all experiments, mice had *ad libitum* access to food and water. Where indicated, mice were fed a control diet (CD, 10% kcal fat, Research Diets, New Brunswick, New Jersey) or high fat diet (HFD, 45% or 60% kcal fat as indicated, Research Diets) for the indicated period of time starting at 6-8 weeks of age. CD, 45% HFD and 60% HFD were gamma-irradiated (10-20 kGy) and stored at 4 °C under dry conditions until use, and rodents were provided fresh chow weekly. In all experiments that did not employ CD or HFD, mice were fed a standard autoclavable rodent chow (5% kcal fat, #5010, Lab Diets, St. Louis, Missouri) that had been autoclaved and allowed to cool overnight before use.

2.3.4 *In vivo* cytokine treatments

Mice were administered 12.5 μg/kg carrier-free recombinant murine IL-33 (rmIL-33, R&D Systems, Minneapolis, Minnesota) in sterile phosphate buffered saline (PBS) by intraperitoneal (i.p.) injection daily for the indicated number of days. In HFD studies, mice were treated with 12.5 μg/kg recombinant murine IL-33 or PBS once every 4 days by i.p. injection. All injections were performed between the hours of 4:00 PM and 7:00 PM.

2.3.5 *In vivo* metabolic phenotyping

Mice were single-housed in an OxyMax Comprehensive Laboratory Animal Monitoring System (CLAMS, Columbus Instruments, Columbus, Ohio) for 24 hours. Mice were acclimated to the CLAMS cages for 24 hours before measurements commenced. Caloric expenditure (kcal/hour) was measured by indirect calorimetry. Food intake was also measured throughout the 24 hour period. Fat mass and adiposity were measured by ^{1}H-nuclear magnetic resonance (NMR) spectroscopy.

For glucose tolerance tests, mice were fasted overnight for 14-16 hours (h) and injected with 2 g/kg D-glucose by i.p. injection. Blood glucose values were measured just prior to injection (time 0) and at 20, 40, 60, 90 and 120 minutes (min) post-injection. For insulin tolerance tests, mice were fasted for 4-6h and then injected with bovine insulin (0.5 U/kg). Blood glucose values were measured just prior to injection (time 0) and at 20, 40 and 60 min post-injection. To measure fasting blood glucose and insulin concentrations, mice were fasted overnight for 14-16 hours, and blood glucose values were measured followed by collection of approximately 20-30 μL blood for serum insulin concentration determination using the Ultra Sensitive Mouse Insulin ELISA Kit (Crystal Chem). Homeostatic model assessment of insulin resistance (HOMA-IR) index values were calculated as described previously (Matthews et al., 1985). All blood

glucose measurements were performed using FreeStyle Lite handheld glucometer (Abbott) in duplicate or triplicate.

2.3.6 Adipocyte area quantification.

Inguinal white adipose tissue (iWAT) sections were H&E stained and imaged at 40X magnification. White adipocyte area was calculated using ImageJ software by drawing ellipses circumscribing white adipocytes. The scale was set to 8 pixels per micron based on the pixel length of a 100 μm scale bar at 40X magnification. Two-to-three images, each from a different area of a given sample, were captured per animal. Adipocyte area was measured in 10-20 adipocytes per image (25-40 adipocytes per mouse) and averaged on a per mouse basis.

2.3.7 Isolation of immune cells from adipose

Murine epididymal white adipose tissue (E-WAT), inguinal WAT (iWAT) or brown adipose tissue (BAT) or human subcutaneous abdominal WAT were harvested and dissected so as to be free of reproductive tissues, lymph nodes and fibrous connective tissue. Tissues were finely minced using sterile scissors to form a slurry that was subsequently digested with 0.1% collagenase type II (Sigma-Aldrich, USA) in high glucose DMEM at 37°C with shaking at 200 rpm for 60-90 min at a 45° angle. Digested tissues were filtered through a 70 μm nylon mesh. The mesh was washed with approximately 20 mL Wash Media (high glucose

DMEM supplemented with 5% heat-inactivated fetal bovine serum [FBS], 100 units/mL penicillin, 100 µg/mL streptomycin and 2 mM L-glutamine). All Wash Media reagents were from Life Technologies (Grand Island, NY) except FBS, which was from Denville Scientific (South Plainfield, NJ). Washed cells were centrifuged at 500 x *g* for 5 min at 4°C, and then floating adipocytes were removed by aspiration and the stromal vascular fraction (SVF) pellet was resuspended in red blood cell lysis buffer (ACK RBC Lysis Buffer) and allowed to incubate at room temperature for 2 min. The RBC Lysis reaction was stopped by addition of 10 volumes Wash Media, and the SVF cells were recovered by centrifugation at 500 x *g* for 5 min at 4°C. Cells were resuspended in 200 µL Wash Media and aliquotted in equal parts for immediate flow cytometric analysis or for re-stimulation as described below for subsequent intracellular cytokine analysis by flow cytometry. In some experiments, all recovered SVF cells were used for immediate flow cytometric analyses.

2.3.8 Surface and nuclear staining of murine cells for flow cytometric analyses

Isolated SVF cells from mice were resuspended in 100 µL FACS PBS (sterile 1X phosphate buffered saline [Invitrogen] supplemented with 2% heat-inactivated FBS and 1 mM EDTA [Invitrogen]) containing LIVE/DEAD Fixable Aqua Dead Cell Stain (1:600) and anti-mouse IL-33R-biotin (T1/S2, clone DJ8) from MD Bioproducts (St. Paul, MN) (1:300). Cells were incubated on ice for 30 min in the

dark and were washed twice in 250 µL FACS PBS with centrifugation at 500 x *g* for 5 min at 4°C before each wash. Washed cells were stained with combinations of the following antibodies (all of which were used at 1:300 dilutions unless otherwise noted) in a volume of 90 µL staining buffer (FACS PBS supplemented with 20 µg/mL rat IgG): anti-mouse CD45-eFluor 605NC (clone 30-F11; 1:200), CD45.1-eFluor 450 (A20; 1:100), CD45.2-AlexaFluor 700 (104), F4/80-eFluor 450 (BM8), CD3e-PerCP-Cy5.5 (145-2C11), CD5-PerCP-Cy5.5 (53-7.3), CD19-PerCP-Cy5.5 (1D3), NK1.1-PerCP-Cy5.5 (PK136), CD11c-PerCP-Cy5.5 (N418), FcεRIα-FITC (MAR-1), Foxp3-FITC (FJK-16s; 1:100), GATA-3-PE (TWAJ; 1:100) and CD25-PE-Cy7 (clone PC61.5) from eBioscience (San Diego, CA); CD11b-PE-Texas Red (M1/70.15; 1:500) from Life Technologies (Grand Island, NY); CD90.2-Alexa Fluor 700 (30-H12; 1:400) and CD4-Brilliant Violet-650 (RM4-5) from BioLegend (San Diego, CA); SiglecF-PE (E50-2440) and CD3e-PE-CF594 (145-2C11) from BD Biosciences (San Jose, CA); CD206-Alexa Fluor 647 (MR5D3; 1:200) from AbD Serotec (Raleigh, NC); and Streptavidin-APC (1:300) from eBioscience. Foxp3, GATA-3 and CD206 staining was performed following fixation and permeabilization with the Foxp3 Staining Buffer Set (eBioscience) according to the manufacturer's protocol. All intracellular stains were performed in 1X Permeabilization Buffer (PB, eBioscience) for 45 min on ice. Cells were washed 3 times in 250 µL 1X PB with centrifugation at 500 *x* g for 5 minutes at 4 °C between washes, and recovered cells were resuspended in 200 µL FACS Buffer before flow cytometric analyses.

2.3.9 Surface and nuclear staining of human cells for flow cytometric analyses

Isolated SVF cells from human tissues were resuspended in 100 µL FACS PBS (sterile 1X phosphate buffered saline [Invitrogen] supplemented with 2% heat-inactivated FBS and 1 mM EDTA [Invitrogen]) containing LIVE/DEAD Fixable Aqua Dead Cell Stain (1:600) and anti-human FcεRIα-biotin (AER-37; eBioscience; 1:100). Cells were incubated on ice for 30 min in the dark and were washed twice in 250 µL FACS PBS with centrifugation at 500 x *g* for 5 min at 4°C before each wash. Washed cells were stained with combinations of the following antibodies in a volume of 90 µL FACS PBS (all of which were used at 1:100 dilutions unless otherwise noted): anti-human GATA-3-PE (TWAJ), TCRαβ-PerCP-Cy5.5 (IP26), CD5-PerCP-Cyanin5.5 (L17F12), CD19-Alexa Fluor 700 (HIB19), CD11c-Alexa Fluor 700 (3.9), CD127-eFluor 780 (eBioRDR5; 1:50), CD45-eFluor 605NC (HI30; 1:50), FcεRIα-biotin (AER-37) and Streptavidin-eFluor 650NC from eBioscience; CD56-Alexa Fluor 700 (B159), CD16-Alexa Fluor 700 (3G8), CD3 (SP34-2) and CD25-PE-Cy7 (M-A251; 1:50) from BD Pharmingen; CD11b-PE-Texas Red (M1/70.15; 1:300) from Life Technologies; and ST2L-FITC (B4E6; 1:50) from MD Bioproducts. GATA-3 and CD3 staining was performed following fixation and permeabilization with the Foxp3 Staining Buffer Set (eBioscience) according to the manufacturer's protocol. All intracellular stains were performed in 1X Permeabilization Buffer (PB,

eBioscience) for 45 min on ice. Cells were washed 3 times in 250 µL 1X PB with centrifugation at 500 *x* g for 5 minutes at 4 °C between washes, and recovered cells were resuspended in 200 µL FACS Buffer before flow cytometric analyses.

2.3.10 Intracellular cytokine analysis

To examine ILC2 effector cytokine production, single cell suspensions of E-WAT or iWAT SVF were stimulated for 4 hours *ex vivo* with Phorbol 12-myristate 13-acetate (PMA) (100 ng/mL) and ionomycin (1 ng/mL) in the presence of Brefeldin A (10 µg/mL) (all from Sigma-Aldrich) in a 37°C incubator (5% CO_2). Cells were then surface stained and fixed/permeabilized using Cyto Fix/Perm (BD Pharmingen) according to manufacturer's instructions before intracellular staining for IL-5 (APC-IL-5, clone TRFK5, 1:200, eBioscience) and IL-13 (PE-IL-13, eBio13A, 1:200, eBioscience). All intracellular stains were performed in 90 µL 1X Permeabilization Buffer (PB, eBioscience) for 45 min on ice. After each intracellular stain, cells were washed 3 times in 250 µL 1X PB with centrifugation at 500 *x* g for 5 minutes at 4°C between washes. Recovered cells after the final wash were resuspended in 200 µL FACS Buffer before flow cytometric analyses.

2.3.11 Flow cytometry

For all flow cytometry analyses, stained cells were acquired on a BD LSRII flow cytometer (BD Biosciences). The entirety of each sample was acquired to obtain total cell counts, which were subsequently normalized to tissue weight. Flow

cytometry data were analyzed using FlowJo software version 9.6.4 (Tree Star, Inc.).

2.3.12 Statistical analyses

Data are expressed as mean ± standard error of the mean (SEM). Statistical significance was determined for Normally-distributed data by using the two-tailed Student's *t* test or a one-way or two-way analysis of variance (ANOVA) followed by Sidak or Tukey post-hoc tests. If variance differed between groups, the appropriate statistical correction was applies (e.g. Welch's correction). Correlation analyses were conducted using Pearson linear regression. Proportions among human samples were compared by Chi-squared tests. Significance was set at $P<0.05$. Statistical analyses were performed with Prism 6 (GraphPad Software, Inc.) or SPSS Statistics version 22 (IBM).

2.4 Results

2.4.1 Identification of ILC2s in human and murine white adipose tissue

To address whether ILC2s are present in human and murine WAT, we first obtained abdominal subcutaneous white adipose tissues (WAT) from non-obese human donors and identified a lineage (Lin)-negative cell population that expresses CD25 (IL-2Rα) and CD127 (IL-7Rα) (Fig. 5a,b). This cell population was positive for GATA binding protein 3 (GATA-3) and the IL-33 receptor (IL-

33R) (Fig. 5c), a phenotype that is consistent with ILC2s identified in other human tissues (Kim et al., 2013; Mjosberg et al., 2012; Mjosberg et al., 2011; Monticelli et al., 2011). A Lin^- $CD25^+$ $CD127^+$ cell population (Fig. 6a) that expresses CD90, GATA-3 and IL-33R but not CCR6 (Fig. 6b) was also identified in epididymal WAT (E-WAT) of mice, similar to murine ILC2s described previously (Furusawa et al., 2013; Molofsky et al., 2013; Monticelli et al., 2011; Moro et al., 2010; Neill et al., 2010; Price et al., 2010; Saenz et al., 2013). In mice, Lin^- $CD25^+$ $CD127^+$ cells in E-WAT were developmentally dependent on Id2, TCF-7 and γ_c (Fig. 7a-c), indicating that these cells exhibit a developmental profile similar to ILC2s described in other murine tissues (Monticelli et al., 2011; Moro et al., 2010; Neill et al., 2010; Yang et al., 2013a). In addition, Lin^- $CD25^+$ $CD127^+$ cells from murine E-WAT produced the type 2 effector cytokines IL-5 and IL-13 (Fig. 7d). Collectively, these data identify ILC2s in human and murine WAT and indicate that murine E-WAT ILC2s exhibit phenotypic, developmental and functional similarities to ILC2s found in other mammalian tissues.

2.4.2 Obesity is associated with decreased ILC2 populations in white adipose tissue in both mice and humans

To examine whether human ILC2 responses are dysregulated in the setting of obesity, we compared ILC2 frequencies in abdominal subcutaneous WAT from non-obese versus obese donors (Table 1). Donors were categorized as non-obese (n=7) if their body mass index (BMI) was less than 30.0 kg/m^2 or as obese

if their BMI was greater than or equal to 30.0 kg/m^2 (n=7), a standardized threshold for defining an individual as clinically obese (Flegal et al., 2014). Strikingly, WAT from obese donors exhibited significantly decreased frequencies of ILC2s compared to non-obese controls (Fig. 8a,b). In linear regression analyses ILC2 frequencies in WAT were also inversely correlated with BMI (Fig. 8c). These findings suggest that ILC2s in WAT are decreased human obesity compared to the non-obese state.

To examine the association between human ILC2 frequencies in WAT and obesity, potential confounding variables including source of tissue, age, sex and some co-morbidities were analyzed to determine whether these factors might explain observed differences in ILC2 frequencies (Table 1). As tissues were obtained from the New York Organ Donor Network (NYODN) and the Cooperative Human Tissue Network-Eastern Division (CHTN), the source of tissue was assessed. The obese donors from each source tended to have lower WAT ILC2 frequencies compared to non-obese donors from the same source (Fig. 9a). Although WAT ILC2 frequencies in obese donors tended to be lower in obese donors from CHTN vs NYODN (Fig. 9a), this difference appeared to be explained by higher BMI values in the obese group from CHTN (Fig. 9b).

In addition, analyses showed that the obese donors were significantly older than the non-obese donors (Table 1, P=0.042). Therefore, we performed additional

analyses comparing WAT ILC2 frequencies between the younger 50%ile (n=7, 36.0 +/- 3.5 years) and the older 50%ile (n=7, 55.9 +/- 1.9 years). WAT ILC2 frequencies did not differ according to age groups (P=0.71, Fig. 10a), indicating that age does not explain differences observed in WAT ILC frequencies between non-obese and obese donors. In addition, the obese donors were predominantly females (6 of 7 donors) in contrast to the non-obese donors (3 of 7 donors) (Table 1, P=0.094). This distribution of biological sex precluded comparisons of ILC2 frequencies in males vs females, and analyzes comparing non-obese versus obese WAT ILC2 frequencies in only males were not possible due to small sample sizes in the obese group. However, when analyses were restricted to females only, WAT ILC2 frequencies remained significantly decreased in obese vs non-obese donors (Fig. 10b). These results suggest that biological sex also does not explain differences observed in WAT ILC frequencies between non-obese and obese donors. The non-obese and obese donors did not differ significantly for history of type 2 diabetes, liver disease or cardiovascular disease (Table 1), suggesting that these co-morbidities also do not explain differences observed in WAT ILC2 frequencies between non-obese and obese donors.

Next, to test whether ILC2s in WAT are also dysregulated in murine obesity, mice were fed a control diet (CD) or high fat diet (HFD). HFD feeding was associated decreased frequencies and numbers of ILC2s in E-WAT of HFD-fed mice compared to CD-fed controls (Fig. 11a,b). These data indicate that ILC2s are

also decreased in WAT of diet-induced obese mice and suggest that decreased ILC2 populations are a conserved characteristic of obesity in mice and humans.

2.4.3 Endogenous IL-33 sustains ILC2 responses in WAT and limits the development of spontaneous obesity

Previous studies demonstrated that IL-33 promotes ILC2 responses in WAT and other murine tissues in inflammatory settings (Furusawa et al., 2013; Imai et al., 2013; Molofsky et al., 2013; Monticelli et al., 2011; Moro et al., 2010; Neill et al., 2010; Saenz et al., 2013), however it is unclear whether IL-33 regulates basal ILC2 responses. We therefore employed IL-33-deficient mice to test whether endogenous IL-33 regulates ILC2 responses. Strikingly, *Il33*$^{-/-}$ mice exhibited decreased frequencies and numbers of ILC2s in E-WAT (Fig. 12a) and iWAT (Fig. 12b) compared to *Il33*$^{+/+}$ controls at steady state. Further, expression of IL-5 and IL-13 by ILC2s from E-WAT or iWAT was decreased in *Il33*$^{-/-}$ mice compared to controls (Fig. 13). These data indicate that endogenous IL-33 is required to maintain normal ILC2 frequencies and numbers and functional potential in WAT.

As ILC2s have previously been implicated in limiting weight gain in the context of HFD feeding and in enhancing glucose homeostasis (Hams et al, 2013), we next sought to test whether IL-33-deficient mice exhibited abnormal metabolic homeostasis under basal conditions. Male IL-33-deficient or -sufficient mice

were fed a CD (10% kcal fat) starting at 7 weeks of age for a period of 12 weeks. Strikingly, over the first 10 weeks of the feeding regimen, mice lacking IL-33 gained more weight than controls in terms of absolute and relative mass (Fig. 14a,b). This was associated with increased E-WAT and iWAT accumulation (Fig. 14c), increased white adipocyte size (Fig. 14d) and higher whole body adiposity (Fig. 14e) in IL-33-deficient mice compared controls. In addition, *Il33*$^{-/-}$ mice exhibited impaired glucose homeostasis as evidenced by fasting euglycemic hyperinsulinemia (Fig. 15a,b), increased homeostatic model assessment of insulin resistance (HOMA-IR) index values (Fig. 15c), impaired glucose tolerance (Fig. 15d) and impaired insulin tolerance (Fig. 15e). Together, these results indicate that endogenous IL-33 is required to maintain normal ILC2 responses in WAT and to limit the development of spontaneous obesity.

2.4.4 Recombinant IL-33 treatment elicits ILC2 responses in white adipose tissue and decreases adiposity

We next employed a complementary gain-of-function approach to examine whether IL-33 treatment could elicit ILC2 responses in WAT of HFD-fed mice and limit the development of obesity. Mice were fed a CD or HFD for 4 weeks, and HFD-fed mice were treated with PBS or rmIL-33 once every 4 days starting on the first day of the feeding regimen. At this early time point (4 weeks), HFD-fed mice treated with PBS exhibited decreased ILC2 numbers in E-WAT compared to controls (Fig. 16a), a result that is similar to longer HFD feeding regimens (Fig

11b). Further, rmIL-33 treatment was associated with markedly increased ILC2 numbers in E-WAT (Fig. 16a), indicating that rmIL-33 treatment produced a robust ILC2 response in the setting of HFD feeding. Strikingly, HFD mice treated with rmIL-33 exhibited decreased body weight (Fig. 16b) and lower accumulation of E-WAT and iWAT mass (Fig. 16c,d) compared to HFD mice treated with PBS. These changes were associated with improved fasting blood glucose levels (Fig. 16e) and enhanced glucose tolerance (Fig. 16f). Collectively, these data indicate that exogenous IL-33 can promote ILC2 responses and ameliorate HFD-induced obesity in association with improved glucose tolerance.

We next tested whether rmIL-33 treatment for 7 days could decrease adiposity in lean mice. As expected, rmIL-33 treatment resulted in increased frequencies and numbers of ILC2s in E-WAT (Fig. 17a) and iWAT (Fig. 17b). Although body weight did not differ between groups (Fig. 17c), mice treated with rmIL-33 had significantly decreased whole body adiposity compared to controls (Fig. 17d), indicating that exogenous rmIL-33 can decrease fat mass in lean mice.

2.4.5 Recombinant IL-33 treatment increases caloric expenditure of mice

To examine the mechanisms by which IL-33 regulates adiposity, we assessed energy homeostasis in lean mice treated with PBS or rmIL-33 daily for 7 day and employed Comprehensive Laboratory Animal Monitoring System (CLAMS) cages to simultaneously assess caloric expenditure and intake during days 6-to-7 over

a 24 hour period. rmIL-33 treatment resulted in a significantly increased caloric expenditure compared to controls (Fig. 17e). However, rmIL-33 treatment did not result in altered food intake (Fig. 18a). The absence of hyperphagia in the setting of increased caloric expenditure, as observed in this experimental system, appeared to be related to decreased ambulatory activity levels. Supporting this, mice treated with rmIL-33 exhibited decreased ambulatory activity compared to controls (Fig. 18b). In addition, decreases in ambulatory activity over 15 min intervals in rmIL-33- vs PBS-treated mice were significantly correlated with decreased food intake over the same time intervals in rmIL-33- vs PBS-treated mice (Fig. 18c). Taken together, these data suggest that increased caloric expenditure in rmIL-33-treated mice could not be explained by the thermic effect of food or physical activity levels but was regulated by other physiologic processes.

2.5 Discussion

Data presented in this Chapter identify IL-33R$^+$ ILC2s in human and murine WAT and demonstrate that decreased ILC2 populations in WAT is a conserved characteristic of obesity in both humans and mice. Furthermore, this Chapter demonstrates that IL-33 is critical for regulating ILC2 responses in WAT and for limiting obesity in mice. Mice lacking IL-33 had impaired ILC2 responses and developed spontaneous obesity on a low fat diet. Further, treatment of HFD-fed wildtype mice with recombinant murine IL-33 increased ILC2 accumulation in

WAT and ameliorated the development of obesity. IL-33-mediated decreases in adiposity were associated with increased caloric expenditure.

Previous studies demonstrated that ILC2s in WAT are decreased in mice fed a HFD compared to lean controls (Molofsky et al., 2013) and that transfer of IL-25-elicited ILC2s could decrease body weight and improve insulin sensitivity in HFD-fed mice (Hams et al., 2013). ILC2s are known to produce the effector cytokines IL-5 and IL-13 to promote eosinophil and AAMac responses, respectively, in WAT (Molofsky et al., 2013), and both eosinophils and AAMacs are reported to limit obesity (Chang et al., 2012; Odegaard et al., 2007; Odegaard et al., 2008; Ricardo-Gonzalez et al., 2010; Wu et al., 2011). These studies provoke the hypothesis that the function of ILC2s in WAT is to sustain eosinophils and AAMacs to maintain optimal metabolic homeostasis. Consistent with this, treatment of mice with exogenous IL-33 is associated with increased ILC2, eosinophil and AAMac frequencies and numbers in WAT and attenuated weight gain in genetically obese *ob/ob* mice (Miller et al., 2010; Molofsky et al., 2013). Further, IL-33R-deficient mice are reported to be more susceptible to diet-induced obesity compared to IL-33R-sufficient controls (Miller et al., 2010). However, ILC2s have not been previously identified in human WAT, and the endogenous factors that regulate ILC2s in WAT remain poorly characterized. In this Chapter, we identify a lineage-negative $CD25^+$ $CD127^+$ GATA-3^+ IL-$33R^+$ cell population in human WAT consistent with ILC2s identified in other human tissues

(Bartemes et al., 2014; Hams et al., 2014; Kim et al., 2013; Kim et al., 2014; Mjosberg et al., 2012; Mjosberg et al., 2011; Monticelli et al., 2011; Spits et al., 2013; Xue et al., 2014), and demonstrate that obesity in both humans and mice is associated with decreased ILC2 populations in WAT. Through loss-of-function studies we also identify that IL-33 is necessary to maintain ILC2 responses and limit the development of obesity. Collectively, these results indicate that the IL-33/ILC2 axis is operational in the steady state to limit adiposity and suggest that decreases in ILC2s in WAT in the context of obesity might be one factor that contributes to weight gain.

IL-33 is highly expressed in white adipose tissue (Thorrez et al., 2008) and is produced predominantly by adipocytes and endothelial cells (Zeyda et al., 2013). Expression levels of IL-33 mRNA and protein are reported to be increased in WAT of obese humans compared to non-obese controls and in HFD-fed mice compared to LFD-mice (Zeyda et al., 2013). In serum, however, IL-33 levels in sera of humans and mice appear to be unchanged (Zeyda et al., 2013) or decreased (Hasan et al., 2014) in the context of obesity, suggesting that there may be tissue-specific effects of obesity on IL-33 levels. Although increased IL-33 levels in WAT would be expected to elicit WAT ILC2 responses, our observation that ILC2s are decreased in obesity suggests that perhaps the IL-33/ILC2 axis might be dysregulated in established obesity. Future studies to address this topic are warranted.

The data in this Chapter also indicate that administration of exogenous IL-33 can elicit ILC2 responses in association with decreased adiposity and enhanced glucose tolerance. These beneficial metabolic effects of the IL-33/ILC2 pathway are consistent with previous studies showing a protective role for IL-33 in genetically obese mice and may be related to obesity-associated pathologies such as atherosclerosis that are limited by IL-33 (Hasan et al., 2014; Miller et al., 2010; Miller et al., 2008). However, whether IL-33 has protective effects against obesity through regulation of caloric expenditure or intake remains poorly characterized. In this Chapter, we demonstrate that chronic IL-33 treatment is associated with increased caloric expenditure but not decreased food intake. Although increased metabolic rate would be expected to result in compensatory increases in food intake to maintain energy balance, IL-33 did not have this effect, apparently due to decreased activity levels and possibly other processes. Importantly, these data suggest that IL-33 does not increase caloric expenditure via the thermic effect of food or through increased activity levels, two important factors that influence metabolic rate (Poehlman and Horton, 1989), and suggest that other physiologic processes are responsible for the increased energy expenditure following IL-33 treatment.

At steady state WAT contains a diverse set of type 2 cytokine-associated immune cells that are critical for the maintenance of metabolic homeostasis

(Gregor and Hotamisligil, 2011; Jin et al., 2013; Lumeng and Saltiel, 2011; Odegaard and Chawla, 2011; Osborn and Olefsky, 2012). Emerging studies suggest that ILC2s are a critical upstream mediator of the eosinophil/IL-4/AAMac pathway in WAT that has been previously demonstrated to maintain metabolic homeostasis and limit the development of obesity (Chang et al., 2012; Hams et al., 2013; Molofsky et al., 2013; Odegaard et al., 2007; Qiu et al., 2014; Ricardo-Gonzalez et al., 2010; Wu et al., 2011; Xu et al., 2013). The data in this Chapter indicate that decreased ILC2s in WAT is a conserved feature of obesity in mice and humans. In addition, we demonstrate that IL-33 is necessary and sufficient to promote ILC2 responses in WAT and limit the development of obesity. As adipocytes are an important source of IL-33 in the context of increased weight gain (Zeyda et al., 2013), the IL-33/ILC2 axis may represent one mechanism for mammals to couple metabolic changes in adipose to innate immune pathways that increase caloric expenditure. Dysregulation of the IL-33/ILC2 pathway may therefore promote increases in adiposity. In addition, these findings suggest that the IL-33/ILC2 axis might be a useful therapeutic target to treat obesity.

2.6 Tables and Figures

Table 1. Characteristics of non-obese and obese human donors.

Characteristic	Non-obese (n=7)	Obese (n=7)	P-value*
Source of tissue (% CHTN/% NYODP)	29/71	43/57	P=0.43
Age	39.3 +/- 5.2	52.6 +/- 2.7	P=0.042
Sex, % female	43	87	P=0.094
BMI (kg/m^2)	23.5 +/- 1.4	42.6 +/- 3.9	P=0.0006
History of Type 2 diabetes (%)	14	43	P=0.24
History of liver disease (%)	0	0	n/a
History of cardiovascular disease (%)	0	13	P=0.30

BMI, body mass index; CHTN, Cooperative Human Tissue Network; NYODP, New York Organ Donor Program

*Proportions were compared by X^2 tests. Continuous variables were compared by Student's *t*-test. Exact P-values are shown.

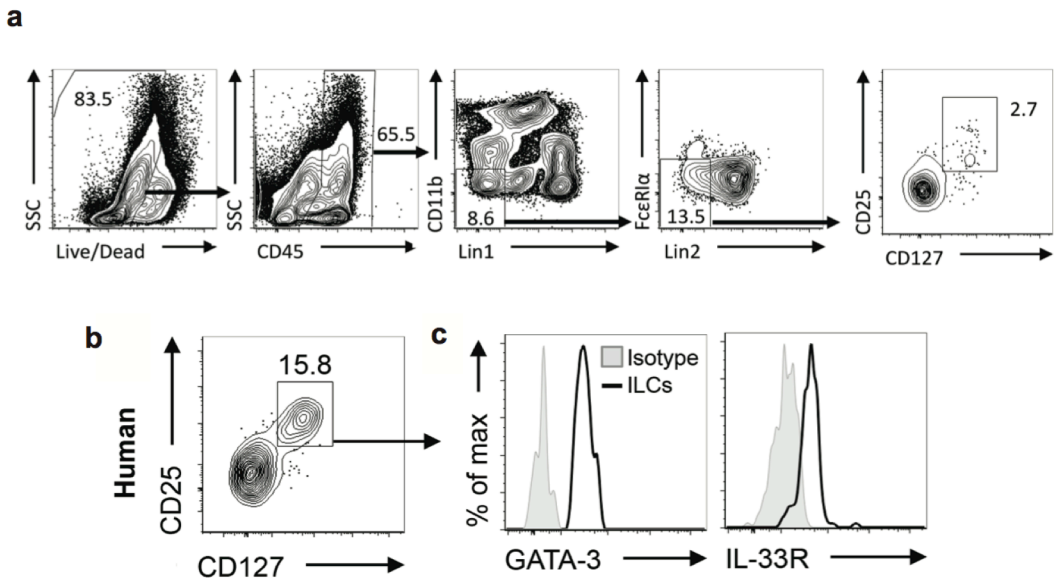

Figure 5. Identification of human Group 2 innate lymphoid cell (ILC2s) in white adipose tissue (WAT). **(a)** Gating strategy to identify human ILCs. Stromal vascular fraction (SVF) cells from human abdominal subcutaneous WAT were isolated and subjected to flow cytometric analyses. First plot pre-gated on singlets. Lineage cocktail 1 (Lin1): CD3, CD5, TCRαβ. Lineage cocktail 2 (Lin2): CD19, CD56, CD11c, CD16. ILCs are identified as Lin-negative cells that are $CD25^+$ $CD127^+$. Plots shown are from an obese donor. **(b)** Identification of lineage (Lin)-negative $CD25^+$ $CD127^+$ innate lymphoid cells (ILCs) in human abdominal subcutaneous WAT from a lean donor. Pre-gated on live $CD45^+$ Lin^- cells that lack CD3, CD5, TCRαβ, CD19, CD56, CD11c, CD11b, CD16, and FcεRIα. **(c)** Histograms of GATA-3 and IL-33R expression by human WAT ILCs (line). Shaded histogram, isotype control. Gated on live $CD45^+$ Lin^- $CD25^+$ $CD127^+$ ILCs.

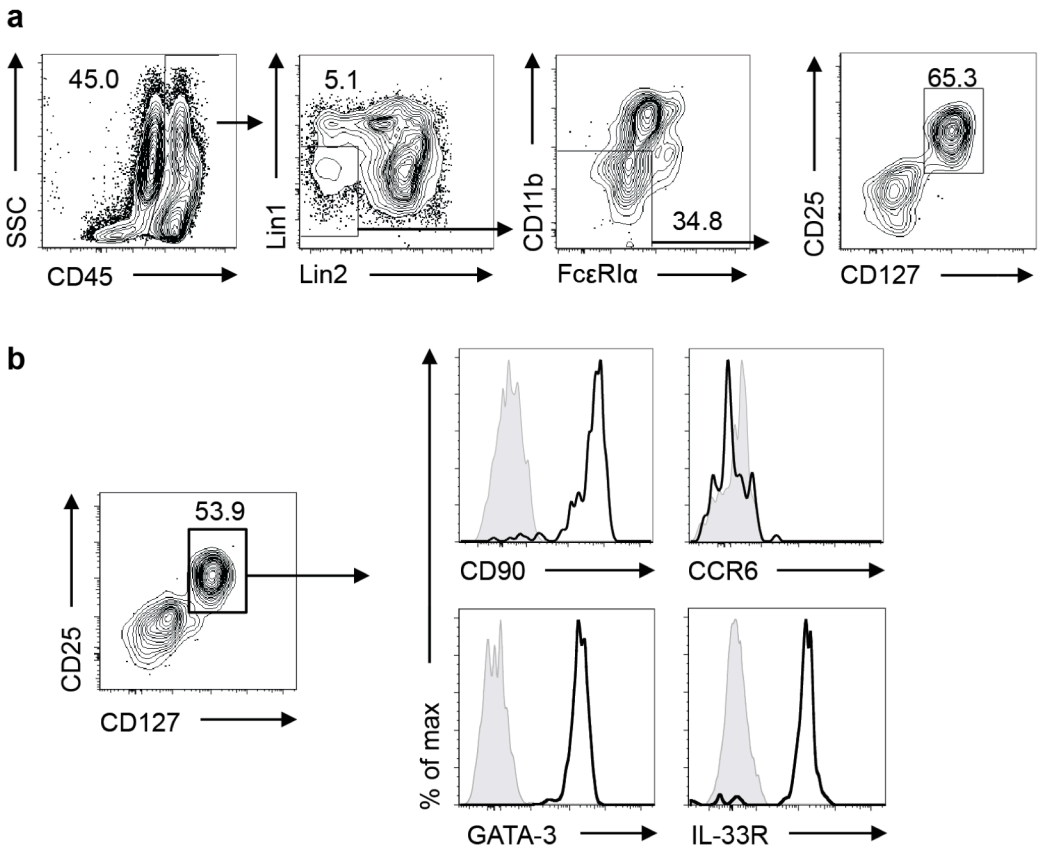

Figure 6. Identification of murine Group 2 innate lymphoid cell (ILC2s) in white adipose tissue (WAT). (a) Gating strategy to identify murine ILCs. Stromal vascular fraction (SVF) cells from murine epididymal (E)-WAT were isolated and subjected to flow cytometric analyses. First plot pre-gated on singlet live cells. Lineage cocktail 1 (Lin1): CD3, CD5, CD19, NK1.1. Lineage cocktail 2 (Lin2): CD19, CD11c. ILCs are identified as Lin-negative cells that are $CD25^+$ $CD127^+$. (**b**) Phenotypic characterization of ILCs from murine E-WAT. Left-hand plot shows Identification of Lin^- $CD25^+$ $CD127^+$ ILCs in murine epididymal (E)-WAT. Pre-gated on live $CD45^+$ Lin^- cells that lack CD3, CD5, CD19, NK1.1, CD11c, CD11b and FcεRIα. Right-hand plots are gated on live $CD45^+$ Lin^- $CD25^+$ $CD127^+$ ILCs and show histograms of CD90, CCR6, GATA-3 and IL-33R expression by murine E-WAT ILCs (line). Shaded histogram, isotype control.

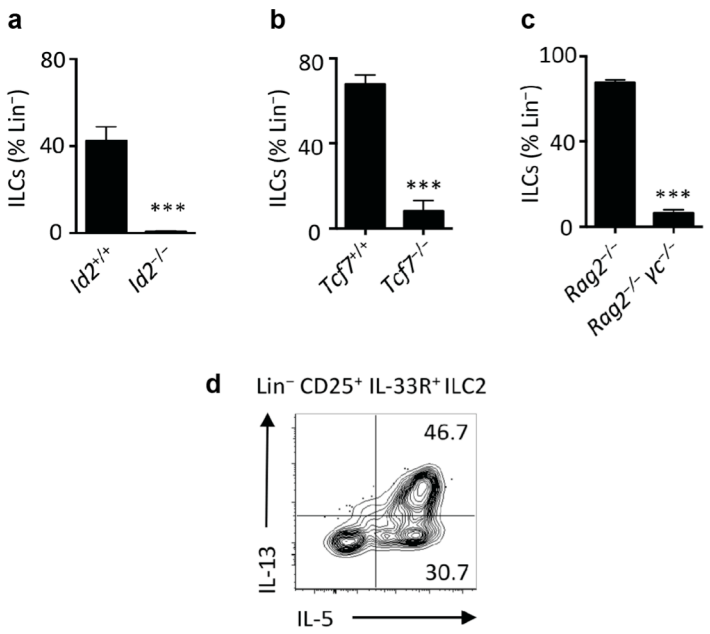

Figure 7. Developmental and functional characteristics of murine ILCs from epididymal white adipose tissue (E-WAT). (a-c) Stromal vascular fraction (SVF) cells from murine E-WAT were isolated and subjected to flow cytometric analyses. ILCs were defined as live $CD45^+$ Lin^- $CD25^+$ $CD127^+$ cells. The lineage (Lin) cocktail included CD3, CD5, CD19, NK1.1, CD11c, CD11b and FcεRIα. Comparison of Lin^- $CD25^+$ $CD127^+$ cells in E-WAT of **(a)** *Id2*$^{+/+}$ versus *Id2*$^{-/-}$ bone marrow chimeras, **(b)** *Tcf7*$^{+/+}$ versus *Tcf7*$^{-/-}$ mice and **(c)** *Rag2*$^{-/-}$ versus *Rag2*$^{-/-}$ $\gamma_c^{-/-}$ mice. N=3-8 mice per group from 2 independent experiments. **(d)** E-WAT SVF cells from C57BL/6 mice were treated with PMA (100 ng/mL) and ionomycin (1 µg/mL) in the presence of Brefeldin A (10 µg/mL) for 4h and stained for ILCs. Live $CD45^+$ Lin^- $CD25^+$ $CD127^+$ $IL\text{-}33R^+$ cells were pre-gated, and IL-5 and IL-13 protein levels were assessed. Plot shown is representative of n=12 mice from 3 independent experiments.

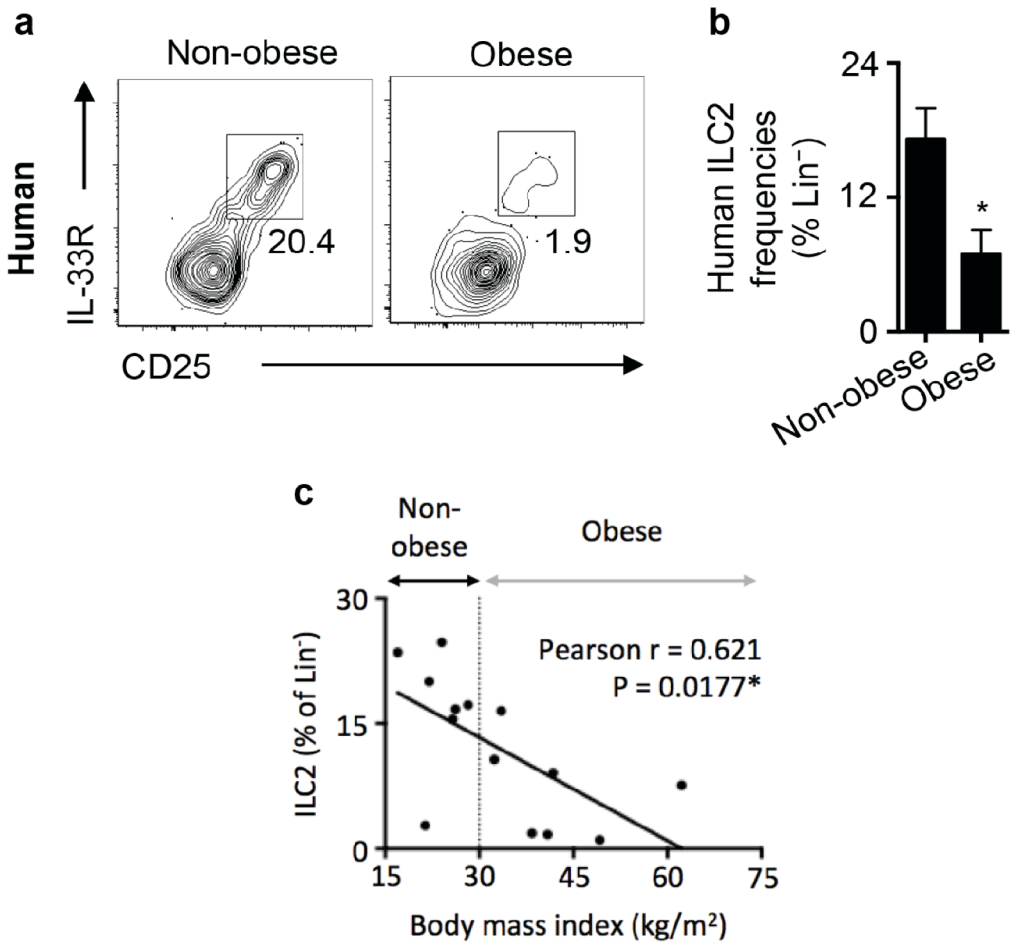

Figure 8. ILC2 populations in human white adipose tissue (WAT) are decreased in obese patients. (a) Representative plots and **(b)** frequencies of human WAT ILC2s from donors stratified into non-obese (body mass index [BMI]<30.0 kg/m^2, n=7) and obese (BMI≥30.0 kg/m^2, n=7) groups. Pre-gated on live CD45$^+$ Lin$^-$ cells that lack CD3, CD5, TCRαβ, CD19, CD56, CD11c, CD11b, CD16, and FcεRIα. Student's t-test, *P<0.05. **(c)** Frequencies of ILC2s are inversely correlated with BMI. Vertical dashed line demarcates BMI = 30.0 kg/m^2. Linear regression. Pearson correlation moment (r) is of the best-fit line, which is shown on the graph. Exact P-value shown. *P<0.05.

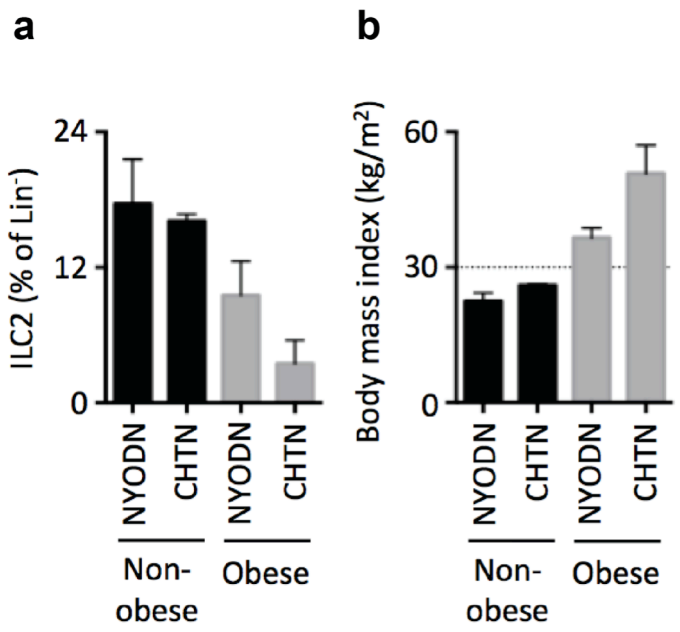

Figure 9. ILC2 frequencies tend to be decreased in human white adipose tissue (WAT) irrespective of source, and differences in ILC2 frequencies between sources are explained by body mass index (BMI). (a) Frequencies of human ILC2s (Lin^- $CD25^+$ IL-$33R^+$ cells) in subcutaneous WAT of non-obese (BMI < 30.0 kg/m^2) and obese (BMI ≥ 30.0 kg/m^2) donors stratified by source of tissue. Gated on live $CD45^+$ Lin^- $CD25^+$ IL-$33R^+$ cells. The lineage (Lin) cocktail included CD3, CD5, TCRαβ, CD19, CD56, CD11c, CD11b, CD16, and FcεRIα. NYODN, New York Organ Donor Network. CHTN, Cooperative Human Tissue Network-Eastern Division. **(b)** BMI of non-obese and obese donors stratified by source of tissue. The horizontal dashed line demarcates the cut off of non-obese vs obese donors. Non-obese from NYODN, n=4. Non-obese from CHTN, n=3. Obese from NYODN, n=4. Obese from CHTN, n=3.

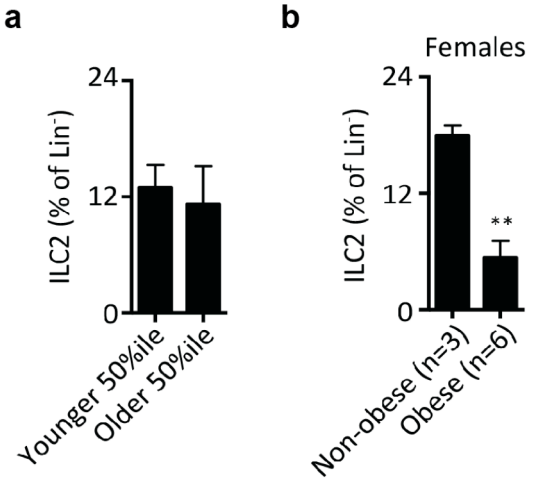

Figure 10. Age and biological sex do not explain differences in WAT ILC2 frequencies observed between non-obese and obese donors. (a) Human WAT ILC2 frequencies were compared in the 7 youngest donors (36.0 +/- 3.5 years old) versus the 7 oldest donors (55.9 +/- 1.9 years old). **(b)** Human WAT ILC2 frequencies in female non-obese donors with body mass index (BMI) <30.0 kg/m^2 versus female obese donors with BMI ≥30.0 kg/m^2. In both panels, ILC2s were defined as live CD45$^+$ Lin$^-$ CD25$^+$ IL-33R$^+$ cells, where the lineage (Lin) cocktail included CD3, CD5, TCRαβ, CD19, CD56, CD11c, CD11b, CD16, and FcεRIα. Student's t-test. **P<0.01, ***P<0.001.

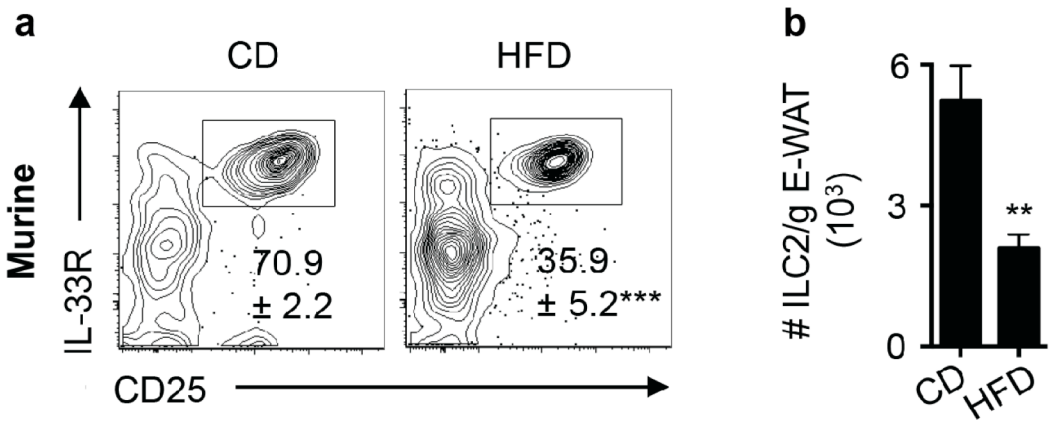

Figure 11. ILC2 populations are decreased in epididymal white adipose tissue (E-WAT) of high fat diet (HFD)-induced obese mice. **(a)** Representative plots and frequencies of murine E-WAT ILC2s from mice fed a control diet (CD, 10% kcal fat, n=5) or high fat diet (HFD, 45% kcal fat, n=4) for 12 weeks. **(h)** Numbers of murine ILC2s/gram E-WAT in mice fed a CD (n=8) or HFD (n=6) for 12 weeks. Student's t-test, **P<0.01, ***P<0.001.

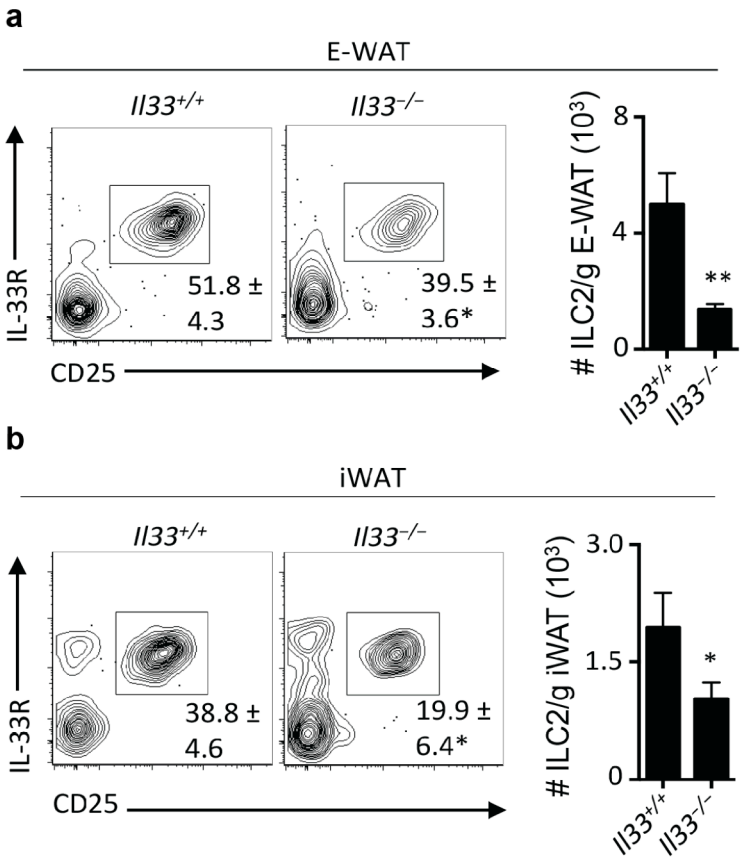

Figure 12. IL-33-deficient mice exhibit decreased frequencies and numbers of ILC2s in white adipose tissue (WAT). *Il33*$^{+/+}$ (n=6) or *Il33*$^{-/-}$ (n=5) mice were fed a low fat diet (10% kcal fat) for 12 weeks starting at 7 weeks of age. **(a)** Frequencies and numbers of live CD45^{+} Lin^{-} CD25^{+} IL-33R^{+} ILC2s in epididymal (E)-WAT. Plots pre-gated on CD45^{+} Lin^{-} cells that lack CD3, CD5, CD19, NK1.1, CD11c, CD11b and FcεRIα. **(b)** Frequencies and numbers of live CD45^{+} Lin^{-} CD25^{+} IL-33R^{+} ILC2s in inguinal (i)WAT. Plots pre-gated on CD45^{+} Lin^{-} cells that lack CD3, CD5, CD19, NK1.1, CD11c, CD11b and FcεRIα. Student's t-test, *P<0.05, **P<0.01.

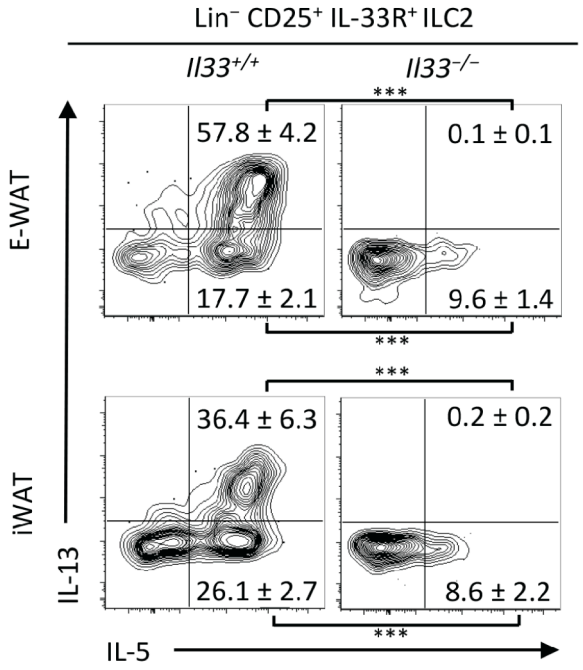

Figure 13. IL-33-deficient mice exhibit decreased frequencies and numbers of ILC2s in white adipose tissue (WAT). *Il33*$^{+/+}$ (n=6) or *Il33*$^{-/-}$ (n=5) mice were fed a low fat diet (10% kcal fat) for 12 weeks starting at 7 weeks of age. Epididymal (E)-WAT and inguinal (i)WAT SVF were treated with PMA (100 ng/mL) and ionomycin (1 µg/mL) in the presence of Brefeldin A (10 µg/mL) for 4h prior to staining for ILC2s and intracellular cytokines. Representative plots and frequencies of IL-5^{+} IL-13^{-} and IL-5^{+} IL-13^{+} ILC2s from E-WAT and iWAT are shown. Plots pre-gated on CD45^{+} Lin^{-} CD25^{+} IL-33R^{+} ILC2s, where the lineage (Lin) cocktail included CD3, CD5, CD19, NK1.1, CD11c, CD11b and FcεRIα. Student's t-test, ***P<0.001.

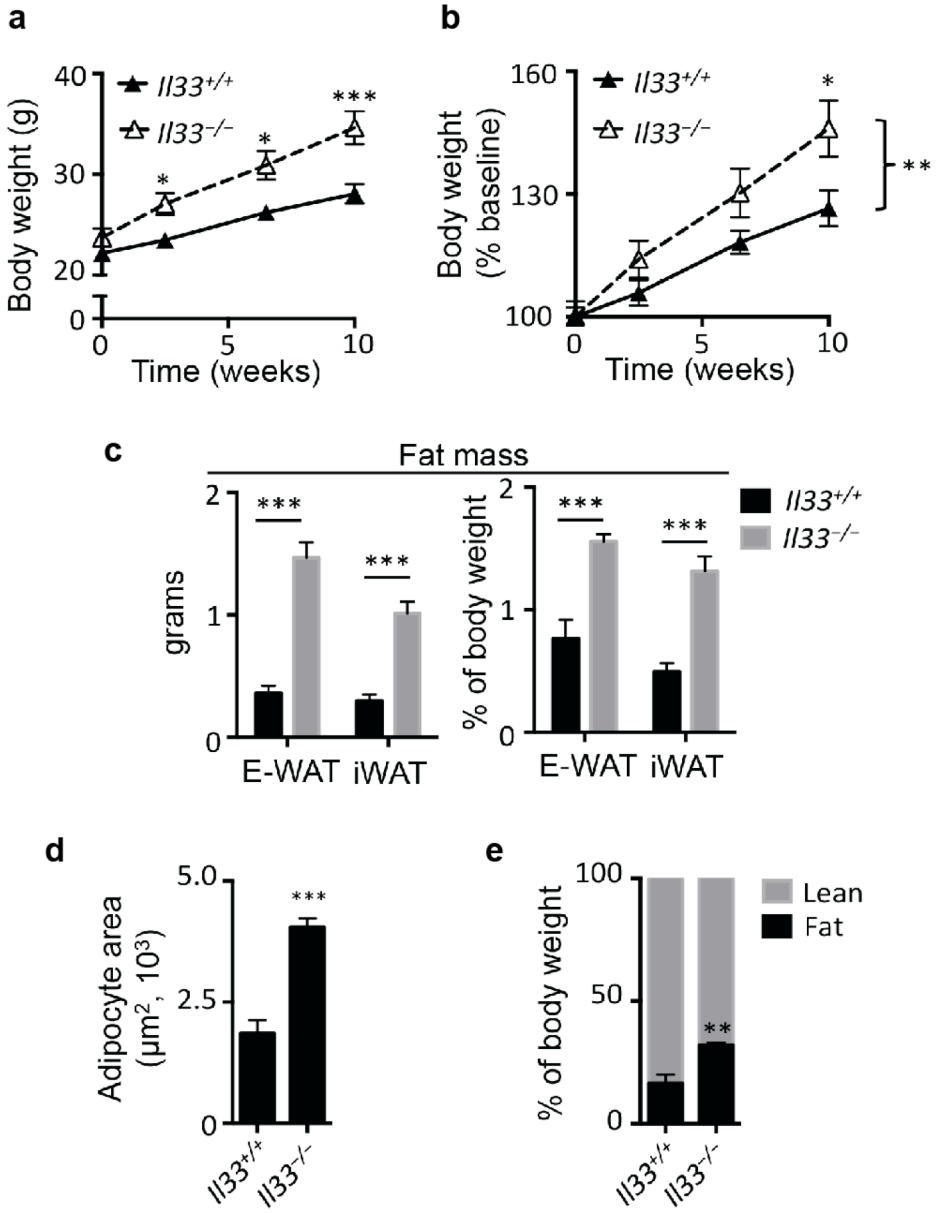

Figure 14. IL-33-deficient mice gain more weight and exhibit increased adiposity compared to IL-33-sufficient mice. *Il33*$^{+/+}$ (n=6) or *Il33*$^{-/-}$ (n=5) mice were fed a low fat diet (10% kcal fat) for 12 weeks starting at 7 weeks of age. **(a)** Absolute and **(b)** relative body weights over the first 10 weeks of feeding. **(c)** Absolute and relative epididymal (E)-WAT and inguinal (i)WAT weights. **(d)** iWAT sections were H&E stained and imaged at 40X magnification. Adipocyte area was calculated from 25-40 adipocytes total from 2-3 images per mouse. **(e)** Body composition analyses. Student's t-test or ANOVA with repeated measures. *P<0.05, **P<0.01, ***P<0.001.

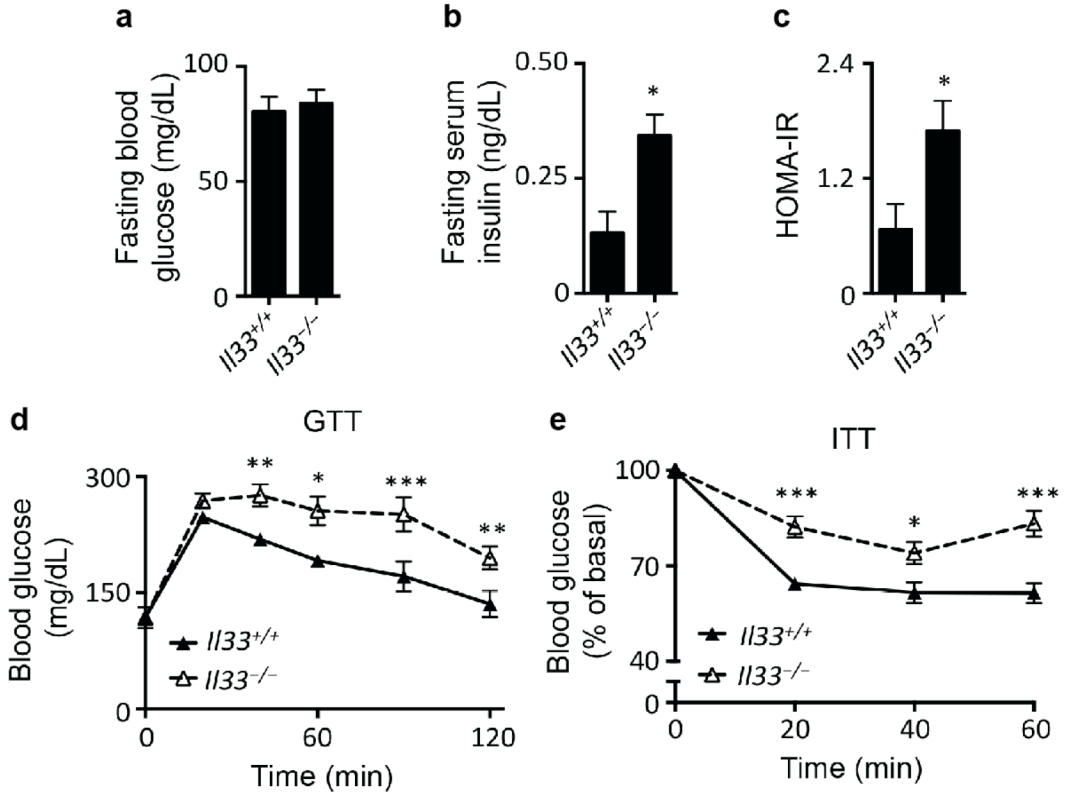

Figure 15. IL-33-deficient mice exhibit impaired glucose homeostasis. *Il33*$^{+/+}$ (n=6) or *Il33*$^{-/-}$ (n=5) mice were fed a low fat diet (10% kcal fat) for 12 weeks starting at 7 weeks of age. On week 10, mice were fasted for 16 hours followed by glucose tolerance testing (GTT). On week 11, mice were fasted for 4-6 hours followed by insulin tolerance testing (ITT). **(a)** 16-hour fasting blood glucose concentrations. **(b)** 16-hour fasting serum insulin concentrations. **(c)** Homeostatic model assessment of insulin resistance (HOMA-IR) index values. **(d)** GTT with 2 g/kg glucose following a 16-hour fast. **(e)** ITT with 0.5 U/kg insulin following a 5-hour fast. For panels **a-c**, groups were compared using Student's t-test, *P<0.05. For panels **d-e**, a two-way ANOVA with repeated measures was performed followed by Tukey post-hoc test. *P<0.05, **P<0.01, ***P<0.001. Data shown are from a single cohort and are representative of 2 independent experiments.

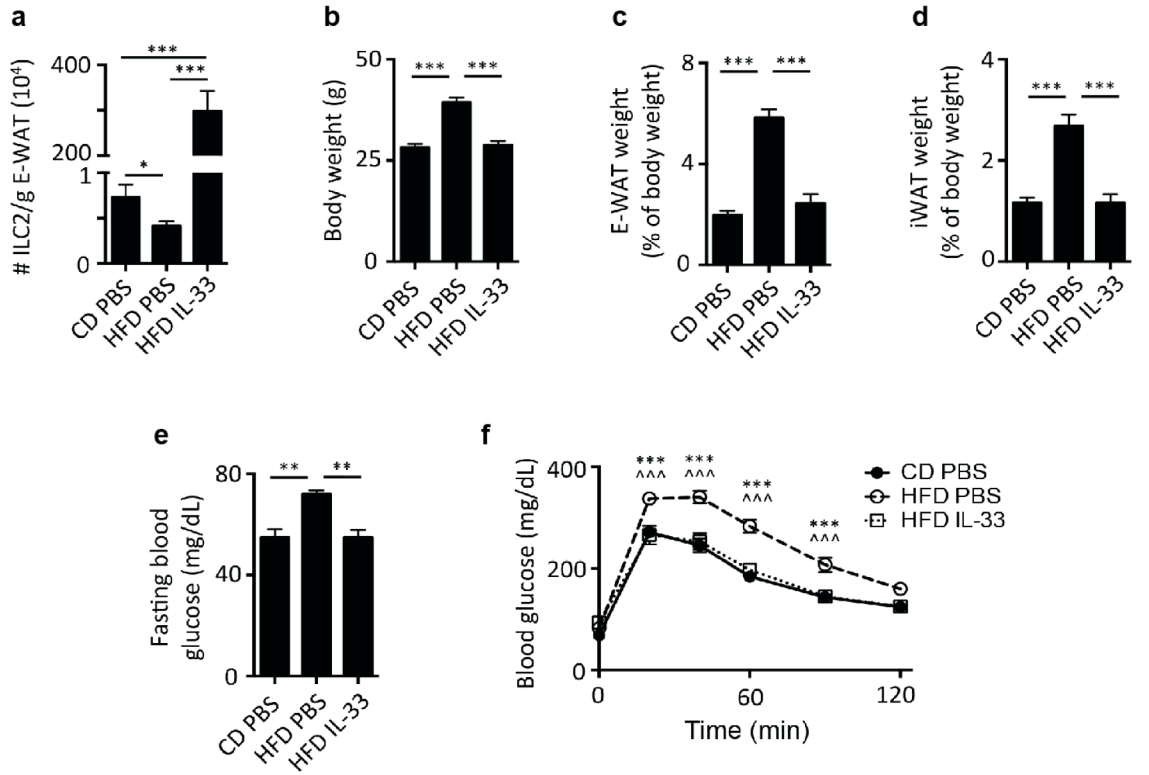

Figure 16. IL-33 increases E-WAT ILC2s and abrogates the development of obesity and glucose intolerance in mice fed a high fat diet (HFD). Male C57BL/6 mice were placed on a control diet (CD) or HFD (60% kcal fat) at age 8 weeks. On the first day of feeding, CD mice were treated with PBS and HFD mice were treated with PBS or recombinant murine (rm)IL-33 (12.5 μg/kg) once every 4 days by intraperitoneal injection for 4 weeks. **(a)** E-WAT ILC2 numbers per gram of adipose, **(b)** body weight, **(c)** relative E-WAT weight and **(d)** relative iWAT weight at week 4. **(e)** 16-hour fasting blood glucose concentrations and **(f)** glucose tolerance testing during week 3. All panels include n=10 mice per group from 2 independent cohorts, except panel A which includes n=16 CD PBS and n=18 HFD PBS from 4 independent cohorts. Panels a-e, One-way ANOVA with Tukey post-hoc test,* P<0.05, **P<0.01, ***P<0.001. Panel f, Two-way ANOVA with repeated measures, ***P<0.001 comparing CD PBS vs HFD PBS, ^^^P<0.001 comparing HFD PBS vs HFD IL-33.

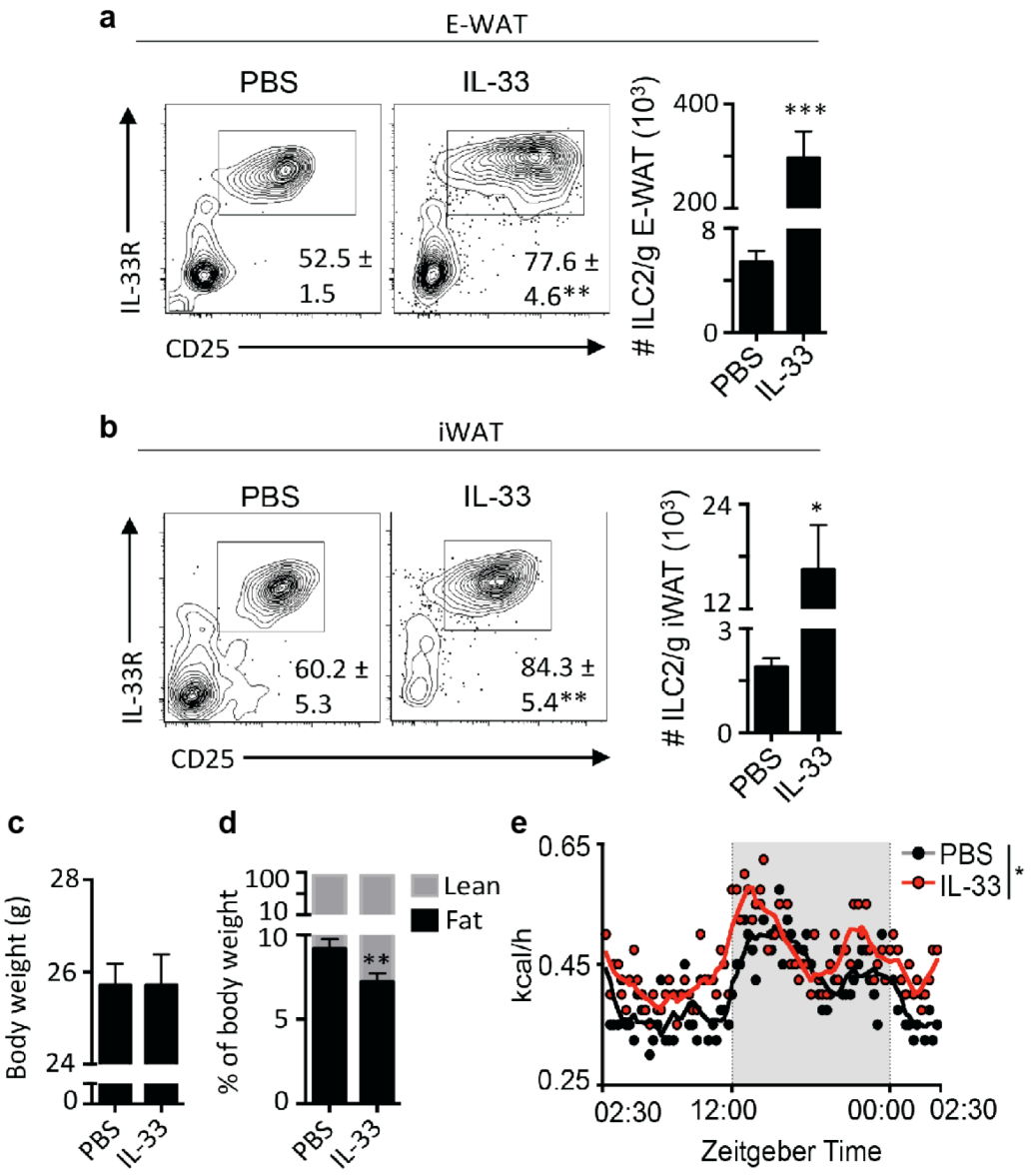

Figure 17. Exogenous IL-33 promotes ILC2 responses in white adipose tissue and limits adiposity in association with increased caloric expenditure. Wildtype mice were treated with phosphate buffered saline (PBS, n=10) or recombinant murine IL-33 (12.5 µg/kg/day, n=12) by intraperitoneal injection for 7 days. **(a-b)** Representative plots with frequencies and numbers of ILC2s in **(a)** epididymal (E)-WAT and **(b)** inguinal (i)WAT. **(c)** Body weight and **(k)** body composition. **(l)** Caloric expenditure over a 24-hour period, days 6-to-7 of treatment. Non-shaded area, lights on. Shaded area, lights off.

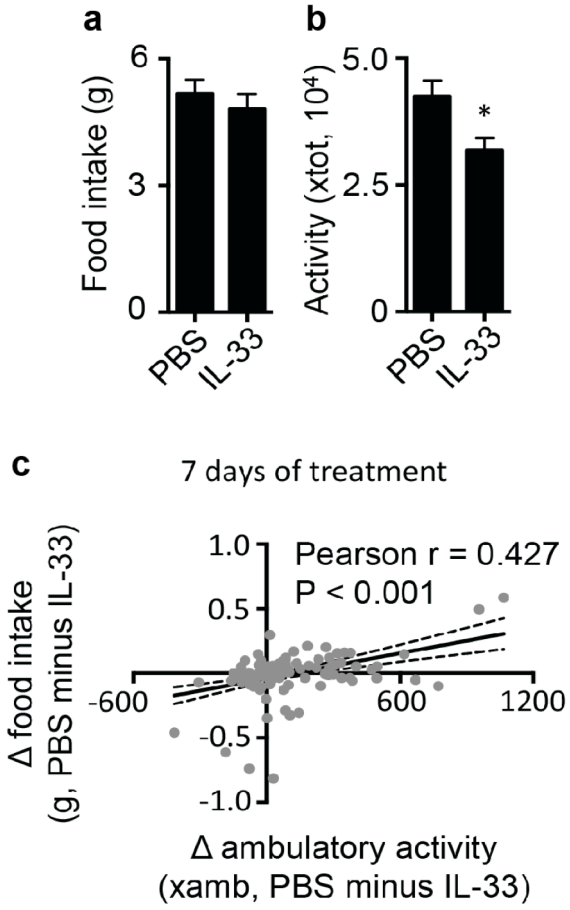

Figure 18. Exogenous IL-33 treatment does not affect food intake, and the absence of hyperphagia following IL-33 treatment may be due to decreased activity levels. Wildtype mice were treated with phosphate buffered saline (PBS, n=10) or recombinant murine IL-33 (12.5 μg/kg/day, n=12) by intraperitoneal injection for 7 days. **(a)** Food intake and **(b)** total activity levels (beam breaks) assessed by Comprehensive Laboratory Animal Monitoring System (CLAMS) cages over a 24 hour period between days 6 and 7 of treatment. Student's t-test, *P<0.05. **(c)** The average difference in food intake or ambulatory activity (beam breaks) between PBS- and rmIL-33-treated mice was calculated for each 15 min interval during the CLAMS cage analyses in panels a-b, and the differences in food intake and ambulatory activity at each time point were related by linear regression. Solid line, best-fit line. Dashed curves, upper and lower 95% confidence intervals around the best-fit line.

Chapter 3: The IL-33/ILC2 pathway promotes beiging of white adipose tissue

3.1 Abstract

Obesity is an increasingly prevalent disease regulated by genetic and environmental factors. Emerging studies indicate that immune cells, including monocytes, granulocytes and lymphocytes, regulate metabolic homeostasis and are dysregulated in obesity. Group 2 innate lymphoid cells (ILC2s) can regulate adaptive immunity and eosinophil and alternatively-activated macrophage responses, and were recently identified in murine white adipose tissue (WAT) where they may act to limit the development of obesity[6]. In the previous Chapter, we demonstrated that decreased ILC2 populations in WAT are a conserved characteristic of obesity in humans and mice and that IL-33 is critical for maintaining ILC2s in WAT and limiting adiposity in mice by increasing caloric expenditure. However the mechanisms by which IL-33 and ILC2s regulate

metabolic homeostasis remain unknown. In this Chapter, we demonstrate that IL-33 treatment is associated with recruitment of uncoupling protein 1 $(UCP1)^{+}$ beige adipocytes in WAT, a process known as beiging or browning that regulates caloric expenditure[7-9]. IL-33-induced beiging appeared to be dependent on ILC2s, and IL-33 treatment or transfer of IL-33-elicited ILC2s was sufficient to drive beiging independently of the adaptive immune system, eosinophils or IL-4 receptor signaling. We found that ILC2s produce methionine-enkephalin peptides that can act directly on adipocytes to upregulate *Ucp1* expression *in vitro* and that promote beiging *in vivo*. Collectively, these studies indicate that in addition to responding to infection or tissue damage, ILC2s can regulate adipose function and metabolic homeostasis in part via production of enkephalin peptides that elicit beiging.

3.2 Introduction

Three adipocyte cell types – white, brown and beige – are regulated by gene-environment interactions to differentially control energy storage and expenditure (Harms and Seale, 2013; Pfeifer and Hoffmann, 2014; Wu et al., 2013). White adipocytes are found in white adipose tissues (WAT), store large amounts of triglycerides (TG) and produce a variety of hormones such as leptin, adiponectin, resistin and adipsin that regulate food intake and glucose homeostasis (Badoud et al., 2014; Peirce et al., 2014; Pfeifer and Hoffmann, 2014). In contrast to white adipocytes, brown adipocytes are found in discrete brown adipose tissue (BAT)

depots, the largest of which is located in the interscapular space in mice, and contain multiple small lipid droplets and abundant Uncoupling protein 1 $(UCP1)^{+}$ mitochondria that uncouple fatty acid and glucose oxidation from ATP synthesis, resulting in the production of heat (Cannon and Nedergaard, 2004; Harms and Seale, 2013). This thermogenic process is dependent on UCP1 and is critical for defending core body temperature and regulating metabolic rate and the development of obesity(Carey et al., 2013; Cohen et al., 2014; Feldmann et al., 2009; Harms and Seale, 2013; Rosen and Spiegelman, 2014; Saito et al., 2009; Wu et al., 2012; Wu et al., 2013; Yoneshiro et al., 2011).

Recent studies have also identified a third adipocyte cell type, the beige adipocyte (also known as brite, brown-like or inducible brown adipocyte) that is dispersed within WAT but with morphologic and functional characteristics of brown adipocytes (Bartelt and Heeren, 2014; Harms and Seale, 2013; Wu et al., 2013). These specialized adipocytes emerge in WAT in response to environmental signals, a process known as beiging or browning, and also act to produce heat in an UCP1-dependent manner(Harms and Seale, 2013; Rosen and Spiegelman, 2014; Shabalina et al., 2013; Wu et al., 2012; Wu et al., 2013). UCP1 is highly expressed in brown and beige but not white adipocytes (Wu et al., 2012). BAT in humans has been shown to contain adipocytes with morphologic and gene expression signatures consistent with beige rather than brown adipocytes (Jespersen et al., 2013; Sharp et al., 2012; Wu et al., 2012).

Activation of these beige/brown fat depots is defective in obese humans (Carey et al., 2013; Saito et al., 2009), and recent studies indicate that selective deletion of beige adipocytes while leaving BAT intact increases susceptibility to obesity in mice (Cohen et al., 2014). Therefore beige adipocytes appear to be critical mediators of energy homeostasis.

Although a variety of factors have been shown to activate both brown and beige adipocytes (Harms and Seale, 2013; Rosen and Spiegelman, 2014; Wu et al., 2013), recent studies suggest that type 2 cytokine-associated immune cells such as eosinophils and alternatively activated macrophages (AAMacs) are necessary for optimal brown and beige adipocyte responses (Nguyen et al., 2011; Qiu et al., 2014; Rao et al., 2014). Mice that lack IL-4 and IL-13 (*Il4/13*$^{-/-}$); the shared receptor for these cytokines, IL-4Rα (*Il4ra*$^{-/-}$); or STAT6, a transcription downstream of IL-4Rα signaling (Stat6$^{-/-}$) have defective AAMac responses (Martinez et al., 2009) and exhibit decreased upregulation of UCP1 expression in BAT and impaired defense of core body temperature following acute exposure to cold environmental temperatures (Nguyen et al., 2011). IL-4 was shown to activate AAMacs to produce catecholamines such as norepinephrine (NE) that act on the β_3 adrenergic receptor (β_3AR) to stimulate lipolysis, elicit mitochondrial biogenesis and activate UCP1 in BAT (Nguyen et al., 2011). However IL-4/IL-4Rα interactions do not appear to be required for BAT responses in the context of chronic exposure to severe cold environmental temperatures over a period of

3 days (Qui et al., 2014). In this context, eosinophils are recruited to WAT and produce IL-4 to stimulate AAMac production of NE to promote beiging of WAT (Qiu et al., 2014; Rao et al., 2014). Mice lacking eosinophils, IL-4Rα or STAT6 failed to undergo optimal beiging of WAT and had decreased metabolic rate compared to wildtype controls in the setting of chronic cold exposure (Qiu et al., 2014; Rao et al., 2014). Thus, the eosinophil/IL-4/AAMac/NE pathway appears to have a critical role in the elicitation of both brown and beige adipocyte responses and in the regulation of metabolic rate.

Group 2 innate lymphoid cells (ILC2s) are a recently described innate immune cell that is a dominant source of IL-5 and IL-13 in WAT to promote eosinophil and AAMac responses, respectively (Molofsky et al., 2013; Moro et al., 2010; Neill et al., 2010; Nussbaum et al., 2013; Price et al., 2010). ILC2s have been previously demonstrated to be decreased in WAT of obese mice (Molofsky et al., 2013) and limit the development of obesity (Hams et al., 2013). However the mechanisms by which ILC2s regulate metabolic homeostasis in WAT remain poorly understood. In the previous Chapter, we demonstrated that decreased ILC2s in WAT is a conserved characteristic of obesity in mice and humans, and that IL-33 is critical for promoting ILC2 responses and decreasing adiposity by increasing caloric expenditure. Collectively, these findings provoke the hypothesis that the IL-33/ILC2 axis might contribute to the regulation of caloric expenditure by promoting the activation of brown and/or beige adipocytes.

In this Chapter, we demonstrate that IL-33 treatment elicits beiging of WAT but does not stimulate expression of *Ucp1* in BAT, suggesting that IL-33 has selective effects on beiging. IL-33-induced beiging appeared to be dependent on ILC2s, and adoptive transfer of IL-33-elicited ILC2s was sufficient to drive beiging of WAT and to increase inguinal (i)WAT oxygen consumption. Surprisingly, IL-33 and ILC2 transfer could elicit beiging in the absence of eosinophils and IL-4Rα-dependent AAMacs, suggesting that the IL-33/ILC2 axis can promote beiging via another mechanism. Gene expression analyses of 69 genes previously linked to the development of obesity in humans revealed that ILC2s produce the neuropeptide methionine-enkephalin (MetEnk). We show that MetEnk treatment is sufficient to drive beiging of WAT *in vivo* and can act directly on primary adipocytes from iWAT but not BAT to upregulate Ucp1 expression. Collectively, these data indicate that the IL-33/ILC2 axis elicits beiging via production of MetEnk peptides.

3.3 Methods

3.3.1 Mice

C57BL/6, CD45.1^{+} C57BL/6, *Rag1*$^{-/-}$ and *DblGata1* (Balb/c background) mice were obtained from Jackson Labs. *Rag2*$^{-/-}$, *Rag2*$^{-/-}$ *cy*$^{-/-}$, *Il33*$^{+/+}$, Balb/c and *Il4ra*$^{-/-}$ (Balb/c background) mice were obtained from Taconic. *Il33*$^{-/-}$ mice were

provided by Amgen Inc via Taconic. All mice were males and had *ad libitum* access to food and water and were maintained in a specific pathogen free facility with a 12h:12h light:dark cycle (lights on at 7:00 AM, lights off at 7:00 PM). Animals were randomly assigned to groups of n=3-5 mice per group per experiment, and at least two independent experiments were performed throughout. In all *in vivo* experiments, a single technical replicate per mouse was performed. For all *in vitro* experiments, 2-3 technical replicates were performed in each independent experiment. Sample sizes in each independent experiment were selected to have power of at least 90% using published sample size/power formulas (Brestoff and Van den Broeck, 2013). All experiments were carried out under the guidelines of the Institutional Animal Care and Use Committee at the University of Pennsylvania.

3.3.2 Rodent chow and diet-induced obesity

In all experiments, mice had *ad libitum* access to food and water. Where indicated, mice were fed a control diet (CD, 10% kcal fat, Research Diets, New Brunswick, New Jersey) for the indicated period of time starting at 6-8 weeks of age. CD was gamma-irradiated (10-20 kGy) and stored at 4 °C under dry conditions until use, and rodents were provided fresh chow weekly. In all experiments that did not employ CD, mice were fed a standard autoclavable rodent chow (5% kcal fat, #5010, Lab Diets, St. Louis, Missouri) that had been autoclaved and allowed to cool overnight before use.

3.3.3 *In vivo* cytokine and enkephalin peptide treatments.

Mice were administered 12.5 µg/kg carrier-free recombinant murine IL-33 (rmIL-33, R&D Systems, Minneapolis, Minnesota) in sterile phosphate buffered saline (PBS) by intraperitoneal (i.p.) injection daily for the indicated number of days. In some studies, mice were treated with a previously reported dose (Zagon et al., 2010) of 10 mg/kg [Met^5]-enkephalin acetate salt hydrate (MetEnk, amino acid sequence YGGFM, ≥95.0% purity by HPLC, Sigma Aldrich, St. Louis, MO) in PBS or with PBS alone by bilateral subcutaneous injection near the iWAT daily for 5 days (approximately 200 µL per side). MetEnk or vehicle injections were performed under 2% isoflurane anesthesia. All injections were performed between the hours of 4:00 PM and 7:00 PM.

3.3.4. Tissue oxygen consumption

A ~20 mg biopsy of iWAT was isolated from directly below the lymph node and minced in PBS containing 2% BSA, 1.1 mM sodium pyruvate and 25 mM glucose. Samples were placed in an MT200A Respirometer Cell (Strathkelvin), and oxygen consumption was measured for approximately 5 min. Oxygen consumption rates were normalized to minced tissue weight.

3.3.5 Isolation of immune cells from adipose

Murine epididymal white adipose tissue (E-WAT), inguinal WAT (iWAT) or brown adipose tissue (BAT) or human subcutaneous abdominal WAT were harvested and dissected so as to be free of reproductive tissues, lymph nodes and fibrous connective tissue. Tissues were finely minced using sterile scissors to form a slurry that was subsequently digested with 0.1% collagenase type II (Sigma-Aldrich, USA) in high glucose DMEM at 37°C with shaking at 200 rpm for 60-90 min at a 45° angle. Digested tissues were filtered through a 70 µm nylon mesh. The mesh was washed with approximately 20 mL Wash Media (high glucose DMEM supplemented with 5% heat-inactivated fetal bovine serum [FBS], 100 units/mL penicillin, 100 µg/mL streptomycin and 2 mM L-glutamine). All Wash Media reagents were from Life Technologies (Grand Island, NY) except FBS, which was from Denville USA. Washed cells were centrifuged at 500 x *g* for 5 min at 4 °C, and then floating adipocytes were removed by aspiration and the stromal vascular fraction (SVF) pellet was resuspended in red blood cell lysis buffer (ACK RBC Lysis Buffer) and allowed to incubate at room temperature for 2 min. The RBC Lysis reaction was stopped by addition of 10 volumes Wash Media, and the SVF cells were recovered by centrifugation at 500 x *g* for 5 min at 4 °C. Cells were resuspended in 200 µL Wash Media and aliquotted in equal parts for immediate flow cytometric analysis or for re-stimulation as described below for subsequent intracellular cytokine analysis by flow cytometry. In some

experiments, all recovered SVF cells were used for immediate flow cytometric analyses.

3.3.6 Surface and nuclear staining of murine cells for flow cytometric analyses

Isolated SVF cells from mice were resuspended in 100 µL FACS PBS (sterile 1X phosphate buffered saline [Invitrogen] supplemented with 2% heat-inactivated FBS and 1 mM EDTA [Invitrogen] containing LIVE/DEAD Fixable Aqua Dead Cell Stain (1:600) and anti-mouse IL-33R-biotin (T1/S2, clone DJ8) from MD Bioproducts (St. Paul, MN) (1:300). Cells were incubated on ice for 30 min in the dark and were washed twice in 250 µL FACS PBS with centrifugation at 500 x *g* for 5 min at 4 °C before each wash. Washed cells were stained with combinations of the following antibodies (all of which were used at 1:300 dilutions unless otherwise noted) in a volume of 90 µL staining buffer (FACS PBS supplemented with 20 µg/mL rat IgG): anti-mouse CD45-eFluor 605NC (clone 30-F11; 1:200), CD45.1-eFluor 450 (A20; 1:100), CD45.2-AlexaFluor 700 (104), F4/80-eFluor 450 (BM8), CD3e-PerCP-Cy5.5 (145-2C11), CD5-PerCP-Cy5.5 (53-7.3), CD19-PerCP-Cy5.5 (1D3), NK1.1-PerCP-Cy5.5 (PK136), CD11c-PerCP-Cy5.5 (N418), FcεRIα-FITC (MAR-1), Foxp3-FITC (FJK-16s; 1:100), GATA-3-PE (TWAJ; 1:100) and CD25-PE-Cy7 (clone PC61.5) from eBioscience (San Diego, CA); CD11b-PE-Texas Red (M1/70.15; 1:500) from Life Technologies (Grand Island, NY); CD90.2-Alexa Fluor 700 (30-H12; 1:400) and

CD4-Brilliant Violet-650 (RM4-5) from BioLegend (San Diego, CA); SiglecF-PE (E50-2440) and CD3e-PE-CF594 (145-2C11) from BD Biosciences (San Jose, CA); CD206-Alexa Fluor 647 (MR5D3; 1:200) from AbD Serotec (Raleigh, NC); and Streptavidin-APC (1:300) from eBioscience. CD206 staining was performed following fixation and permeabilization with the Foxp3 Staining Buffer Set (eBioscience) according to the manufacturer's protocol. All intracellular stains were performed in 1X Permeabilization Buffer (PB, eBioscience) for 45 min on ice. Cells were washed 3 times in 250 µL 1X PB with centrifugation at 500 *x* g for 5 minutes at 4 °C between washes, and recovered cells were resuspended in 200 µL FACS Buffer before flow cytometric analyses.

3.3.7 Intracellular cytokine analysis

To examine ILC2 MetEnk production, ILC2s were sort-purified from E-WAT of IL-33-treated mice, as described below. Ten thousand ILC2s were re-stimulated for 4 days with rmIL-2 (10 ng/ml) and rmIL-7 (10 ng/mL) in the presence or absence of rmIL-33 (30 ng/mL) in complete media (Wash Media with 10% FBS, 55 µM 2-mercaptoethanol and 25 mM HEPES) at 37 °C with 5% CO_2. All cytokines were from R&D Systems (Minneapolis, Minnesota). During the final 4 hours of treatment, cells were treated with Brefeldin A (10 µg/mL) (Sigma-Aldrich) and monensin (1:1500) in a 37°C incubator (5% CO_2). Cells were then surface stained and fixed/permeabilized using Cyto Fix/Perm (BD Pharmingen) according to manufacturer's instructions before intracellular staining with rabbit anti-mouse

MetEnk (bs-1759R, Bioss USA, Woburn, MA; 1:200) or rabbit anti-mouse IgG (Isotype control, Bioss USA; 1:200) followed by staining with goat anti-rabbit PE (sc-3739, 1:400; Santa Cruz Biotechnology, Dallas, TX). All intracellular stains were performed in 1X Permeabilization Buffer (PB, eBioscience) for 45 min on ice. After each intracellular stain, cells were washed 3 times in 250 µL 1X PB with centrifugation at 500 *x* g for 5 minutes at 4 °C between washes. Recovered cells after the final wash were resuspended in 200 µL FACS Buffer before flow cytometric analyses.

3.3.8 Flow cytometry

For all flow cytometry analyses, stained cells were acquired on a BD LSRII flow cytometer (BD Biosciences). The entirety of each sample was acquired to obtain total cell counts, which were subsequently normalized to tissue weight. Flow cytometry data were analyzed using FlowJo software version 9.6.4 (Tree Star, Inc.).

3.3.9 Sort-purification and transfer of ILC2s

E-WAT was harvested from male CD45.1$^+$ C57BL/6 mice that received daily injections of rmIL-33 (12.5 µg/kg) for 7 days by intraperitoneal injection. The stromal vascular fraction (SVF) was isolated as described above, and Live CD45$^+$ Lin$^-$ CD25$^+$ IL-33R$^+$ ILC2s were sort-purified using an Aria Cell Sorter (BD) to ≥98% purity. The lineage cocktail for sorts included CD3, CD5, CD19,

NK1.1, CD11c, CD11b, FcεRIα and SiglecF. CD45.1$^+$ ILC2s (10^5) were immediately transferred to the indicated recipient mice by intraperitoneal injection (5 x 10^4 cells) and by subcutaneous injection near iWAT (5 x 10^4 cells split evenly for bilateral injections). Daily transfers were performed for 4 consecutive days, and tissues were harvested on day 5. In ILC2 reconstitution experiments involving *Rag2*$^{-/-}$ *γc*$^{-/-}$ recipient mice, 10^5 CD45.1$^+$ ILC2s were transferred by a single intraperitoneal injection, and the next day mice were treated with PBS or rmIL-33 (12.5 μg/kg) by daily intraperitoneal injection for 7 days. In ILC2 transfer experiments involving recipient mice on a Balb/c background (*Db*l*Gata1* or *Il4ra*$^{-/-}$), donor ILC2s were sort-purified as described above from E-WAT of Balb/c mice that received daily injections of rmIL-33 (12.5 μg/kg) daily for 5-7 days by intraperitoneal injection. Balb/c ILC2s (10^5) were immediately transferred to the indicated recipient mice by intraperitoneal injection (5 x 10^4 cells) and by subcutaneous injection near iWAT (5 x 10^4 cells split evenly for bilateral injections). Daily transfers were performed for 4 consecutive days, and tissues were harvested on day 5.

3.3.10 Histologic analysis

Tissues were fixed in 4% paraformaldehyde in PBS for at least 48 hours at 4°C and embedded in paraffin before cutting 5 μm sections and staining with hematoxylin and eosin (H&E) or performing immunohistochemistry (IHC) with rabbit anti-UCP1 antibody (Abcam, ab10983). For IHC, rehydrated sections

were microwaved in 10 mM citric acid buffer (pH 6.0) for antigen retrieval, and endogenous peroxidases were quenched with 3% hydrogen peroxide. Sections were blocked with Avidin D, biotin and protein blocking agent in sequential order followed by application of the anti-UCP1 antibody (1:500). A biotinylated anti-rabbit antibody was used as a secondary antibody. Horseradish peroxidase-conjugated ABC reagent was applied, and then DAB reagent was used to develop the signal before counterstaining in hematoxylin and dehydrating the sections in preparation for mounting. Stained sections were visualized and photographed using a Nikon E600 brightfield microscope.

3.3.11 Real-time PCR

Adipose tissues were snap-frozen in 1.0 mL TRIzol (Invitrogen) and homogenized using a Tissue Lyser (Qiagen) with a 5mm RNase-free metal bead (Qiagen). Homogenates were centrifuged at 10,000 x *g* for 15 min at room temperature, and 700 µL of the TRIzol interphase was collected to exclude the top lipid phase and cellular debris and genomic DNA in the pellet. Chloroform (200 µL; Fisher Scientific) was added to the lipid-extracted TRIzol fraction and shaken vigorously for 15 seconds before benchtop incubation at room temperature for 2-3 min. Samples were centrifuged at 10,000 x *g* for 15 min at room temperature, and the top aqueous phase was collected (250 µL) into tubes containing 500 µL isopropanol (Sigma Aldrich) to precipitate the RNA. Samples were mixed gently by vortexing on setting 4 (of 10) for 3-5 seconds and allowed

to incubate at room temperature for 10 min. Samples were then applied to RNeasy Mini columns (Qiagen), and RNA was purified and isolated in accordance with the manufacturer's instructions. Purified total RNA samples were eluted in 30-50 µL RNase-free water (Qiagen), and total RNA concentrations were determined using a Nanodrop 2000c (Thermo Scientific, Wilmington, DE).

cDNA was synthesized in 20 µL reactions from 1.0 µg aliquots of RNA using Superscript II Reverse Transcriptase (Invitrogen) and oligo(dT) (Invitrogen) according to manufacturer's instructions. cDNA was diluted with 180 µL nuclease-free water (Promega) before used. Real-time PCR was performed using 10 µL reactions consisting of 5 µL Power SYBR Green 2X Master Mix (Applied Biosystems), 3 µL nuclease-free water (Promega or Qiagen), 1 µL diluted cDNA and 1 µL primers (1 µM). Previously published primer sequences for murine *Ucp1*[17] and Qiagen Quantitect real-time PCR primers for *β-actin, Il33, Penk, Oprd1 and Ogfr*. Reactions were performed in duplicate or triplicate using the 7500 Fast Real-Time PCR System (Applied Biosystems) or the QuantStudio 6 Flex Real-Time PCR System (Applied Biosystems). C^T values were normalized to the endogenous housekeeping gene *β-actin*. The $\Delta\Delta C^T$ method was employed for all real-time PCR analyses with expression levels for each sample expressed relative to the average gene expression level of the indicated control group.

3.3.12 Microarrays and ILC2 vs ILC3 gene enrichment analyses

Microarray analyses (~25,000 genes) were performed using previously published microarray datasets (GEO GSE46468) (Monticelli et al., 2011). In brief, Lin^- $CD90^+$ $CD25^+$ $IL\text{-}33R^+$ ILC2s from the lung (4 biological replicates each comprising 6 pooled lungs) and Lin^- $CD90^+$ $CD25^+$ $CD4^+$ ILC3s from the spleen (4 biological replicates each comprising 10 pooled spleens) were sorted using a FACS Aria (BD) directly into TRIzol LS (Invitrogen) at a purity of >97% (1.5-2.0 x 10^4 cells/replicate). mRNA was isolated, amplified, labeled and hybridized to Affymetrix GeneChip (Mouse Gene 1.0 ST) as described previously (Monticelli et al., 2011). Gene expression Z-scores were calculated for each of 69 obesity-associated genes in ILC2s or ILC3s (see Table 2 for a complete list of genes). First, the average and standard deviation of all microarray probe intensities were calculated for each cell type. The average probe intensity of the array was subtracted from average probe intensity of each of the 69 obesity-associated genes. The difference in average probe intensities (single gene minus array) was divided by the array standard deviation to calculate the Z-score. Genes that were significantly enriched compared to the average gene expression level of the entire microarray dataset in one cell population but not the other ($Z > +2.20$) were considered to be differentially enriched in that cell population. The Bonferroni correction was used to determine the level of significance with 69 comparisons to

account for multiple testing (α=0.05; k=69). The Bonferroni-corrected P-value for level of significance was P = 0.014, which corresponds to a Z-score of ±2.20.

3.3.13 Primary adipocyte culture

iWAT or BAT was dissected from 4 week-old C57BL/6 mice (n=5 per experiment, pooled) and digested as described above. Stromal vascular fraction (SVF) cells were plated in 12-well CellBind plates, and adherent cells were grown to confluence. Cells were differentiated into adipocytes as previously described (Seale et al., 2011). Briefly, cells were cultured for 2 days with 850 nM insulin, 1 nM T_3, 1 μM rosiglitazone, 125 nM indomethacin (125 μM for BAT primary adipocytes), 0.5 mM isobutylmethylxanthine (IBMX) and 1 μM dexamethasone in adipocyte culture media (DMEM:F12 [50:50] supplemented with 10% heat-inactivated FBS, penicillin, streptomycin and L-glutamine). Cells were then maintained in adipocyte culture media supplemented with 850 nM insulin and 1 nM T3 with either PBS or 50 μM MetEnk for 6 days, with fresh media replacement every 2 days. Cells were harvested on day 8 in TRIzol.

3.3.14 Statistical analyses

All data are expressed as mean ± standard error of the mean (SEM), except some human subject data that are expressed as proportions. Statistical significance was determined using the two-tailed Student's *t* test or a one-way or

two-way analysis of variance (ANOVA) followed by Sidak or Tukey post-hoc tests. If variance differed between groups, the appropriate statistical correction was applies (e.g. Welch's correction). Correlation analyses were conducted using Pearson linear regression. Proportions among human samples were compared by χ^2 tests. Significance was set at $P<0.05$ except for microarray analyses, in which case the Bonferroni correction was applied to account for multiple testing ($\alpha=0.05$, $k=69$), resulting in a level of significance of $P<0.014$. Statistical analyses were performed with Prism 6 (GraphPad Software, Inc.) or SPSS Statistics version 22 (IBM).

3.4 Results

3.4.1 IL-33 regulates beiging of white adipose tissue

Given the thermogenic properties of beige and brown adipocytes (Harms and Seale, 2013; Pfeifer and Hoffmann, 2014; Rosen and Spiegelman, 2014; Wu et al., 2013), we tested whether IL-33 treatment regulates the morphology or *Ucp1* expression levels in WAT and BAT. In PBS-treated controls, E-WAT and iWAT from PBS-treated mice exhibited predominantly unilocular white adipocytes, and iWAT had interspersed paucilocular beige adipocytes that are characterized morphologically by multiple small lipid droplets and increased $UCP1^+$ cytoplasm (Fig 19a). Mice receiving rmIL-33 exhibited increased $UCP1^+$ beige adipocytes in E-WAT and iWAT compared to PBS-treated controls (Fig. 19a). In addition, expression levels of *Ucp1* in E-WAT and iWAT were significantly increased in

mice treated with rmIL-33 compared to controls (Fig. 19b). These results suggest that IL-33 can promote beiging of WAT. rmIL-33 also resulted in increased frequencies (Fig. 20a) and numbers (Fig. 20b) of Lin^- $CD25^+$ IL-$33R^+$ ILC2s in BAT. However, in contrast to WAT, BAT from rmIL-33-treated mice exhibited decreased *Ucp1* expression (Fig. 20c) without apparent morphologic changes to brown adipocytes (Fig. 20d,e). Taken together, these results indicate that the stimulatory effect of rmIL-33 treatment on UCP1 expression was selective to WAT but not BAT.

To further test whether IL-33 regulates beiging, we examined WAT morphology and *Ucp1* expression levels of $Il33^{+/+}$ versus $Il33^{-/-}$ mice that had been fed a 10% fat diet for 12 weeks. iWAT from $Il33^{+/+}$ mice was predominantly comprised of white adipocytes with interspersed $UCP1^+$ beige adipocytes (Fig. 21a), whereas iWAT from $Il33^{-/-}$ mice had few beige adipocytes (Fig. 21b). Consistent with this, *Ucp1* expression was significantly lower in iWAT of $Il33^{-/-}$ mice compared to $Il33^{+/+}$ controls (Fig. 21c). These findings indicate that endogenous IL-33 is a critical regulator of beiging.

3.4.2 IL-33-elicited ILC2s are sufficient to drive beiging of white adipose tissue

To test whether IL-33-elicited ILC2s can promote beiging, congenically marked $CD45.1^+$ ILC2s from E-WAT of IL-33-treated donor mice were sort-purified and

adoptively transferred into wildtype CD45.2^{+} recipient mice (Fig. 22a). CD45.1^{+} donor ILC2s could be identified in iWAT of mice that received ILC2s but not control mice that received PBS (Fig. 22b), and total ILC2 numbers were significantly increased in iWAT of mice receiving CD45.1^{+} ILC2s compared to controls (Fig. 22c). Transferred ILC2s could also be identified in E-WAT but were not found in BAT, mesenteric lymph nodes or lung (Fig. 23), demonstrating selective accumulation of WAT-derived ILC2s in WAT of recipient mice. Mice that received ILC2s had increased UCP1^{+} beige adipocytes (Fig. 22d) and augmented expression of *Ucp1* (Fig. 22e) in iWAT compared to controls. In addition, iWAT from mice that received ILC2s had elevated oxygen consumption (Fig. 22f) in iWAT. Collectively, these results indicate that activated ILC2s can promote beiging in wildtype mice.

ILC2s have been shown to regulate both T and B cell responses (Halim et al., 2014; Mirchandani et al., 2014; Moro et al., 2010; Oliphant et al., 2014), and IL-33 treatment is associated with increased regulatory T cells (T_{reg}) responses in mice (Schiering et al., 2014), a cell population previously implicated in regulation of metabolic homeostasis in obese mice (Cipolletta et al., 2012; Zhong et al., 2014) (Feuerer et al., 2009). Therefore we sought to test whether transferring IL-33-elicited ILC2s could promote beiging in the absence of an adaptive immune system. CD45.1^{+} donor ILC2s could be identified in iWAT of CD45.2^{+} *Rag1*$^{-/-}$ recipients that received ILC2s (Fig. 24a), and this was associated with increased

ILC2 numbers in iWAT compared to controls (Fig. 24b). Similar to wildtype recipients, *Rag1*$^{-/-}$ hosts demonstrated increased UCP1^{+} beige adipocytes (Fig. 24c) and upregulated expression of *Ucp1* in iWAT (Fig. 24d) following ILC2 transfer. These data indicate that IL-33-elicited ILC2s are sufficient to promote beiging in the absence of the adaptive immune system.

3.4.3 IL-33 may promote beiging in an ILC2-dependent manner

The findings that IL-33 treatment and ILC2 transfer could promote beiging of WAT provoked the hypothesis IL-33 promotes beiging in an ILC2-dependent manner. To test this, we first sort-purified ILC2s from IL-33-treated CD45.1+ mice and reconstituted *Rag2*$^{-/-}$ *γc*$^{-/-}$ mice with ILC2s by a single adoptive transfer by intraperitoneal injection. The next day, ILC2-sufficient *Rag2*$^{-/-}$ mice, ILC2-deficient *Rag2*$^{-/-}$ *γc*$^{-/-}$ mice and ILC2-reconstituted *Rag2*$^{-/-}$ *γc*$^{-/-}$ mice were treated with PBS or rmIL-33 daily for 7 days (Fig. 25a). Following IL-33 treatment, ILC2-sufficient *Rag2*$^{-/-}$ control mice but not ILC2-deficient *Rag2*$^{-/-}$ *γc*$^{-/-}$ mice demonstrated population expansion of E-WAT ILC2s (Fig. 25b,c). Furthermore, *Rag2*$^{-/-}$ *γc*$^{-/-}$ mice supported accumulation and IL-33-induced population expansion of donor ILC2s in host E-WAT (Fig. 25b,c). IL-33 treatment increased expression of *Ucp1* in E-WAT of ILC2-sufficient *Rag2*$^{-/-}$ mice but not ILC2-deficient *Rag2*$^{-/-}$ *γc*$^{-/-}$ mice treated with rmIL-33 (Fig. 25d). Strikingly, IL-33-induced increases in expression of *Ucp1* and beiging were restored in ILC2-reconstituted *Rag2*$^{-/-}$ *γc*$^{-/-}$ mice (Fig. 25d,e). Collectively, these results indicate

that IL-33-induced beiging of WAT requires a γ_c-dependent cell population and that ILC2s are sufficient to rescue this defect, suggesting that IL-33-induced beiging is critically dependent on ILC2s.

3.4.4 IL-33 and ILC2s can elicit beiging independently of eosinophils and the IL-4 receptor

In addition to regulating adaptive immune cell responses, ILC2s are known to promote eosinophil and alternatively-activated macrophage (AAMac) responses in multiple tissue compartments including WAT(Molofsky et al., 2013; Wu et al., 2011). Recent studies indicate that eosinophils and IL-4Rα-dependent AAMac responses are critical for beiging in the context of chronic exposure to cold environmental temperatures (Qiu et al., 2014). We therefore tested whether IL-33 or ILC2s could elicit beiging of WAT independently of eosinophils or IL-4Rα. At steady state, $UCP1^+$ beige adipocytes could be identified in iWAT of Balb/c (wildtype), *DblGata1* mice (that lack eosinophils) and *Il4ra*$^{-/-}$ mice (that have dysregulated AAMac responses), and rmIL-33 treatment was associated with elevated ILC2 responses in iWAT and increased $UCP1^+$ beige adipocytes in each of these strains (Fig. 26a-f). Further, adoptive transfer of IL-33-elicited ILC2s was sufficient to promote beiging in *DblGata1* and *Il4ra*$^{-/-}$ mice (Fig. 27a-d). Eosinophils are reported to be increased in iWAT from mice exposed to cold environmental conditions (Qiu et al., 2014; Rao et al., 2014), and ILC2s control eosinophils responses in multiple tissues including WAT (Molofsky et al., 2013;

Nussbaum et al., 2013). However, exposure of C57BL/6 mice to 4 °C temperatures for 72 hours resulted in upregulation of *Ucp1* expression (Fig. 28a) without altering the numbers of ILC2s (Fig. 28b) or expression of *Il33* (Fig. 28c) in iWAT or BAT. Thus, while eosinophils and AAMacs may contribute to optimal beiging under some physiologic settings such as chronic exposure to severe cold environmental temperatures (Qiu et al., 2014; Rao et al., 2014), these data indicate that the IL33/ILC2 axis can promote beiging independently of the eosinophil/IL-4Rα/AAMac pathway and may be associated with beiging in other physiologic contexts.

3.4.5 ILC2s express methionine-enkephalin peptides that are upregulated by IL-33 treatment

Obesity is associated with both decreased ILC2s (Chapter 2) and defective beige adipocytes (Carey et al., 2013; Cohen et al., 2014; Molofsky et al., 2013; Saito et al., 2009). To address whether ILC2s produce obesity-associated factors that could regulate beiging, we employed genome-wide transcriptional profiling of ILC2s versus group 3 ILCs (ILC3s), a related innate immune cell population (Constantinides et al., 2014; Diefenbach et al., 2014; Monticelli et al., 2012; Spits and Cupedo, 2012), to compare gene expression enrichment scores of 69 genes previously linked to human obesity (Fig. 29a and Table 2) (McCarthy, 2010; Walley et al., 2009). This analysis identified that one gene, proprotein convertase subtilisin/kexin type 1 (*Pcsk1*) (also known as prohormone

convertase 1 [*Pc1*]), was significantly enriched in ILC2s but not ILC3s (Fig. 29b, P<0.01). PCSK1 is an endopeptidase involved in processing some prohormones into active forms (Seidah, 2011; Seidah et al., 2013), and loss-of-function mutations in both mice and humans are associated with increased susceptibility to obesity (Benzinou et al., 2008; Creemers et al., 2012; Lloyd et al., 2006) in association with decreased caloric expenditure (Lloyd et al., 2006). Of the prohormones known to be processed by PCSK1, the most differentially expressed in ILC2s compared to ILC3s was Proenkephalin A (*Penk*) (Fig. 29c), which encodes endogenous opioid-like peptides such as methionine-enkephalin (MetEnk, also known as opioid growth factor [OGF]). Production of MetEnk by ILC2s was confirmed by flow cytometric analysis of sort-purified ILC2s re-stimulated with IL-2 and IL-7 (Fig. 29d). Following IL-33 stimulation of sort-purified ILC2s, production of MetEnk peptides on a per-cell basis was increased (Fig. 29e). Together, these findings demonstrate that ILC2s express Proenkephalin A and its processing machinery to produce enkephalin peptides.

3.4.6 Methionine-enkephalin appears to have tissue-specific effects on white versus brown adipose tissue

Tissue-level gene expression analyses in wildtype mice at steady state indicated that *Il33* and *Penk* expression levels were increased in iWAT compared to BAT (Fig. 30a), and *Il33* and *Penk* expression levels were correlated in iWAT but not BAT of naïve C57BL/6 mice (Fig. 30b). In addition, expression of the MetEnk

receptor δ1 opioid receptor (*Oprd1*) was higher in iWAT compared to BAT, whereas expression of the other known MetEnk receptor opioid growth factor receptor (*Ogfr*) was lower in iWAT compared to BAT (Fig. 30c). Together, these gene expression analyses suggest that there may be tissue-specific regulation of the IL-33/PENK/MetEnk receptor pathways in iWAT compared to BAT. These data also suggest that there might be tissue-specific of effects of MetEnk in iWAT compared to BAT. Consistent with this, MetEnk stimulation of cultured primary adipocytes from iWAT (Fig. 31a), but not cultured primary adipocytes from BAT (Fig. 31b), induced *Ucp1* expression. This suggests that MetEnk has a stimulatory effect on the expression of *Ucp1* in adipocytes from iWAT but not BAT.

3.4.7 Methionine-enkephalin administration is associated with increased beiging of white adipose tissue *in vivo*

To test whether MetEnk can promote beiging in *in vivo*, MetEnk peptides (amino acid sequence YGGFM) were delivered by subcutaneous injection into wild-type mice. MetEnk treatment was associated with elicitation of $UCP1^{+}$ beige (Fig. 32a) and upregulated expression of *Ucp1* in iWAT (Fig. 32b). These changes were associated with increased iWAT oxygen consumption (Fig. 32c), collectively indicating the formation of functional beige fat. Consistent with this, MetEnk treatment was also associated with decreased iWAT mass (Fig. 32d). These

changes were not associated with increased expression of *Il-4* or *Il-13* (Fig. 32e) or with altered eosinophil or AAMac numbers (Fig. 32f) in iWAT.

3.5 Discussion

In this Chapter, we demonstrate that IL-33 is a critical regulator of beiging of WAT. IL-33-induced beiging was mediated by ILC2s, and IL-33-elicited ILC2s were sufficient to drive the formation of functional beige fat in wildtype mice. In addition, IL-33 and ILC2s could elicit beiging in mice that lack an adaptive immune system, eosinophils or IL-4Rα signaling. This suggests that the IL-33/ILC2 axis has the capacity to promote beiging of WAT independent of T cells and the eosinophil/IL-4Rα/AAMac/norepinephrine pathway. Employing analyses of obesity-associated genes, we identify that ILC2s produce the previously unappreciated effector molecule MetEnk. Finally, we demonstrate that MetEnk can drive beiging *in vivo* and upregulate Ucp1 expression levels in primary adipocytes from iWAT.

Previous studies indicate that the immune system can have an important role in the generation of beige adipose. Specifically, eosinophils are suggested to be activated and produce IL-4 in iWAT of mice exposed to cold environmental temperatures (Qiu et al., 2014). This leads to IL-4/IL-4Rα-dependent stimulation of AAMacs in iWAT to produce norepinephrine and possibly other catecholamines that elicit beiging and increase the metabolic rate of mice (Qiu et

al., 2014). Meteorin-like (Metrnl) is a hormone produced by adipose and muscle tissue and elicits beiging in iWAT by inducing local eosinophil accumulation and AAMac activation (Rao et al., 2014). Mice that lack eosinophils (*dblGata1* mutant mice) or IL-4/IL-13-dependent signaling (*Il4/13*$^{-/-}$ mice) have impaired *Ucp1* upregulation following cold exposure (Qiu et al., 2014), and administration of exogenous Meteorin-like produces attenuated beiging in *dblGata1* or STAT6-deficient mice that have defective AAMacs (Rao et al., 2014). However, cold exposure and exogenous Meteorin-like can elicit beiging in these strains albeit in a less efficient manner (Qiu et al., 2014; Rao et al., 2014). This provokes the hypothesis that there are other pathways beyond the eosinophil/IL-4Rα/AAMac/norepinephrine pathway that can contribute to beiging in mice. Consistent with this, we observe that IL-33 treatment or adoptive transfer of IL-33-elicited ILC2s form E-WAT is sufficient to drive beiging of iWAT in wildtype mice as well as *dblGata1* mice that lack eosinophils and IL-4Rα-deficient mice that have dysregulated AAMacs. Although it is likely that eosinophils and AAMacs contribute to optimal beiging in some physiologic contexts such as cold exposure (Qiu et al., 2014; Rao et al., 2014), the data presented in this Chapter indicate that the IL-33/ILC2 axis can elicit beiging independently of these pathways.

Supporting this, we identified that ILC2s produce the pentapeptide MetEnk and reveal a previously unappreciated role for MetEnk in stimulation of beiging *in*

vivo. Delivery of MetEnk peptides to mice elicited beiging of WAT without affecting the numbers of eosinophils or AAMacs, suggesting that the IL-33/ILC2/MetEnk pathway might elicit beiging independently of these cell types. Consistent with this, treatment of primary adipocytes from iWAT with MetEnk increased *Ucp1* expression levels, indicating a direct stimulatory effect of MetEnk on adipocytes. Recent studies suggest that there are multiple developmental pathways to beige adipocytes, including differentiation form a bipotent white/beige pre-adipocyte (Lee et al., 2012) and transdifferentiation of mature white adipocytes to beige adipocytes (Barbatelli et al., 2010; Rosenwald et al., 2013). Future studies will be required to investigate the mechanisms through which MetEnk elicits beiging.

MetEnk has previously been to be produced by neurons to limit anxiety, pain and aggression levels in mice (Konig et al., 1996) and to promote conditioned learning and addiction in mice (Tseng et al., 2013). In addition to these neuronal processes, MetEnk was shown to act directly on adipocytes to stimulate lipolysis (Nencini and Paroli, 1981), indicating that this neuronal-associated peptide also has metabolic effects. Importantly, lipolysis is critical for the maintenance of beige adipocyte function (Dong et al., 2013; Mottillo et al., 2012; Nguyen et al., 2011). Further, UCP1 functions as a long-chain fatty acid-proton symporter and employs long-chain fatty acids for efficient uncoupling (Fedorenko et al., 2012). Thus, while MetEnk upregulates *Ucp1* transcript levels in adipocytes, the lipolytic

effects of MetEnk may also contribute to beiging and the regulation of beige adipocyte function.

MetEnk peptides are derived from Proenkephalin A (PENK) via PCSK1-dependent processing (Seidah, 2011; Seidah et al., 2013). Single nucleotide polymorphisms in PCSK1 have been previously linked to the development of obesity in humans (Benzinou et al., 2008; Creemers et al., 2012; Lloyd et al., 2006), and this has been associated with PCSK1 effects on both food intake and energy storage (Lloyd et al., 2006). Obesity has also been associated with decreased beige fat activation in humans (Carey et al., 2013; Saito et al., 2009), and murine studies demonstrate that defective beige fat leads to increased susceptibility to obesity (Cohen et al., 2014). The previous Chapter indicated that decreased ILC2 responses in WAT are a conserved feature of obesity in mice and humans and suggested the IL-33/ILC2 pathway may be dysregulated in obese WAT. In light of these findings, the data in the present Chapter suggest that PCSK1 mutations might affect weight gain through regulation of the PENK/MetEnk/beiging pathway.

Collectively, the data in this Chapter provide the first demonstration that the IL-33/ILC2 axis regulates metabolic homeostasis by eliciting beiging of WAT. Production of enkephalin peptides is a previously unrecognized effector mechanism employed by ILC2s to regulate metabolic homeostasis. From an

evolutionary perspective, coupling ILC2-dependent innate immune effector functions with the maintenance of systemic metabolic homeostasis could provide a rapid, integrated multi-organ response that allows mammals to surmount multiple environmental challenges including infection, nutrient stress or changes in temperature. Given that impaired UCP1 and beige adipocyte function is associated with increased weight gain and obesity in mice (Cohen et al., 2014; Feldmann et al., 2009) and that activity of brown/beige (Sharp et al., 2012; Wu et al., 2012) adipose tissue is dysregulated in obese patients (Carey et al., 2013; Saito et al., 2009), targeting the IL-33/ILC2/beiging pathway could represent a new approach for treating obesity and obesity-associated diseases.

3.6 Tables and Figures

Table 2. List of genes with single nucleotide polymorphisms associated with human obesity

Human gene symbol	Human gene name	Murine ortholog gene symbol	Inclusion in Microarray
ADAMTS9	A disintegrin-like and metallopeptidase (reprolysin type) with thrombospondin type 1 motif, 9	*Adamts9*	Yes
BCDIN3D	BCDIN3 domain containing	*Bcdin3d*	Yes
BDNF	Brain-derived neurotrophic factor	*Bdnf*	Yes
CADM2	Cell adhesion molecule 2	*Cadm2*	Yes
CNR1	Cannabinoid type 1 receptor	*Cnr1*	Yes
CPEB4	Cytoplasmic polyadenylation element binding protein 4	*Cpeb4*	Yes
CTNNBL1	Catenin, beta like 1	*Ctnnbl1*	Yes
DLK1	Delta-like homologue 1	*Dlk1*	Yes
ENPP1	Ectonucleotide pyrophasphatase/phosphodiesterase 1	*Enpp1*	Yes
ETV5	Ets variant 5	*Etv5*	Yes
FAIM2	Fas apoptotic inhibitory molecule 2	*Faim2*	Yes
FANCL	Fanconi anemia, complementation group L	*Fancl*	Yes
FTO	fat mass and obesity associated	*Fto*	Yes
GHSR	Growth hormone receptor secretogogue receptor	*Ghsr*	Yes
GIPR	Gastric inhibitory polypeptide receptor	*Gipr*	Yes
GNPDA2	Glucosamine-6-phosphate deaminase 2	*Gnpda2*	Yes
GPRC5B	G protein-coupled receptor, family C, group 5, member B	*Gprc5b*	Yes
GRB14	Growth factor receptor-bound protein 14	*Grb14*	Yes
HMGA1	High mobility group AT-hook 1	*Hmga1*	Yes
HMGCR	3-hydroxy-3-methylglutaryl-CoA reductase	*Hmgcr*	Yes
HOXC13	Homeobox C13	*Hoxc13*	Yes
ITPR2	Inositol 1,4,5-trisphosphate receptor, type 2	*Itpr2*	Yes

KCTD15	Potassium channel tetramerization domain containing 15	*Kctd15*	Yes	
KLF7	Kruppel-like factor 7	*Klf7*	Yes	
LEP	Leptin	*Lep*	Yes	
LEPR	Leptin receptor	*Lepr*	Yes	
LMNA	Lamin A/C	*Lmna*	Yes	
LRP1B	Low density lipoprotein receptor-related protein 1B	*Lrp1b*	Yes	
LINGO2 (LRRN6C)	Leucine rich repeat and Ig domain containing 2	*Lingo2*	Yes	
LY86	Lymphocyte antigen 86	*Ly86*	Yes	
LYPLAL1	Lysophospholipase-like 1	*Lyplal1*	Yes	
MAF	v-maf avian musculoaponeurotic fibrosarcoma oncogene homolog	*Maf*	Yes	
MAP2K5	Mitogen-activated protein kinase kinase 5	*Map2k5*	Yes	
MC4R	Melanocortin 4 receptor	*Mc4r*	Yes	
MSRA	Methionine sulfoxide reductase A	*Msra*	Yes	
MTCH2	Mitochondrial carrier 2	*Mtch2*	Yes	
MTIF3	Mitochondrial translational initiation factor 3	*Mtif3*	Yes	
MTMR9	Myotubularin related protein 9	*Mtmr9*	Yes	
NAMPT	Nicotinamide phosphoribosyltransferase	*Nampt*	Yes	
NCR3	Natural cytotoxicity triggering receptor 3	*Ncr3*		No
NEGR1	Neuronal growth regulator 1	*Negr1*	Yes	
NFE2L3	Nuclear factor, erythroid 2-like 3	*Nfe2l3*	Yes	
NPC1	Niemann-Pick disease, type C1	*Npc1*	Yes	
NPY2R	Neuropeptide Y receptor Y2	*Npy2r*	Yes	
NRXN3	Neurexin 3	*Nrxn3*	Yes	
PCSK1	Proprotein convertase subtilisin/kexin type 1	*Pcsk1*	Yes	
PIGC	Phosphatidylinositol glycan anchor biosynthesis, class C	*Pigc*	Yes	
POMC	Proopiomelanocortin	*Pomc*	Yes	
PRKD1	Protein kinase D1	*Prkd1*	Yes	
PRL	Prolactin	*Prl*	Yes	
PTBP2	Polypyrimidine tract binding protein 2	*Ptbp2*	Yes	
PTER	Phosphotriesterase related	*Pter*	Yes	
RSPO3	R-spondin 3	*Rspo3*	Yes	
SDCCAG8	Serologically defined colon cancer antigen 8	*Sdccag8*	Yes	
SEC16B	SEC16 Homolog B	*Sec16b*	Yes	

SH2B1	SH2B adaptor protein 1	*Sh2b1*	Yes	
SLC39A8	Solute carrier family 39 (zinc transporter), member 8	*Slc39a8*	Yes	
SNRPN	Small nuclear ribonucleoprotein polypeptide N	*Snrpn*	Yes	
SOCS1	Suppressor of cytokine signaling 1	*Socs1*	Yes	
SOCS3	Suppressor of cytokine signaling 3	*Socs3*	Yes	
STAB1	Stabilin 1	*Stab1*	Yes	
TBC1D1	TBC1 (tre-2/USP6, BUB2, cdc16) domain family, member 1	*Tbc1d1*	Yes	
TBX15	T-box 15	*Tbx15*	Yes	
TFAP2B	Transcription factor AP-2 beta (activating enhancer binding protein 2 beta)	*Tfap2b*		No
TMEM160	Transmembrane protein 160	*Tmem160*	Yes	
TMEM18	Transmembrane protein 18	*Tmem18*	Yes	
TNNI3K	TNNI3 interacting kinase	*Tnni3k*	Yes	
TUB	Tubby bipartite transcription factor	*Tub*	Yes	
VEGFA	Vascular endothelial growth factor A	*Vegfa*	Yes	
ZNF608	Zinc finger protein 608	*Zfp608*	Yes	
ZNRF3	Zinc and ring finger 3	*Znrf3*	Yes	

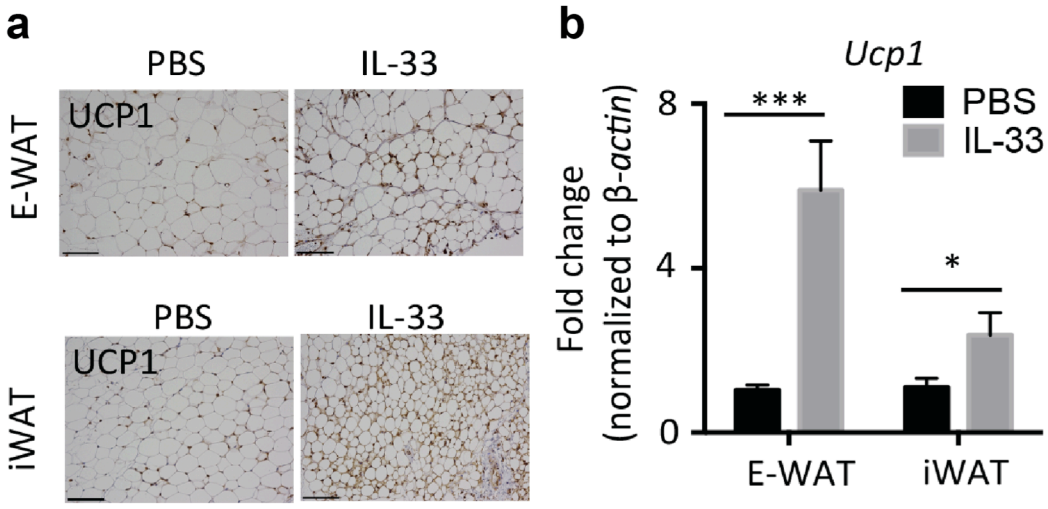

Figure 19. Administration of recombinant murine IL-33 is associated with increased beiging of white adipose tissue (WAT). Wildtype C57BL/6 mice were treated with PBS or recombinant murine IL-33 (12.5 µg/kg/day) by intraperitoneal injection for 7 days. **(a)** Epididymal (E)-WAT and inguinal (i)WAT Uncoupling protein 1 (UCP1) immunohistochemistry. Scale bars, 100 µm. **(b)** *Ucp1* transcript levels in E-WAT and iWAT. Student's t-test, *P<0.05, ***P<0.001.

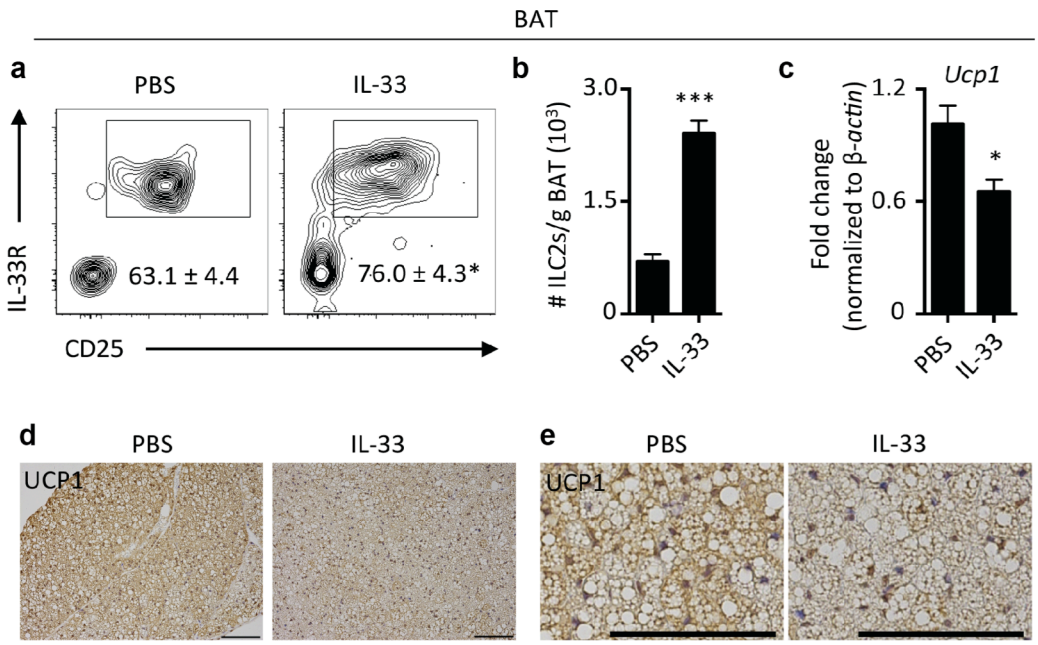

Figure 20. Brown adipose tissue (BAT) contains Lin$^-$ CD25$^+$ IL-33R$^+$ ILC2s that expand in response to IL-33 in association with decreased *Ucp1* expression. C57BL/6 male mice (10 weeks old) were treated with PBS (n=8) or IL-33 (12.5 µg/kg, n=8) daily by intraperitoneal injection for 7 days. **(a)** Representative plots and frequencies of Lin$^-$ CD25$^+$ IL-33R$^+$ ILC2s in interscapular BAT. Gated on live CD45$^+$ Lin$^-$ cells. **(b)** Numbers of ILC2s per gram of BAT. **(c)** *Ucp1* expression in BAT by real-time PCR. **(d)** Uncoupling protein 1 (UCP1) immunohistochemistry of BAT at 10X magnification. Scale bars, 100 µm. **(e)** 40X magnification of panel d. Scale bars, 100 µm. Student's t-test, *<0.05, ***P<0.001.

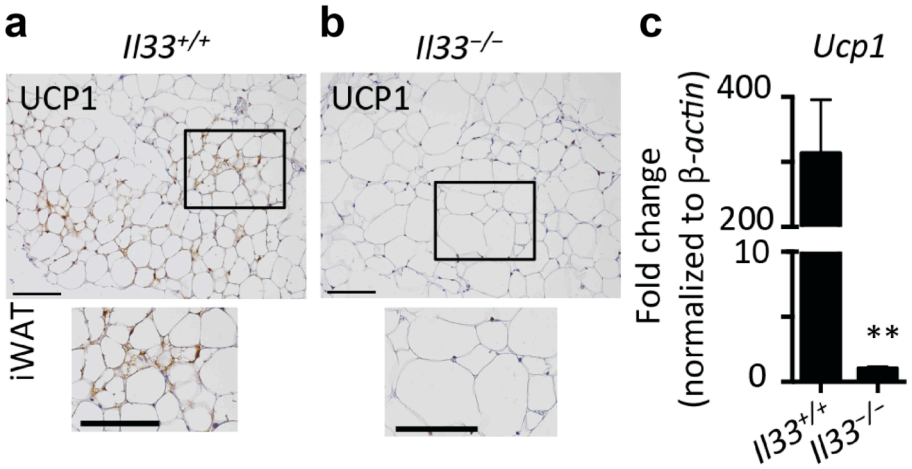

Figure 21. IL-33-deficient mice exhibit defective beiging of white adipose tissue (WAT). (a-c) *Il33*$^{+/+}$ (n=6) or *Il33*$^{-/-}$ (n=5) mice were fed a low fat diet (10% kcal fat) for 12 weeks starting at age 7 weeks. Uncoupling protein 1 (UCP1) immunohistochemistry (IHC) in inguinal (i)WAT from **(a)** *Il33*$^{+/+}$ or **(b)** *Il33*$^{-/-}$ mice. Scale bars, 100 μm. **(c)** *Ucp1* transcript levels in iWAT.

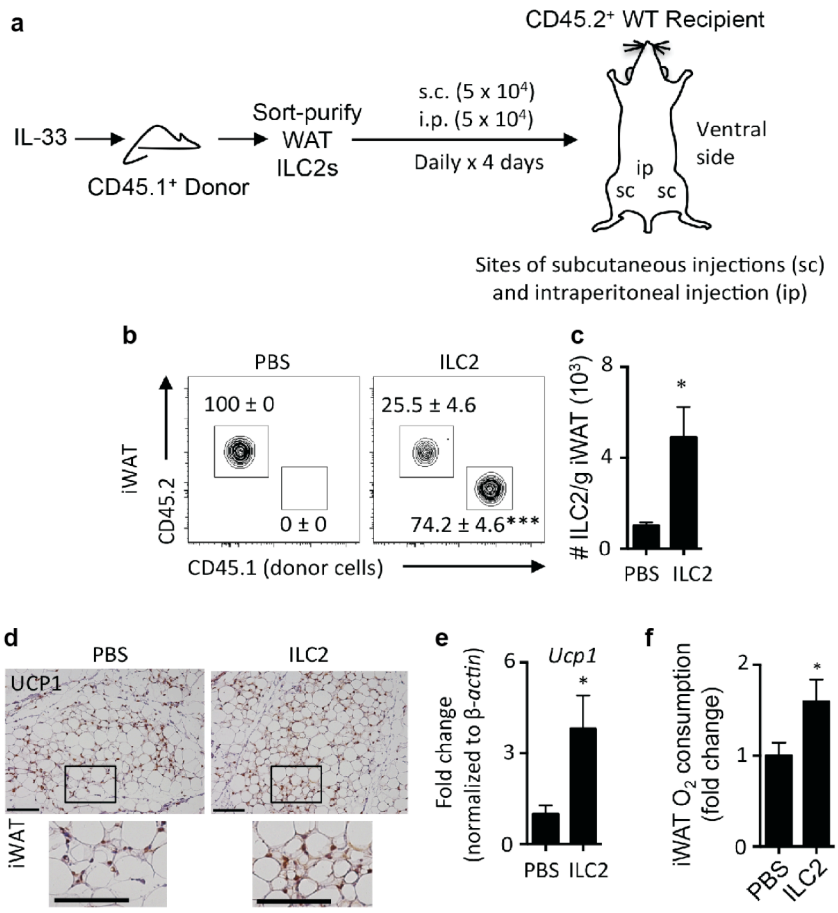

Figure 22. Adoptive transfer of IL-33-elicited ILC2s is sufficient to drive beiging. **(a)** Experimental design for panels **b-f**. Live CD45$^+$ Lin$^-$ CD25$^+$ IL-33R$^+$ ILC2s were sort-purified from E-WAT of CD45.1$^+$ mice treated with 12.5 µg/kg recombinant murine (rm)IL-33 daily for 7 days by intraperitoneal injection. ILC2s (1 x 10^5 total) were transferred to CD45.2$^+$ recipient mice daily for 4 days by subcutaneous injection near inguinal (i)WAT (5 x 10^4 ILC2s, split evenly bilaterally) and intraperitoneal injection (5 x 10^4 ILC2s). Tissues were harvested on day 5 for analyses (PBS, n=8; ILC2, n=8 except panel **f**). **(b)** Representative plots identifying donor and recipient ILC2s in iWAT. Plots pre-gated on live CD45$^+$ Lin$^-$ CD25$^+$ IL33R$^+$ cells. Lineage cocktail: CD3, CD5, CD19, NK1.1, CD11c, CD11b and FcεRIα. **(c)** Total numbers of ILC2s per gram iWAT. **(d)** iWAT Uncoupling protein 1 (UCP1) immunohistochemistry, bar 100 µm. **(e)** *Ucp1* expression in iWAT. **(f)** iWAT oxygen consumption (PBS, n=14; ILC2, n=15).

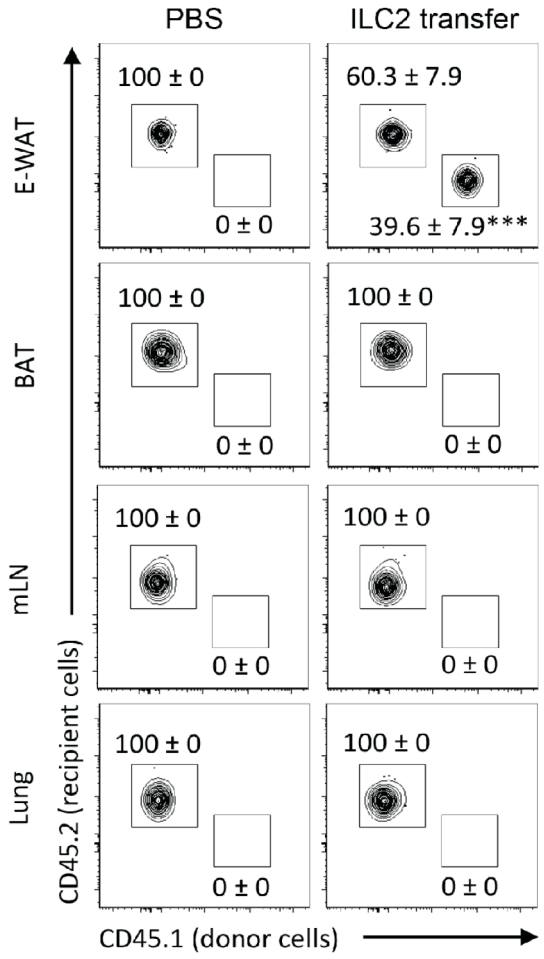

Figure 23. IL-33-elicited ILC2s derived from white adipose tissue (WAT) selectively accumulate in recipient WAT. Live $CD45^+$ Lin^- $CD25^+$ $IL\text{-}33R^+$ ILC2s were sort-purified from E-WAT of $CD45.1^+$ mice treated with 12.5 µg/kg recombinant murine (rm)IL-33 daily for 7 days by intraperitoneal injection. ILC2s (1 x 10^5 total) were transferred to $CD45.2^+$ recipient mice daily for 4 days by subcutaneous injection near iWAT (5 x 10^4 ILC2s, split evenly bilaterally) and intraperitoneal injection (5 x 10^4 ILC2s). Tissues were harvested on day 5 for analyses. **(b)** Donor and recipient ILC2s in E-WAT, brown adipose tissue (BAT), mesenteric lymph nodes (mLN) and lung. iWAT ILC2 plots from this experiment are shown in the previous figure. Pre-gated on Live $CD45^+$ Lin^- $CD25^+$ $IL\text{-}33R^+$ ILC2s. Donor ILC2s are defined as $CD45.1^+$ $CD45.2^-$, whereas recipient ILC2s are defined as $CD45.1^-$ $CD45.2^+$. Representative plots shown. Frequencies represent percent of ILC2s that are recipient or donor cells. Student's t-test, ***P<0.001.

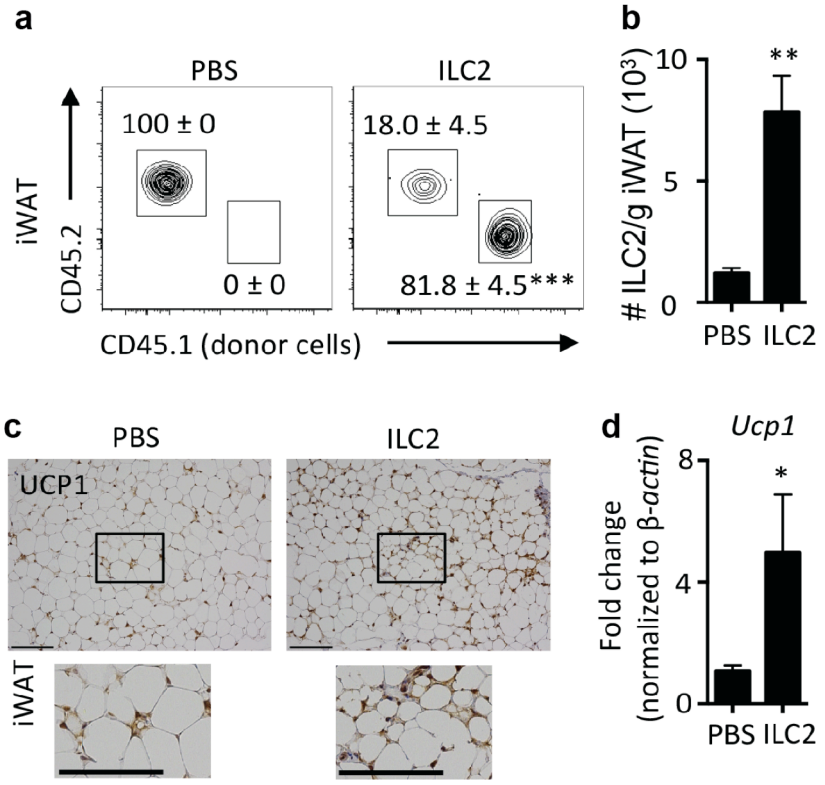

Figure 24. IL-33-elicited ILC2s can elicit beiging independently of the adaptive immune system. Live CD45$^+$ Lin$^-$ CD25$^+$ IL-33R$^+$ ILC2s were sort-purified from E-WAT of C57BL/6 mice treated with rmIL-33 (12.5 μg/kg) daily for 7 days by intraperitoneal injection. ILC2s (1 x 10^5 total) were transferred to *Rag1*$^{-/-}$ recipient mice on a C57BL/6 background daily for 4 days by subcutaneous injection (n=8 mice per group). **(a)** Representative plots identifying donor and recipient ILC2s in iWAT. Plots pre-gated on live CD45$^+$ Lin$^-$ CD25$^+$ IL33R$^+$ cells. Lineage cocktail: CD3, CD5, CD19, NK1.1, CD11c, CD11b and FcεRIα. **(b)** Total numbers of ILC2s per gram iWAT. **(c)** iWAT Uncoupling protein 1 (UCP1) immunohistochemistry, bar 100 μm. (d) iWAT Ucp1 expression levels. Student's *t*-test, *P<0.05, **P<0.01.

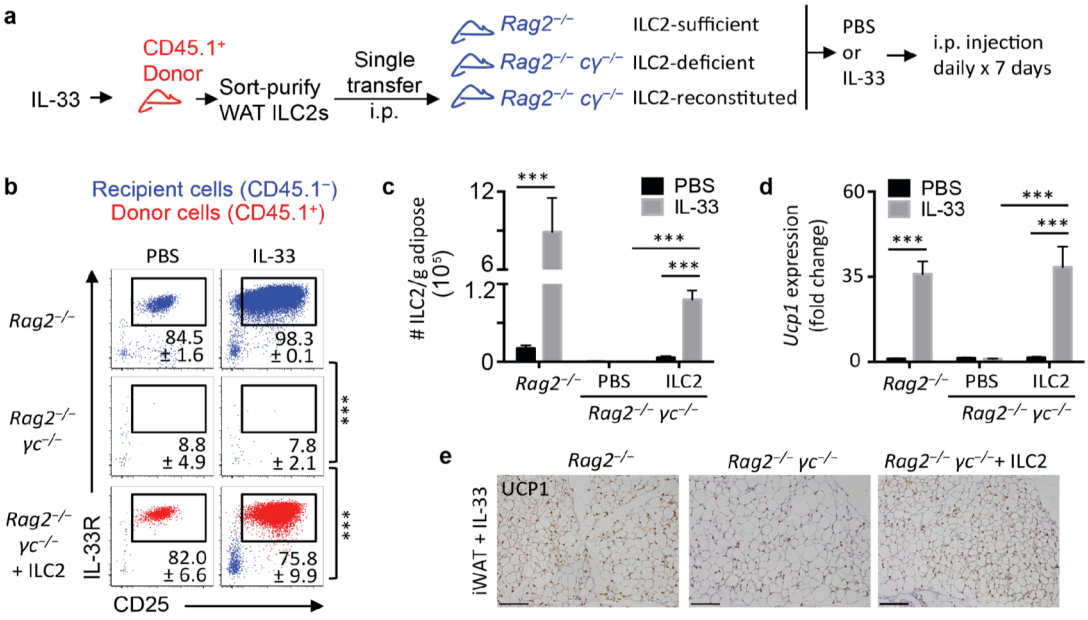

Figure 25. ILC2s from E-WAT accumulate in white adipose tissue (WAT) of recipient mice and expand in response to IL-33 to promote beiging. Experimental design for panels **b-e**. Sort-purified CD45.1$^+$ ILC2s (10^5) from E-WAT of IL-33-treated mice (12.5 µg/kg/day for 7 days by intraperitoneal [i.p.] injection) were transferred into *Rag2*$^{-/-}$ *γc*$^{-/-}$ recipients by a single i.p. injection. ILC2-sufficient *Rag2*$^{-/-}$ mice, ILC2-deficient *Rag2*$^{-/-}$ *γc*$^{-/-}$ mice and ILC2-reconstituted *Rag2*$^{-/-}$ *γc*$^{-/-}$ mice were treated with PBS or rmIL-33 (12.5 µg/kg) by intraperitoneal injection daily for 7 days (n=4 mice per group). **(b)** Representative plots of live CD45.1$^+$ Lin$^-$ CD25$^+$ IL33R$^+$ ILC2s in E-WAT. Blue, recipient cells. Red, donor cells. Lineage cocktail includes CD3, CD5, CD19, NK1.1, CD11c, CD11b and FcεRIα. **(c)** ILC2 numbers per gram of E-WAT. **(d)** *Ucp1* expression in E-WAT. **(e)** iWAT UCP1 immunohistochemistry, bar 100 µm. ANOVA with Tukey post-hoc test, ***P<0.001.

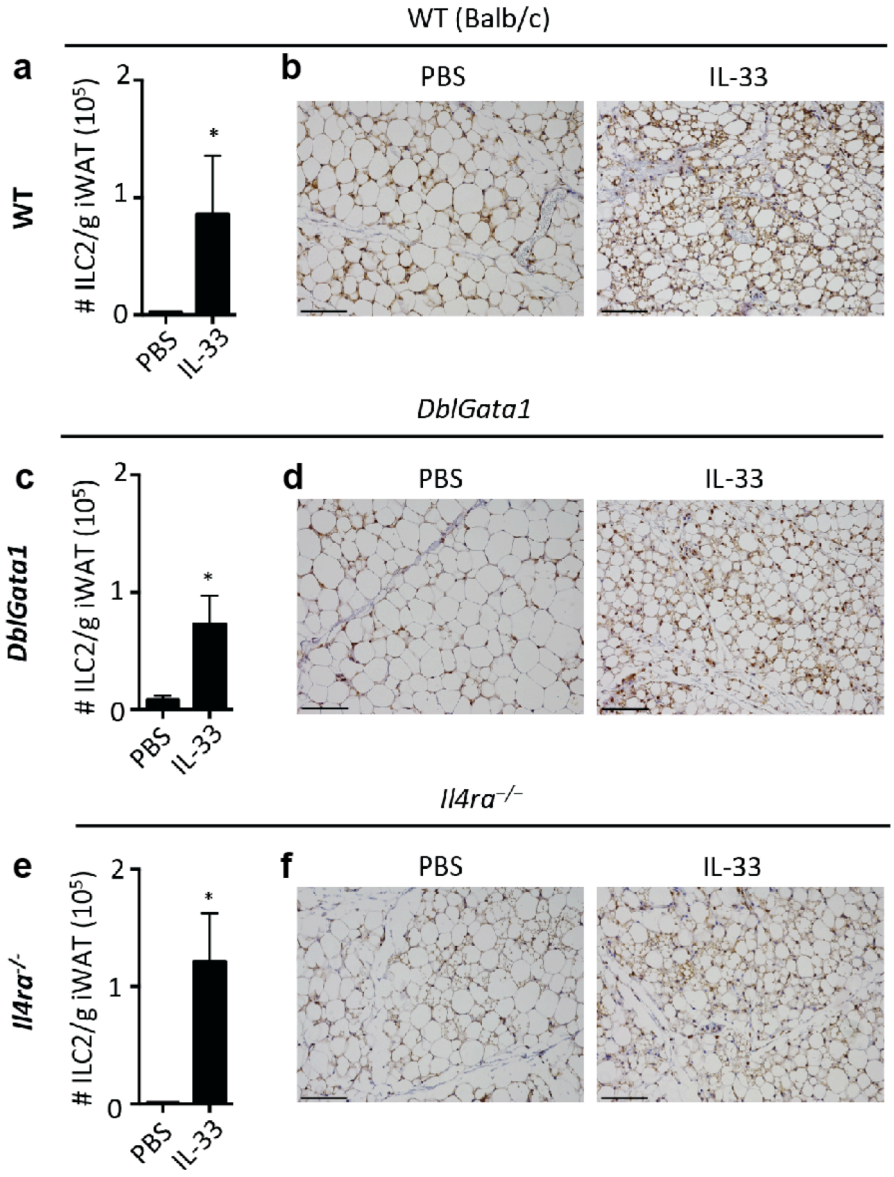

Figure 26. IL-33 treatment can elicit beiging independently of eosinophils and IL-4Rα signaling. Wildtype (Balb/c), *DblGata1* mice that lack eosinophils or *Il4ra*$^{-/-}$ mice that have dysregulated alternatively activated macrophages (AAMacs) (both mutant strains on a Balb/c background) were treated with PBS or recombinant murine (rm)IL-33 (12.5 µg/kg) daily by intraperitoneal injection for 7 days. **(a)** ILC2 numbers/gram iWAT and **(b)** iWAT UCP1 immunohistochemistry (IHC) in Balb/c mice. **(c)** iWAT ILC2 numbers per gram of adipose and **(d)** iWAT UCP1 IHC in *DblGata1* mice. **(e)** ILC2 numbers/gram iWAT and **(f)** iWAT UCP1 IHC in *Il4ra*$^{-/-}$ mice. Student's *t*-test, *P<0.05. There were 3-6 mice per group from 2 independent experiments. Scale bars, 100 µm.

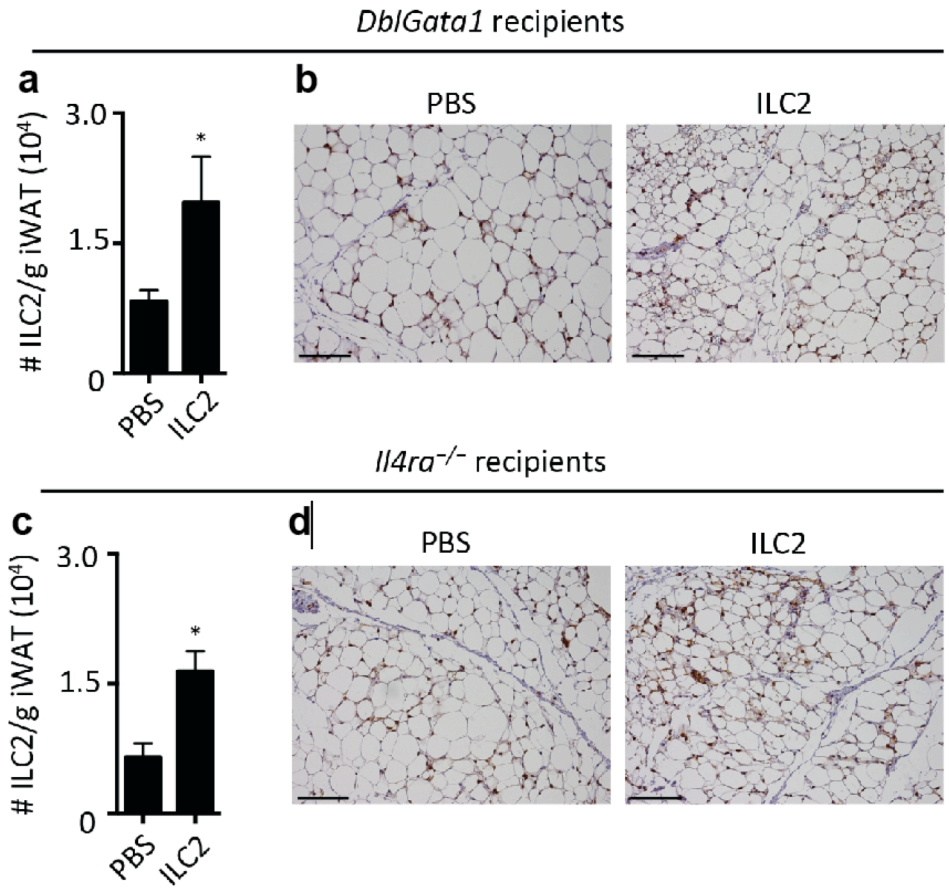

Figure 27. IL-33-elicited ILC2s can promote beiging independently of eosinophils and IL-4Rα signaling. Live CD45^{+} Lin^{-} CD25^{+} IL-33R^{+} ILC2s were sort-purified from E-WAT of Balb/c mice treated with rmIL-33 (12.5 µg/kg) daily for 5-7 days by intraperitoneal injection. ILC2s (1 x 10^{5} total) were transferred to the indicated recipient mice daily for 4 days by subcutaneous injection. **(a)** iWAT ILC2 numbers per gram of adipose and **(b)** iWAT Uncoupling protein 1 (UCP1) immunohistochemistry (IHC) in *DblGata1* recipients. **(c)** iWAT ILC2 numbers per gram of adipose and **(d)** iWAT UCP1 IHC in *Il4ra*$^{-/-}$ recipients. Student's t-test, *P<0.05. Data are from n=3-6 mice per group pooled over 2-3 independent experiments. Scale bars, 100 µm.

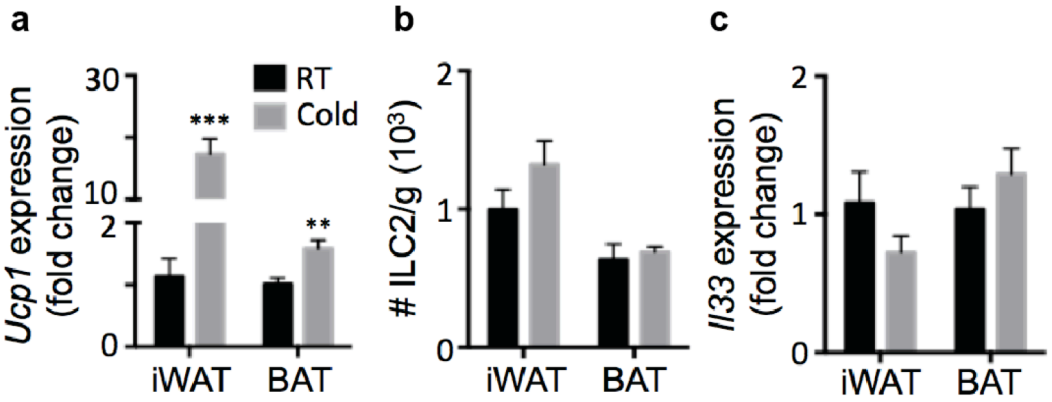

Figure 28. Chronic exposure to severe cold environmental temperatures is not associated with accumulation of ILC2s in inguinal white adipose tissue (iWAT) or brown adipose tissue (BAT). C57BL/6 mice were single-housed at room temperature (n=7) or 4 °C (n=8) for 72 hours. **(a)** Uncoupling protein 1 (*Ucp1*) mRNA levels in iWAT and BAT. **(b)** ILC2 numbers per gram of adipose tissue in iWAT and BAT. **(c)** Interleukin 33 (*Il33*) mRNA levels in iWAT and BAT. Student's t-test, **P<0.01, ***P<0.001.

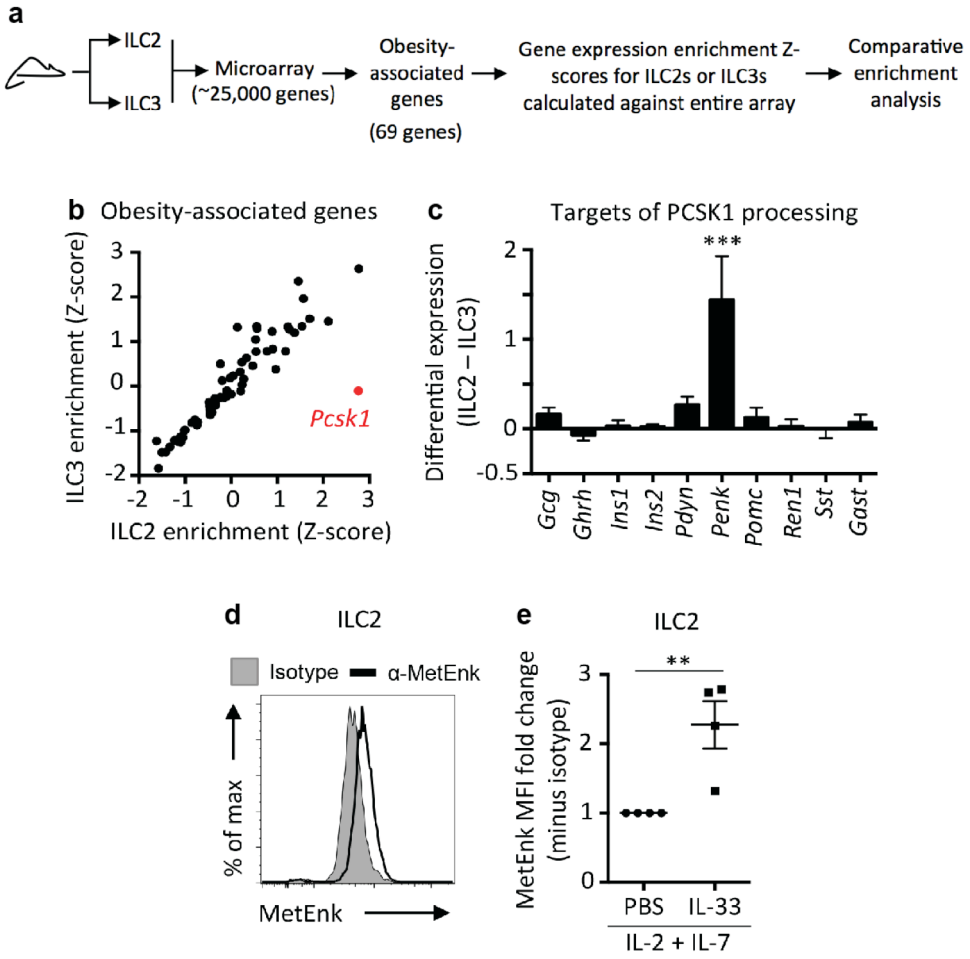

Figure 29. ILC2s produce the obesity-associated gene PCSK1 and the PCSK1 target methionine-enkephalin. **(a)** Gene expression enrichment analyses of 69 obesity-associated genes in ILC2s (x-axis) versus ILC3s (y-axis). Genes significantly enriched in one cell type but not the other are red. **(b)** Differential expression of PCSK1 target genes in ILC2s vs ILC3s. **(c)** Intracellular staining of MetEnk (black line) or rabbit IgG isotype control (shaded histogram) in ILC2s sort-purified from E-WAT and re-stimulated *in vitro* with IL-2 and IL-7 (10 ng/mL) for 4 days. **(d)** MetEnk mean fluorescence intensity (MFI) in sort-purified E-WAT ILC2s re-stimulated *in vitro* with IL-2 and IL-7 (10 ng/mL) with or without IL-33 (30 ng/mL) for 4 days. Isotype control MFI for each group was subtracted before calculating relative expression. Shown are averages from 4 independent experiments, each representing pooled cells from n=3-5 mice and measured in duplicate or triplicate.

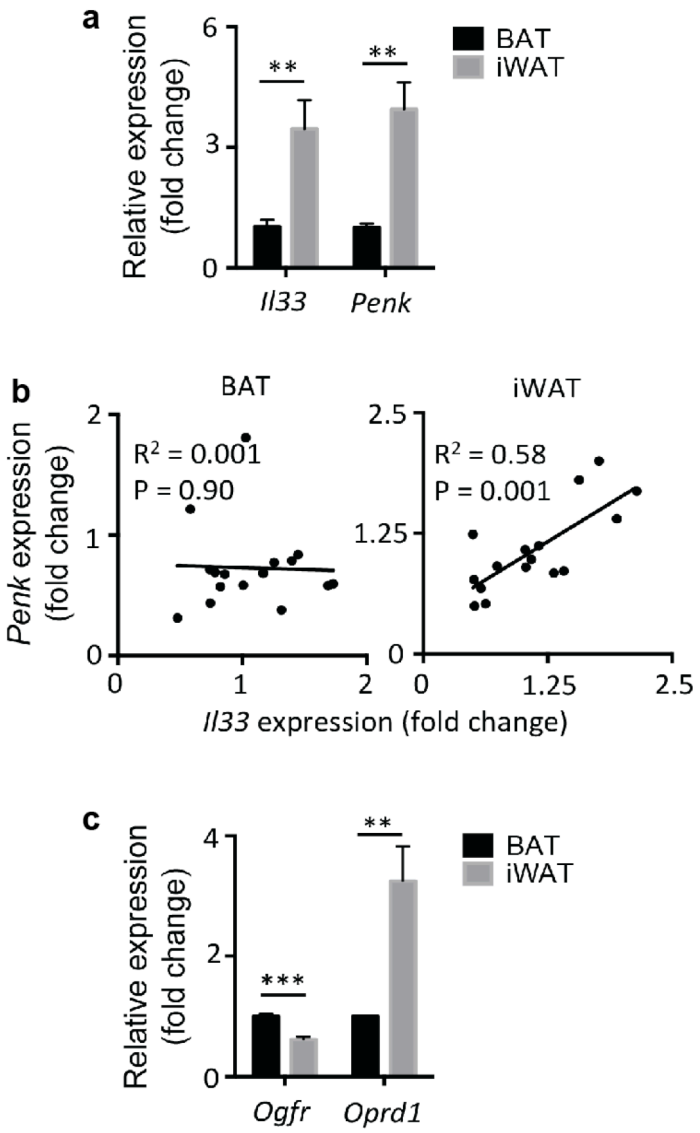

Figure 30. Interleukin 33 (Il33) and Proenkephalin A (Penk) expression levels are tissue specific. (a) *Il33* and *Penk* mRNA levels in inguinal white adipose tissue (iWAT) vs brown adipose tissue (BAT), n=8 mice, paired samples. (b) Il33 and Penk mRNA expression levels are correlated in iWAT but not BAT. Linear regression, n=16 mice, naïve C57BL/6 mice. **(c)** *Ogfr* and *Oprd1* mRNA levels in inguinal white adipose tissue (iWAT) vs brown adipose tissue (BAT), n=8 mice, paired samples. For panels a and c, Paired Student's t-test, *P<0.01, ***P<0.001. For panel b, Pearson linear regression.

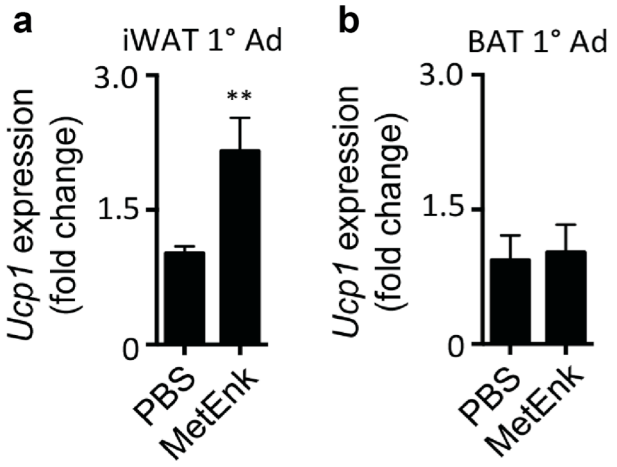

Figure 31. Methionine-enkephalin (MetEnk) treatment upregulates Uncoupling protein 1 (*Ucp1*) expression in primary adipocytes from inguinal white adipose tissue (iWAT). Adherent stromal vascular fraction (SVF) cells from **(a)** iWAT or **(b)** BAT of 4-week-old C57BL/6 mice were differentiated into adipocytes for 2 days, treated with PBS or 50 μM MetEnk from days 2-8 and harvested on day 8 (iWAT: n=7 PBS, n=8 MetEnk; BAT: n=6 PBS, n=6 MetEnk from 2-3 independent experiments). Student's t-test, **P<0.01.

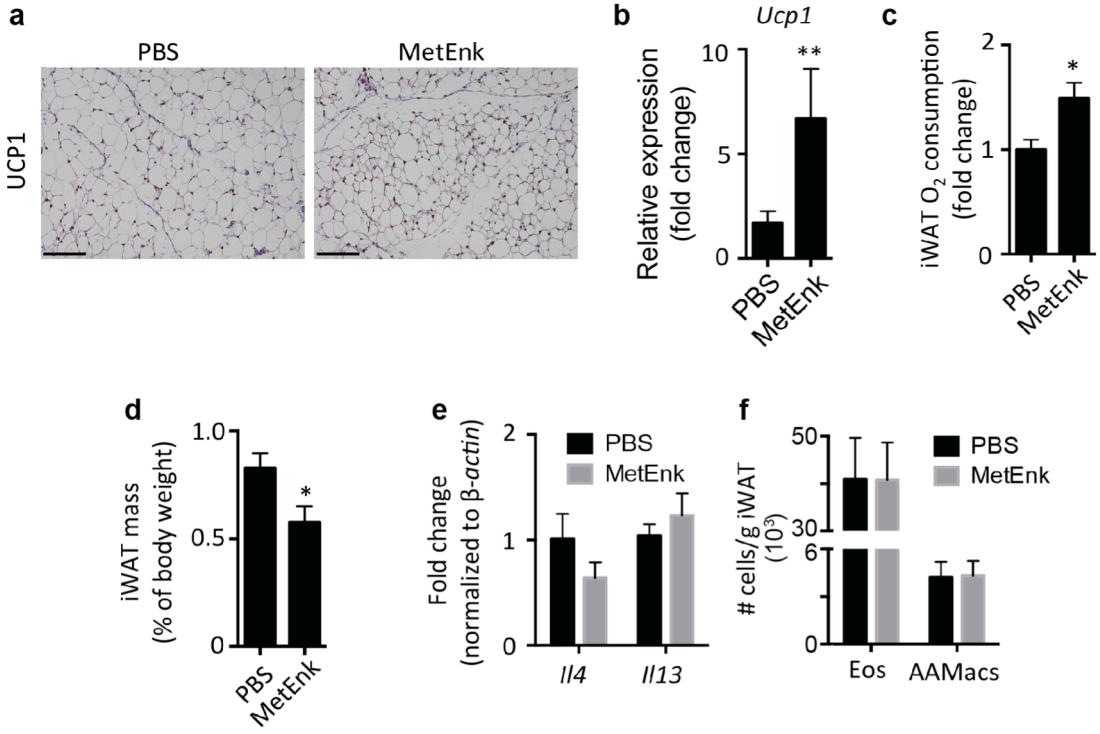

Figure 32. Methionine-enkephalin (MetEnk) treatment can elicit beiging *in vivo*. Wildtype mice were treated with PBS (n=7) or MetEnk (n=9) by subcutaneous injection (10 mg/kg/day) for 5 days. **(a)** Uncoupling protein 1 (UCP1) immunohistochemistry (IHC) in inguinal white adipose tissue (iWAT). Scale bars, 100 μm. **(b)** iWAT *Ucp1* expression, **(c)** iWAT oxygen consumption, **(d)** iWAT relative mass, **(e)** iWAT *Il4* and *Il13* expression and **(f)** numbers of eosinophils (Eos, live $CD45^+$ $SiglecF^+$ SSC^{hi}) and alternatively activated macrophages (AAMacs, live $CD45^+$ $SiglecF^-$ $F4/80^+$ $CD206^+$) per gram of iWAT. Student's t-test, *P<0.05, **P<0.01.

CHAPTER 4: Summary, Discussion and Future Directions

4.1 Characterization of Group 2 innate lymphoid cell responses in white adipose tissue

Group 2 innate lymphoid cells (ILC2s) are a recently described immune cell type (Moro et al., 2009; Price et al., 2010; Neill et al. 2010) that respond to epithelial-derived cytokines that include IL-33, IL-25 and thymic stromal lymphopoietin (TSLP) to initiate type 2 immune responses that promote host protective immunity against helminth pathogens or pathologic allergic inflammation (Kim, 2014; Monticelli et al., 2012; Sonnenberg et al., 2013; Spits et al., 2013; Spits and Cupedo, 2012). ILC2s initiate type 2 immune responses in multiple tissues by producing IL-5 and IL-13 that act to promote eosinophil and AAMac responses, respectively (Molofsky et al., 2013; Nussbaum et al., 2013), although these cells can also promote adaptive T helper type 2 (Th2) and B cell responses in some contexts (Halim et al., 2014; Mirchandani et al., 2014; Moro et al., 2010;

Oliphant et al., 2014). Production of type 2 cytokines by ILC2s is critically regulated by the transcription factor GATA-3 (Furusawa et al., 2013; Mjosberg et al., 2012), a transcription factor that also controls ILC2 development (Monticelli et al., 2012; Sonnenberg et al., 2013; Spits and Cupedo, 2012). Although ILC2 responses are associated with immune responses at barrier surfaces such as the gut and lung, ILC2s were also recently demonstrated to be present in WAT, where these cells constitutively produce IL-5 and IL-13 to sustain eosinophils and AAMacs (Molofsky et al., 2013). ILC2-mediated activation of the eosinophil/IL-4/AAMac pathway in WAT has been implicated in limiting obesity (Hams et al., 2013; Molofsky et al., 2013; Wu et al., 2011). In addition, IL-33 has been shown to have protective effects on inflammatory responses in WAT and for limiting obesity (Miller et al., 2010). Based on these findings, the goal of this thesis was to investigate ILC2 responses in WAT in the setting of murine and human obesity and the mechanisms through which the IL-33/ILC2 pathway influences metabolic homeostasis.

The results presented in this thesis identify IL-33R$^+$ GATA-3$^+$ ILC2s in human and murine WAT and reveal a previously unappreciated link between IL-33-dependent ILC2 responses and beiging of WAT. In **Chapter 2**, decreased WAT ILC2 populations were found to be a conserved feature of obesity in humans and mice. In mice, IL-33 was critical for promoting ILC2 responses in WAT and limiting the development of obesity in mice, and treatment of mice with IL-33 was

associated with increased metabolic rate. In **Chapter 3**, IL-33 is shown to promote beiging of WAT in a process mediated by ILC2s. IL-33-elicited ILC2s could drive beiging independently of the adaptive immune system and the eosinophil/IL-4Rα/AAMac pathway. It was found that ILC2s produced methionine-enkephalin (MetEnk) peptides, which were sufficient to drive beiging *in vivo* and *in vitro*, indicating that the IL-33/ILC2 axis elicits beiging via production of MetEnk peptides.

Previous studies have implicated ILC2s in limiting obesity in mice and have indicated that ILC2s in WAT can expand in response to exogenous IL-33 (Hams et al., 2013; Molofsky et al., 2013). However, the relevance of ILC2 responses in human obesity remained unknown. In addition, the endogenous factors that control ILC2 responses in WAT and the mechanisms through which ILC2s regulate metabolic homeostasis remain poorly understood. In Chapter 2, using human subcutaneous WAT and murine epididymal (E)-WAT, we identified Lineage $(Lin)^-$ $CD25^+$ $CD127^+$ ILCs that were uniformly positive for the $IL\text{-}33R^+$ $GATA\text{-}3^+$ ILC2s in both species. WAT ILC2 populations were decreased in both murine and human obesity, suggesting that there may be a conserved immunologic response in human and murine obesity that suppresses ILC2s.

The mechanisms of this decrease in ILC2s is not clear, however one possibility is that ILC2s become resistant to the effects of IL-33 (i.e., hypo-responsiveness to IL-33). Consistent with this hypothesis are recent studies indicating that IL-33 production is elevated in WAT of obese mice and humans (Zeyda et al., 2013), which would be expected to result in increased ILC2 responses rather than the observed decrease in ILC2s. Supporting this possibility are data in Chapter 2 indicating that endogenous IL-33 is necessary to sustain ILC2 responses in WAT. Therefore, loss of IL-33-dependent signaling may contribute to decreased ILC2 responses in obesity. Another possible explanation for why ILC2s are decreased in WAT may be related to decreases in other immune cell populations in WAT that produce factors that stimulate ILC2s. For example, iNKT cells in WAT are decreased in obesity and produce substantial amounts of IL-4 (Lynch et al., 2014; Lynch et al., 2012), a factor that stimulates ILC2 proliferation and effector cytokine production in the skin and lung (Kim et al., 2014; Motomura et al., 2014). Direct associations between iNKT and ILC2 responses have not been investigated. In addition, alternative mechanisms that might decrease ILC2s in WAT are potential direct effects of fatty acids on ILC2s, or inflammatory signals from other immune cell populations that suppress ILC2 responses. Future studies will be required to understand the mechanisms associated the decreased ILC2 response in WAT in the context of obesity.

IL-33 was previously shown to be an important regulator of adiposity and inflammation in obese WAT (Miller et al., 2010), and exogenous IL-33 has been shown to elicit ILC2 responses in WAT (Molofsky et al., 2013). The studies in Chapter 2 support and extend these prior observations by indicating that endogenous IL-33 is necessary to sustain ILC2s and to limit the development of obesity. Recent studies showed that antibody-mediated depletion of ILC2s is associated with increased weight gain and more severe insulin resistance in mice fed a high fat diet (Hams et al., 2013), and transferring IL-25-elicted ILC2s is sufficient to promote weight loss in diet-induced obese mice (Hams et al., 2013). This suggests that ILC2s negatively regulate the development of obesity, although the mechanisms of this remain poorly understood. The studies in Chapter 2 indicate that administration of exogenous IL-33 promoted ILC2 responses in WAT and decreased adiposity in association with increased energy expenditure. This finding is consistent with earlier studies indicating that the eosinophil/IL-4Rα/AAMac pathway can regulate caloric expenditure of mice (Molofsky et al., 2013; Qiu et al., 2014; Rao et al., 2014; Wu et al., 2011). Therefore, it is likely that ILC2s regulate metabolic homeostasis by eliciting the eosinophil/IL-4Rα/AAMac pathway in WAT.

4.2 IL-33 and ILC2s promote beiging of white adipose tissue

Previous studies have indicated that the eosinophil/IL-4Rα/AAMac pathway regulates energy expenditure by eliciting beiging of WAT (Liu et al., 2014; Qiu et

al., 2014; Rao et al., 2014), a process in which UCP1-expressing beige adipocytes emerge within WAT (Bartelt and Heeren, 2014; Harms and Seale, 2013; Rosen and Spiegelman, 2014; Wu et al., 2013). Eosinophils are recruited to WAT in the setting of chronic exposure to severe cold environmental temperatures (4°C), and these cells produce IL-4 to elicit AAMac production of norepinephrine (Qiu et al., 2014; Rao et al., 2014). Although ILC2s are known to be upstream mediators of eosinophil and AAMac responses in WAT (Molofsky et al., 2013), whether ILC2s can contribute to beiging was unknown. Data in Chapter 3, indicate that IL-33 treatment and adoptive transfer of IL-33-elicited ILC2s derived from WAT are sufficient to promote beiging. Surprisingly, however, the IL-33/ILC2 pathway could elicit beiging independently of eosinophils and IL-4Rα. Gene expression enrichment analyses of obesity-associated genes in ILC2s indicated that ILC2s express PCSK1, a gene previously linked to human and murine obesity by regulating both food intake and caloric expenditure (Benzinou et al., 2008; Lloyd et al., 2006) by processing various pro-hormones into their active forms (Seidah, 2011; Seidah et al., 2013). We found that ILC2s produce the PCSK1 target gene Proenkephalin A and its active form methionine-enkephalin, and this peptide could upregulate *Ucp1* expression in adipocytes *in vitro* and elicit beiging *in vivo*.

Collectively, these findings suggest that ILC2s can elicit beiging via multiple mechanisms (Fig. 33). First, ILC2s likely induce the eosinophil/IL-4Rα/AAMac

pathway to promote beiging via production of norepinephrine (NE). In addition ILC2s can produce MetEnk peptides that can directly stimulate beiging. It is not yet clear whether NE and MetEnk elicit the same beige adipocyte subset. However, we propose that NE and MetEnk cooperatively support optimal beiging to regulate metabolic homeostasis. Supporting this are prior studies suggesting that NE and MetEnk signaling pathways might interact to cooperatively stimulate lipolysis in adipocytes (Nencini and Paroli, 1981), a process that is critical for beige adipocyte responses and UCP1 function (Fedorenko et al., 2012; Harms and Seale, 2013; Rosen and Spiegelman, 2014; Wu et al., 2013). Future studies focused on MetEnk and NE interactions in adipocytes are warranted to better understand that mechanisms by which ILC2s, eosinophils and AAMacs contribute to the regulation of beiging and metabolic rate.

Another possibility is that ILC2-derived MetEnk and AAMac-derived NE elicit distinct populations of beige adipocytes involved in the regulation of metabolic homeostasis in different physiologic contexts. Supporting this, the eosinophil/IL-4Rα/AAMac pathway is activated in WAT in the setting of chronic cold exposure (Qiu et al., 2014; Rao et al., 2014), whereas data in Chapter 3 indicate that ILC2 numbers and *Il33* expression were unchanged in iWAT following 3 days of exposure to severe cold environmental temperatures. This suggests that the IL-33/ILC2 pathway is not activated in the setting of cold exposure and that other factors such as the adipokine/myokine meteorin-like or IL-4/IL-13-producing iNKT

cells might elicit the eosinophil/AAMac-dependent beiging pathway (Lynch et al., 2014; Lynch et al., 2012; Rao et al., 2014). Other metabolic functions of beige adipocytes include limiting weight gain and promoting glucose homeostasis (Cohen et al., 2014). As the IL-33/ILC2 axis appears to be dysregulated in the setting of obesity and to limit weight gain (Chapter 2), the IL-33/ILC2/MetEnk/beiging pathway might be associated with regulation of weight gain or maintenance of glucose homeostasis. Additional studies will be required to dissect the physiologic functions of ILC2s and MetEnk in the regulation of beiging.

4.3 Concluding Remarks

Previous studies have implicated various type 2 immune cells in the regulation of weight gain (see Chapter 1), and emerging work indicates that eosinophils and AAMacs can promote beiging of WAT through AAMac-derived norepinephrine to regulate energy expenditure (Liu et al., 2014; Qiu et al., 2014; Rao et al., 2014). ILC2s produce effector cytokines that elicit type 2 immune responses (Kim, 2014; Monticelli et al., 2012; Spits and Cupedo, 2012) and stimulate eosinophils and AAMacs through production of IL-5 and IL-13 (Molofsky et al., 2013). Although ILC2s have been implicated in limiting weight gain by regulating the eosinophil/IL-4/AAMac pathway (Hams et al., 2013; Molofsky et al., 2013; Wu et al., 2011), the relevance of ILC2 responses in human obesity and the

mechanisms through which ILC2s regulate metabolic homeostasis have remained poorly understood.

Collectively, the data presented in this thesis provide the first demonstration that dysregulated ILC2 responses in WAT are a conserved feature of obesity in humans and mice and that the IL-33-ILC2 axis regulates metabolic homeostasis by eliciting beiging of white adipose tissue. The expression of enkephalin peptides within ILC2s indicates a previously unrecognized effector mechanism employed by ILC2s to regulate metabolic homeostasis. From an evolutionary perspective, coupling ILC2-dependent innate immune effector functions with the maintenance of systemic metabolic homeostasis through beiging of WAT could provide a rapid and integrated multi-organ response that allows mammals to surmount multiple environmental challenges including infection, nutrient stress or changes in temperature. Given that impaired beige adipocyte function is associated with increased weight gain and obesity in mice (Cohen et al., 2014; Feldmann et al., 2009) and that activity of brown/beige (Sharp et al., 2012; Wu et al., 2012) adipose tissue is dysregulated in obese patients (Carey et al., 2013; Saito et al., 2009), targeting the IL-33-ILC2-beiging pathway could represent a new approach for the treatment of obesity and obesity-associated disorders such as type 2 diabetes and atherosclerosis.

4.4 Figures

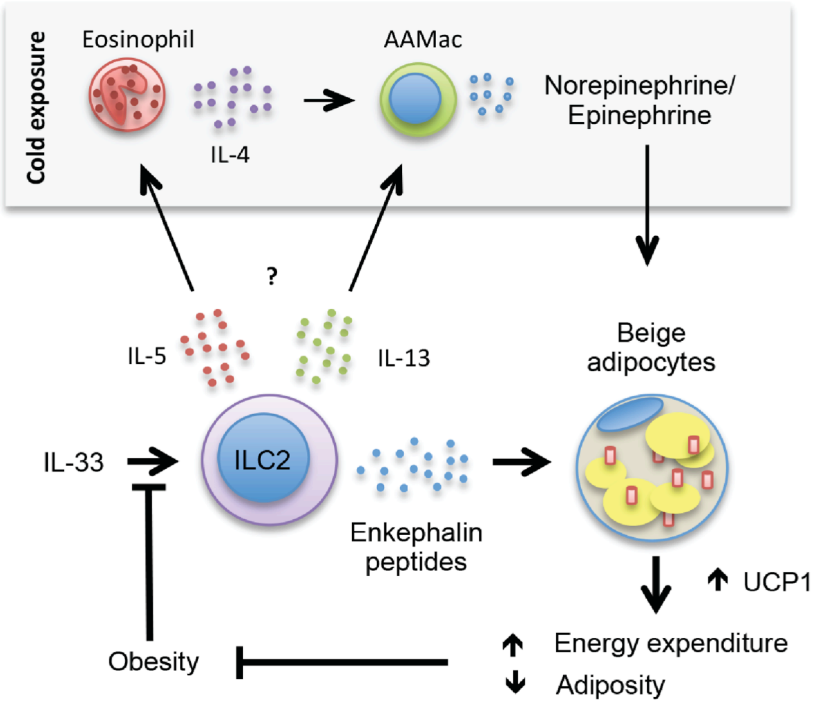

Figure 33. Summary model linking the IL-33/ILC2/MetEnk pathway to the regulation of beiging and obesity. Interleukin (IL)-33 acts on group 2 innate lymphoid cells (ILC2s) to upregulate production of the effector molecules IL-5, IL-13 and enkephalin peptides. ILC2-derived IL-5 promotes eosinophil homeostasis in WAT, and eosinophils in turn produce IL-4 to sustain alternatively activated macrophages (AAMacs) in WAT. ILC2-derived IL-13 can also promote AAMac responses. In the setting of chronic exposure to a cold environment, eosinophil-derived IL-4 stimulates AAMacs to produce catecholamines such as norepinephrine, which acts directly on beige adipocytes to upregulate uncoupling protein 1 (UCP1) expression and promote . Although it remains unknown whether ILC2-derived IL-5 and IL-13 contribute to cold stress-induced beiging, ILC2-derived enkephalin peptides can act directly on beige adipocytes to upregulate UCP1. This results in increased energy expenditure and decreased adiposity that may counteract weight gain. In the setting of obesity, IL-33 expression in WAT is increased, however WAT ILC2s are paradoxically decreased in both mice and humans, suggesting that the IL-33/ILC2 axis is dysregulated in obesity. This may impede the ability of ILC2s to contribute to the function of beige fat, resulting in a vicious cycle that promotes weight gain.

BIBLIOGRAPHY

Allison, M.B., and Myers, M.G., Jr. (2014). 20 years of leptin: connecting leptin signaling to biological function. The Journal of endocrinology *223*, T25-35.

Amano, S.U., Cohen, J.L., Vangala, P., Tencerova, M., Nicoloro, S.M., Yawe, J.C., Shen, Y., Czech, M.P., and Aouadi, M. (2014). Local proliferation of macrophages contributes to obesity-associated adipose tissue inflammation. Cell metabolism *19*, 162-171.

Amar, J., Chabo, C., Waget, A., Klopp, P., Vachoux, C., Bermudez-Humaran, L.G., Smirnova, N., Berge, M., Sulpice, T., Lahtinen, S.*, et al.* (2011). Intestinal mucosal adherence and translocation of commensal bacteria at the early onset of type 2 diabetes: molecular mechanisms and probiotic treatment. EMBO molecular medicine *3*, 559-572.

Arner, P., Bernard, S., Salehpour, M., Possnert, G., Liebl, J., Steier, P., Buchholz, B.A., Eriksson, M., Arner, E., Hauner, H.*, et al.* (2011). Dynamics of human adipose lipid turnover in health and metabolic disease. Nature *478*, 110-113.

Attie, A.D., and Scherer, P.E. (2009). Adipocyte metabolism and obesity. Journal of lipid research *50 Suppl*, S395-399.

Badoud, F., Perreault, M., Zulyniak, M.A., and Mutch, D.M. (2014). Molecular insights into the role of white adipose tissue in metabolically unhealthy normal weight and metabolically healthy obese individuals. FASEB journal : official publication of the Federation of American Societies for Experimental Biology. [Epub ahead of print].

Barbatelli, G., Murano, I., Madsen, L., Hao, Q., Jimenez, M., Kristiansen, K., Giacobino, J.P., De Matteis, R., and Cinti, S. (2010). The emergence of cold-induced brown adipocytes in mouse white fat depots is determined predominantly by white to brown adipocyte transdifferentiation. American journal of physiology. Endocrinology and metabolism *298*, E1244-1253.

Bartelt, A., and Heeren, J. (2014). Adipose tissue browning and metabolic health. Nature reviews. Endocrinology *10*, 24-36.

Bartemes, K.R., Kephart, G.M., Fox, S.J., and Kita, H. (2014). Enhanced innate type 2 immune response in peripheral blood from patients with asthma. The Journal of allergy and clinical immunology *134*, 671-678 e674.

Bartness, T.J., Shrestha, Y.B., Vaughan, C.H., Schwartz, G.J., and Song, C.K. (2010). Sensory and sympathetic nervous system control of white adipose tissue lipolysis. Molecular and cellular endocrinology *318*, 34-43.

Benzinou, M., Creemers, J.W., Choquet, H., Lobbens, S., Dina, C., Durand, E., Guerardel, A., Boutin, P., Jouret, B., Heude, B.*, et al.* (2008). Common nonsynonymous variants in PCSK1 confer risk of obesity. Nature genetics *40*, 943-945.

Bouchard, C. (2008). Gene-environment interactions in the etiology of obesity: defining the fundamentals. Obesity *16 Suppl 3*, S5-S10.

Brestoff, J.R., and Artis, D. (2013). Commensal bacteria at the interface of host metabolism and the immune system. Nature immunology *14*, 676-684.

Brestoff, J.R., and Van den Broeck, J. (2013). Study Size Planning. In Epidemiology: Principles and Practical Guidelines, J.R. Brestoff, and J. Van den Broeck, eds. (Dordrecht: Springer Science+Business Media), pp. 137-155.

Calder, P.C. (2002). Dietary modification of inflammation with lipids. The Proceedings of the Nutrition Society *61*, 345-358.

Cani, P.D., Amar, J., Iglesias, M.A., Poggi, M., Knauf, C., Bastelica, D., Neyrinck, A.M., Fava, F., Tuohy, K.M., Chabo, C.*, et al.* (2007). Metabolic endotoxemia initiates obesity and insulin resistance. Diabetes *56*, 1761-1772.

Cannon, B., and Nedergaard, J. (2004). Brown adipose tissue: function and physiological significance. Physiological reviews *84*, 277-359.

Carey, A.L., Formosa, M.F., Van Every, B., Bertovic, D., Eikelis, N., Lambert, G.W., Kalff, V., Duffy, S.J., Cherk, M.H., and Kingwell, B.A. (2013). Ephedrine activates brown adipose tissue in lean but not obese humans. Diabetologia *56*, 147-155.

Carey, A.L., Vorlander, C., Reddy-Luthmoodoo, M., Natoli, A.K., Formosa, M.F., Bertovic, D.A., Anderson, M.J., Duffy, S.J., and Kingwell, B.A. (2014). Reduced UCP-1 content in in vitro differentiated beige/brite adipocytes derived from preadipocytes of human subcutaneous white adipose tissues in obesity. PloS one *9*, e91997.

Carriere, A., Jeanson, Y., Berger-Muller, S., Andre, M., Chenouard, V., Arnaud, E., Barreau, C., Walther, R., Galinier, A., Wdziekonski, B.*, et al.* (2014). Browning of white adipose cells by intermediate metabolites: an adaptive mechanism to alleviate redox pressure. Diabetes *63*, 3253-3265.

Cawley, J., and Meyerhoefer, C. (2012). The medical care costs of obesity: an instrumental variables approach. Journal of health economics *31*, 219-230.

Chang, Y.H., Ho, K.T., Lu, S.H., Huang, C.N., and Shiau, M.Y. (2012). Regulation of glucose/lipid metabolism and insulin sensitivity by interleukin-4. International journal of obesity *36*, 993-998.

Cho, K.W., Morris, D.L., DelProposto, J.L., Geletka, L., Zamarron, B., Martinez-Santibanez, G., Meyer, K.A., Singer, K., O'Rourke, R.W., and Lumeng, C.N. (2014). An MHC II-Dependent Activation Loop between Adipose Tissue Macrophages and CD4(+) T Cells Controls Obesity-Induced Inflammation. Cell reports *9*, 605-617.

Cipolletta, D., Feuerer, M., Li, A., Kamei, N., Lee, J., Shoelson, S.E., Benoist, C., and Mathis, D. (2012). PPAR-gamma is a major driver of the accumulation and phenotype of adipose tissue Treg cells. Nature *486*, 549-553.

Cohen, P., Levy, J.D., Zhang, Y., Frontini, A., Kolodin, D.P., Svensson, K.J., Lo, J.C., Zeng, X., Ye, L., Khandekar, M.J.*, et al.* (2014). Ablation of PRDM16 and beige adipose causes metabolic dysfunction and a subcutaneous to visceral fat switch. Cell *156*, 304-316.

Collaboration, P.S. (2009). Body-mass index and cause-specific mortality in 900 000 adults: collaborative analyses of 57 prospective studies. Lancet *373*, 1083-1096.

Constantinides, M.G., McDonald, B.D., Verhoef, P.A., and Bendelac, A. (2014). A committed precursor to innate lymphoid cells. Nature *508*, 397-401.

Creemers, J.W., Choquet, H., Stijnen, P., Vatin, V., Pigeyre, M., Beckers, S., Meulemans, S., Than, M.E., Yengo, L., Tauber, M.*, et al.* (2012). Heterozygous mutations causing partial prohormone convertase 1 deficiency contribute to human obesity. Diabetes *61*, 383-390.

Curtis, J.M., Grimsrud, P.A., Wright, W.S., Xu, X., Foncea, R.E., Graham, D.W., Brestoff, J.R., Wiczer, B.M., Ilkayeva, O., Cianflone, K.*, et al.* (2010). Downregulation of adipose glutathione S-transferase A4 leads to increased protein carbonylation, oxidative stress, and mitochondrial dysfunction. Diabetes *59*, 1132-1142.

Curtis, J.M., Hahn, W.S., Stone, M.D., Inda, J.J., Droullard, D.J., Kuzmicic, J.P., Donoghue, M.A., Long, E.K., Armien, A.G., Lavandero, S.*, et al.* (2012). Protein carbonylation and adipocyte mitochondrial function. The Journal of biological chemistry *287*, 32967-32980.

Deiuliis, J., Shah, Z., Shah, N., Needleman, B., Mikami, D., Narula, V., Perry, K., Hazey, J., Kampfrath, T., Kollengode, M.*, et al.* (2011). Visceral adipose inflammation in obesity is associated with critical alterations in tregulatory cell numbers. PloS one *6*, e16376.

Deng, T., Lyon, C.J., Minze, L.J., Lin, J., Zou, J., Liu, J.Z., Ren, Y., Yin, Z., Hamilton, D.J., Reardon, P.R.*, et al.* (2013). Class II major histocompatibility complex plays an essential role in obesity-induced adipose inflammation. Cell metabolism *17*, 411-422.

Diefenbach, A., Colonna, M., and Koyasu, S. (2014). Development, differentiation, and diversity of innate lymphoid cells. Immunity *41*, 354-365.
Dong, M., Yang, X., Lim, S., Cao, Z., Honek, J., Lu, H., Zhang, C., Seki, T., Hosaka, K., Wahlberg, E.*, et al.* (2013). Cold exposure promotes atherosclerotic plaque growth and instability via UCP1-dependent lipolysis. Cell metabolism *18*, 118-129.

Exley, M.A., Hand, L., O'Shea, D., and Lynch, L. (2014). Interplay between the immune system and adipose tissue in obesity. The Journal of endocrinology *223*, R41-48.

Fedorenko, A., Lishko, P.V., and Kirichok, Y. (2012). Mechanism of fatty-acid-dependent UCP1 uncoupling in brown fat mitochondria. Cell *151*, 400-413.
Feldmann, H.M., Golozoubova, V., Cannon, B., and Nedergaard, J. (2009). UCP1 ablation induces obesity and abolishes diet-induced thermogenesis in mice exempt from thermal stress by living at thermoneutrality. Cell metabolism *9*, 203-209.

Feuerer, M., Herrero, L., Cipolletta, D., Naaz, A., Wong, J., Nayer, A., Lee, J., Goldfine, A.B., Benoist, C., Shoelson, S., and Mathis, D. (2009). Lean, but not obese, fat is enriched for a unique population of regulatory T cells that affect metabolic parameters. Nature medicine *15*, 930-939.

Finkelstein, E.A., Trogdon, J.G., Cohen, J.W., and Dietz, W. (2009). Annual medical spending attributable to obesity: payer-and service-specific estimates. Health affairs *28*, w822-831.

Fisher, F.M., Kleiner, S., Douris, N., Fox, E.C., Mepani, R.J., Verdeguer, F., Wu, J., Kharitonenkov, A., Flier, J.S., Maratos-Flier, E., and Spiegelman, B.M. (2012). FGF21 regulates PGC-1alpha and browning of white adipose tissues in adaptive thermogenesis. Genes & development *26*, 271-281.

Flegal, K.M., Carroll, M.D., Kit, B.K., and Ogden, C.L. (2012). Prevalence of obesity and trends in the distribution of body mass index among US adults, 1999-2010. Jama *307*, 491-497.

Flegal, K.M., Kit, B.K., and Graubard, B.I. (2014). Body mass index categories in observational studies of weight and risk of death. American journal of epidemiology *180*, 288-296.

Flegal, K.M., Kit, B.K., Orpana, H., and Graubard, B.I. (2013). Association of all-cause mortality with overweight and obesity using standard body mass index categories: a systematic review and meta-analysis. Jama *309*, 71-82.

Foster, M.T., and Bartness, T.J. (2006). Sympathetic but not sensory denervation stimulates white adipocyte proliferation. American journal of physiology. Regulatory, integrative and comparative physiology *291*, R1630-1637.

Furusawa, J., Moro, K., Motomura, Y., Okamoto, K., Zhu, J., Takayanagi, H., Kubo, M., and Koyasu, S. (2013). Critical role of p38 and GATA3 in natural helper cell function. Journal of immunology *191*, 1818-1826.

Gnad, T., Scheibler, S., von Kugelgen, I., Scheele, C., Kilic, A., Glode, A., Hoffmann, L.S., Reverte-Salisa, L., Horn, P., Mutlu, S.*, et al.* (2014). Adenosine activates brown adipose tissue and recruits beige adipocytes via A receptors. Nature. [Epub ahead of print].

Gordon, S., and Martinez, F.O. (2010). Alternative activation of macrophages: mechanism and functions. Immunity *32*, 593-604.

Graham, T.E., Yang, Q., Bluher, M., Hammarstedt, A., Ciaraldi, T.P., Henry, R.R., Wason, C.J., Oberbach, A., Jansson, P.A., Smith, U., and Kahn, B.B. (2006). Retinol-binding protein 4 and insulin resistance in lean, obese, and diabetic subjects. The New England journal of medicine *354*, 2552-2563.

Greenberg, A.S., and Obin, M.S. (2006). Obesity and the role of adipose tissue in inflammation and metabolism. The American journal of clinical nutrition *83*, 461S-465S.

Gregor, M.F., and Hotamisligil, G.S. (2011). Inflammatory mechanisms in obesity. Annual review of immunology *29*, 415-445.

Halim, T.Y., Steer, C.A., Matha, L., Gold, M.J., Martinez-Gonzalez, I., McNagny, K.M., McKenzie, A.N., and Takei, F. (2014). Group 2 innate lymphoid cells are critical for the initiation of adaptive T helper 2 cell-mediated allergic lung inflammation. Immunity *40*, 425-435.

Hams, E., Armstrong, M.E., Barlow, J.L., Saunders, S.P., Schwartz, C., Cooke, G., Fahy, R.J., Crotty, T.B., Hirani, N., Flynn, R.J.*, et al.* (2014). IL-25 and type 2 innate lymphoid cells induce pulmonary fibrosis. Proceedings of the National Academy of Sciences of the United States of America *111*, 367-372.

Hams, E., Locksley, R.M., McKenzie, A.N., and Fallon, P.G. (2013). Cutting edge: IL-25 elicits innate lymphoid type 2 and type II NKT cells that regulate obesity in mice. Journal of immunology *191*, 5349-5353.

Han, M.S., Jung, D.Y., Morel, C., Lakhani, S.A., Kim, J.K., Flavell, R.A., and Davis, R.J. (2013). JNK expression by macrophages promotes obesity-induced insulin resistance and inflammation. Science *339*, 218-222.

Harms, M., and Seale, P. (2013). Brown and beige fat: development, function and therapeutic potential. Nature medicine *19*, 1252-1263.

Hasan, A., Al-Ghimlas, F., Warsame, S., Al-Hubail, A., Ahmad, R., Bennakhi, A., Al-Arouj, M., Behbehani, K., Dehbi, M., and Dermime, S. (2014). IL-33 is negatively associated with the BMI and confers a protective lipid/metabolic profile in non-diabetic but not diabetic subjects. BMC immunology *15*, 19.

Hausman, D.B., DiGirolamo, M., Bartness, T.J., Hausman, G.J., and Martin, R.J. (2001). The biology of white adipocyte proliferation. Obesity reviews : an official journal of the International Association for the Study of Obesity *2*, 239-254.

Hill, A.A., Reid Bolus, W., and Hasty, A.H. (2014). A decade of progress in adipose tissue macrophage biology. Immunological reviews *262*, 134-152.

Hondares, E., Gallego-Escuredo, J.M., Flachs, P., Frontini, A., Cereijo, R., Goday, A., Perugini, J., Kopecky, P., Giralt, M., Cinti, S.*, et al.* (2014). Fibroblast growth factor-21 is expressed in neonatal and pheochromocytoma-induced adult human brown adipose tissue. Metabolism: clinical and experimental *63*, 312-317.

Hong, J.Y., Bentley, J.K., Chung, Y., Lei, J., Steenrod, J.M., Chen, Q., Sajjan, U.S., and Hershenson, M.B. (2014). Neonatal rhinovirus induces mucous metaplasia and airways hyperresponsiveness through IL-25 and type 2 innate lymphoid cells. The Journal of allergy and clinical immunology *134*, 429-439.

Huh, J.Y., Kim, J.I., Park, Y.J., Hwang, I.J., Lee, Y.S., Sohn, J.H., Lee, S.K., Alfadda, A.A., Kim, S.S., Choi, S.H.*, et al.* (2013). A novel function of adipocytes in lipid antigen presentation to iNKT cells. Molecular and cellular biology *33*, 328-339.

Ibrahim, M.M. (2010). Subcutaneous and visceral adipose tissue: structural and functional differences. Obesity reviews : an official journal of the International Association for the Study of Obesity *11*, 11-18.

Ilan, Y., Maron, R., Tukpah, A.M., Maioli, T.U., Murugaiyan, G., Yang, K., Wu, H.Y., and Weiner, H.L. (2010). Induction of regulatory T cells decreases adipose inflammation and alleviates insulin resistance in ob/ob mice. Proceedings of the National Academy of Sciences of the United States of America *107*, 9765-9770.

Imai, Y., Yasuda, K., Sakaguchi, Y., Haneda, T., Mizutani, H., Yoshimoto, T., Nakanishi, K., and Yamanishi, K. (2013). Skin-specific expression of IL-33 activates group 2 innate lymphoid cells and elicits atopic dermatitis-like inflammation in mice. Proceedings of the National Academy of Sciences of the United States of America *110*, 13921-13926.

Jespersen, N.Z., Larsen, T.J., Peijs, L., Daugaard, S., Homoe, P., Loft, A., de Jong, J., Mathur, N., Cannon, B., Nedergaard, J.*, et al.* (2013). A classical brown adipose tissue mRNA signature partly overlaps with brite in the supraclavicular region of adult humans. Cell metabolism *17*, 798-805.

Jin, C., Henao-Mejia, J., and Flavell, R.A. (2013). Innate immune receptors: key regulators of metabolic disease progression. Cell metabolism *17*, 873-882.

Jung, U.J., and Choi, M.S. (2014). Obesity and its metabolic complications: the role of adipokines and the relationship between obesity, inflammation, insulin resistance, dyslipidemia and nonalcoholic fatty liver disease. International journal of molecular sciences *15*, 6184-6223.

Kadowaki, T., Yamauchi, T., Kubota, N., Hara, K., Ueki, K., and Tobe, K. (2006). Adiponectin and adiponectin receptors in insulin resistance, diabetes, and the metabolic syndrome. The Journal of clinical investigation *116*, 1784-1792.

Kain, L., Webb, B., Anderson, B.L., Deng, S., Holt, M., Constanzo, A., Zhao, M., Self, K., Teyton, A., Everett, C.*, et al.* (2014). The Identification of the Endogenous Ligands of Natural Killer T Cells Reveals the Presence of Mammalian alpha-Linked Glycosylceramides. Immunity *41*, 543-554.

Kajimura, S., Seale, P., Kubota, K., Lunsford, E., Frangioni, J.V., Gygi, S.P., and Spiegelman, B.M. (2009). Initiation of myoblast to brown fat switch by a PRDM16-C/EBP-beta transcriptional complex. Nature *460*, 1154-1158.

Kelly, T., Yang, W., Chen, C.S., Reynolds, K., and He, J. (2008). Global burden of obesity in 2005 and projections to 2030. International journal of obesity *32*, 1431-1437.

Kershaw, E.E., and Flier, J.S. (2004). Adipose tissue as an endocrine organ. The Journal of clinical endocrinology and metabolism *89*, 2548-2556.

Kim, B.S. (2014). Innate Lymphoid Cells in the Skin. The Journal of investigative dermatology. [Epub ahead of print].

Kim, B.S., Siracusa, M.C., Saenz, S.A., Noti, M., Monticelli, L.A., Sonnenberg, G.F., Hepworth, M.R., Van Voorhees, A.S., Comeau, M.R., and Artis, D. (2013). TSLP elicits IL-33-independent innate lymphoid cell responses to promote skin inflammation. Science translational medicine *5*, 170ra116.

Kim, B.S., Wang, K., Siracusa, M.C., Saenz, S.A., Brestoff, J.R., Monticelli, L.A., Noti, M., Tait Wojno, E.D., Fung, T.C., Kubo, M., and Artis, D. (2014). Basophils promote innate lymphoid cell responses in inflamed skin. Journal of immunology *193*, 3717-3725.

Klein Wolterink, R.G., Serafini, N., van Nimwegen, M., Vosshenrich, C.A., de Bruijn, M.J., Fonseca Pereira, D., Veiga Fernandes, H., Hendriks, R.W., and Di Santo, J.P. (2013). Essential, dose-dependent role for the transcription factor Gata3 in the development of IL-5+ and IL-13+ type 2 innate lymphoid cells. Proceedings of the National Academy of Sciences of the United States of America *110*, 10240-10245.

Konig, M., Zimmer, A.M., Steiner, H., Holmes, P.V., Crawley, J.N., Brownstein, M.J., and Zimmer, A. (1996). Pain responses, anxiety and aggression in mice deficient in pre-proenkephalin. Nature *383*, 535-538.

Kotnik, P., Fischer-Posovszky, P., and Wabitsch, M. (2011). RBP4: a controversial adipokine. European journal of endocrinology / European Federation of Endocrine Societies *165*, 703-711.

Kubota, N., Terauchi, Y., Miki, H., Tamemoto, H., Yamauchi, T., Komeda, K., Satoh, S., Nakano, R., Ishii, C., Sugiyama, T.*, et al.* (1999). PPAR gamma mediates high-fat diet-induced adipocyte hypertrophy and insulin resistance. Molecular cell *4*, 597-609.

Lazar, M.A. (2007). Resistin- and Obesity-associated metabolic diseases. Hormone and metabolic research = Hormon- und Stoffwechselforschung = Hormones et metabolisme *39*, 710-716.

Lee, P., Werner, C.D., Kebebew, E., and Celi, F.S. (2014). Functional thermogenic beige adipogenesis is inducible in human neck fat. International journal of obesity *38*, 170-176.

Lee, Y.H., Petkova, A.P., Mottillo, E.P., and Granneman, J.G. (2012). In vivo identification of bipotential adipocyte progenitors recruited by beta3-adrenoceptor activation and high-fat feeding. Cell metabolism *15*, 480-491.

Liu, P.S., Lin, Y.W., Lee, B., McCrady-Spitzer, S.K., Levine, J.A., and Wei, L.N. (2014). Reducing RIP140 Expression in Macrophage Alters ATM Infiltration, Facilitates White Adipose Tissue Browning, and Prevents High-Fat Diet-Induced Insulin Resistance. Diabetes *63*, 4021-4031.

Lloyd, D.J., Bohan, S., and Gekakis, N. (2006). Obesity, hyperphagia and increased metabolic efficiency in Pc1 mutant mice. Human molecular genetics *15*, 1884-1893.

Long, J.Z., Svensson, K.J., Tsai, L., Zeng, X., Roh, H.C., Kong, X., Rao, R.R., Lou, J., Lokurkar, I., Baur, W.*, et al.* (2014). A smooth muscle-like origin for beige adipocytes. Cell metabolism *19*, 810-820.

Lumeng, C.N., Bodzin, J.L., and Saltiel, A.R. (2007). Obesity induces a phenotypic switch in adipose tissue macrophage polarization. The Journal of clinical investigation *117*, 175-184.

Lumeng, C.N., and Saltiel, A.R. (2011). Inflammatory links between obesity and metabolic disease. The Journal of clinical investigation *121*, 2111-2117.

Lynch, L., Michelet, X., Zhang, S., Brennan, P.J., Moseman, A., Lester, C., Besra, G., Vomhof-Dekrey, E.E., Tighe, M., Koay, H.F.*, et al.* (2014). Regulatory iNKT cells lack expression of the transcription factor PLZF and control the homeostasis of T cells and macrophages in adipose tissue. Nature immunology. [Epub ahead of print].

Lynch, L., Nowak, M., Varghese, B., Clark, J., Hogan, A.E., Toxavidis, V., Balk, S.P., O'Shea, D., O'Farrelly, C., and Exley, M.A. (2012). Adipose tissue invariant NKT cells protect against diet-induced obesity and metabolic disorder through regulatory cytokine production. Immunity *37*, 574-587.

Madsen, L., Pedersen, L.M., Lillefosse, H.H., Fjaere, E., Bronstad, I., Hao, Q., Petersen, R.K., Hallenborg, P., Ma, T., De Matteis, R.*, et al.* (2010). UCP1 induction during recruitment of brown adipocytes in white adipose tissue is dependent on cyclooxygenase activity. PloS one *5*, e11391.

Martinez, F.O., Helming, L., and Gordon, S. (2009). Alternative activation of macrophages: an immunologic functional perspective. Annual review of immunology *27*, 451-483.

Matthews, D.R., Hosker, J.P., Rudenski, A.S., Naylor, B.A., Treacher, D.F., and Turner, R.C. (1985). Homeostasis model assessment: insulin resistance and beta-cell function from fasting plasma glucose and insulin concentrations in man. Diabetologia *28*, 412-419.

Matthias, A., Ohlson, K.B., Fredriksson, J.M., Jacobsson, A., Nedergaard, J., and Cannon, B. (2000). Thermogenic responses in brown fat cells are fully UCP1-dependent. UCP2 or UCP3 do not substitute for UCP1 in adrenergically or fatty scid-induced thermogenesis. The Journal of biological chemistry *275*, 25073-25081.

McCarthy, M.I. (2010). Genomics, type 2 diabetes, and obesity. The New England journal of medicine *363*, 2339-2350.

McNelis, J.C., and Olefsky, J.M. (2014). Macrophages, immunity, and metabolic disease. Immunity *41*, 36-48.

McSorley, H.J., Blair, N.F., Smith, K.A., McKenzie, A.N., and Maizels, R.M. (2014). Blockade of IL-33 release and suppression of type 2 innate lymphoid cell responses by helminth secreted products in airway allergy. Mucosal immunology *7*, 1068-1078.

Miller, A.M., Asquith, D.L., Hueber, A.J., Anderson, L.A., Holmes, W.M., McKenzie, A.N., Xu, D., Sattar, N., McInnes, I.B., and Liew, F.Y. (2010). Interleukin-33 induces protective effects in adipose tissue inflammation during obesity in mice. Circulation research *107*, 650-658.

Miller, A.M., Xu, D., Asquith, D.L., Denby, L., Li, Y., Sattar, N., Baker, A.H., McInnes, I.B., and Liew, F.Y. (2008). IL-33 reduces the development of atherosclerosis. The Journal of experimental medicine *205*, 339-346.

Mirchandani, A.S., Besnard, A.G., Yip, E., Scott, C., Bain, C.C., Cerovic, V., Salmond, R.J., and Liew, F.Y. (2014). Type 2 innate lymphoid cells drive CD4+ Th2 cell responses. Journal of immunology *192*, 2442-2448.

Mjosberg, J., Bernink, J., Golebski, K., Karrich, J.J., Peters, C.P., Blom, B., te Velde, A.A., Fokkens, W.J., van Drunen, C.M., and Spits, H. (2012). The transcription factor GATA3 is essential for the function of human type 2 innate lymphoid cells. Immunity *37*, 649-659.

Mjosberg, J.M., Trifari, S., Crellin, N.K., Peters, C.P., van Drunen, C.M., Piet, B., Fokkens, W.J., Cupedo, T., and Spits, H. (2011). Human IL-25- and IL-33-

responsive type 2 innate lymphoid cells are defined by expression of CRTH2 and CD161. Nature immunology *12*, 1055-1062.

Moisan, A., Lee, Y.K., Zhang, J.D., Hudak, C.S., Meyer, C.A., Prummer, M., Zoffmann, S., Truong, H.H., Ebeling, M., Kiialainen, A.*, et al.* (2014). White-to-brown metabolic conversion of human adipocytes by JAK inhibition. Nature cell biology. [Epub ahead of print].

Molofsky, A.B., Nussbaum, J.C., Liang, H.E., Van Dyken, S.J., Cheng, L.E., Mohapatra, A., Chawla, A., and Locksley, R.M. (2013). Innate lymphoid type 2 cells sustain visceral adipose tissue eosinophils and alternatively activated macrophages. The Journal of experimental medicine *210*, 535-549.

Monticelli, L.A., Sonnenberg, G.F., Abt, M.C., Alenghat, T., Ziegler, C.G., Doering, T.A., Angelosanto, J.M., Laidlaw, B.J., Yang, C.Y., Sathaliyawala, T.*, et al.* (2011). Innate lymphoid cells promote lung-tissue homeostasis after infection with influenza virus. Nature immunology *12*, 1045-1054.

Monticelli, L.A., Sonnenberg, G.F., and Artis, D. (2012). Innate lymphoid cells: critical regulators of allergic inflammation and tissue repair in the lung. Current opinion in immunology *24*, 284-289.

Moraes-Vieira, P.M., Yore, M.M., Dwyer, P.M., Syed, I., Aryal, P., and Kahn, B.B. (2014). RBP4 activates antigen-presenting cells, leading to adipose tissue inflammation and systemic insulin resistance. Cell metabolism *19*, 512-526.
Moro, K., Yamada, T., Tanabe, M., Takeuchi, T., Ikawa, T., Kawamoto, H., Furusawa, J., Ohtani, M., Fujii, H., and Koyasu, S. (2010). Innate production of T(H)2 cytokines by adipose tissue-associated c-Kit(+)Sca-1(+) lymphoid cells. Nature *463*, 540-544.

Morris, D.L., Cho, K.W., Delproposto, J.L., Oatmen, K.E., Geletka, L.M., Martinez-Santibanez, G., Singer, K., and Lumeng, C.N. (2013). Adipose tissue macrophages function as antigen-presenting cells and regulate adipose tissue CD4+ T cells in mice. Diabetes *62*, 2762-2772.

Motomura, Y., Morita, H., Moro, K., Nakae, S., Artis, D., Endo, T.A., Kuroki, Y., Ohara, O., Koyasu, S., and Kubo, M. (2014). Basophil-derived interleukin-4 controls the function of natural helper cells, a member of ILC2s, in lung inflammation. Immunity *40*, 758-771.

Mottillo, E.P., Bloch, A.E., Leff, T., and Granneman, J.G. (2012). Lipolytic products activate peroxisome proliferator-activated receptor (PPAR) alpha and delta in brown adipocytes to match fatty acid oxidation with supply. The Journal of biological chemistry *287*, 25038-25048.

Mraz, M., and Haluzik, M. (2014). The role of adipose tissue immune cells in obesity and low-grade inflammation. The Journal of endocrinology *222*, R113-127.

Muoio, D.M., and Newgard, C.B. (2006). Obesity-related derangements in metabolic regulation. Annual review of biochemistry *75*, 367-401.

Murano, I., Barbatelli, G., Parisani, V., Latini, C., Muzzonigro, G., Castellucci, M., and Cinti, S. (2008). Dead adipocytes, detected as crown-like structures, are prevalent in visceral fat depots of genetically obese mice. Journal of lipid research *49*, 1562-1568.

Neill, D.R., Wong, S.H., Bellosi, A., Flynn, R.J., Daly, M., Langford, T.K., Bucks, C., Kane, C.M., Fallon, P.G., Pannell, R.*, et al.* (2010). Nuocytes represent a new innate effector leukocyte that mediates type-2 immunity. Nature *464*, 1367-1370.

Nencini, P., and Paroli, E. (1981). The lipolytic activity of met-enkephalin, leu-enkephalin, morphine, methadone and naloxone in human adipose tissue. Pharmacological research communications *13*, 535-540.

Ng, M., Fleming, T., Robinson, M., Thomson, B., Graetz, N., Margono, C., Mullany, E.C., Biryukov, S., Abbafati, C., Abera, S.F.*, et al.* (2014). Global, regional, and national prevalence of overweight and obesity in children and adults during 1980-2013: a systematic analysis for the Global Burden of Disease Study 2013. Lancet *384*, 766-781.

Nguyen, K.D., Qiu, Y., Cui, X., Goh, Y.P., Mwangi, J., David, T., Mukundan, L., Brombacher, F., Locksley, R.M., and Chawla, A. (2011). Alternatively activated macrophages produce catecholamines to sustain adaptive thermogenesis. Nature *480*, 104-108.

Nguyen, M.T., Favelyukis, S., Nguyen, A.K., Reichart, D., Scott, P.A., Jenn, A., Liu-Bryan, R., Glass, C.K., Neels, J.G., and Olefsky, J.M. (2007). A subpopulation of macrophages infiltrates hypertrophic adipose tissue and is activated by free fatty acids via Toll-like receptors 2 and 4 and JNK-dependent pathways. The Journal of biological chemistry *282*, 35279-35292.

Nishimura, S., Manabe, I., Nagasaki, M., Eto, K., Yamashita, H., Ohsugi, M., Otsu, M., Hara, K., Ueki, K., Sugiura, S.*, et al.* (2009). CD8+ effector T cells contribute to macrophage recruitment and adipose tissue inflammation in obesity. Nature medicine *15*, 914-920.

Nomiyama, T., Perez-Tilve, D., Ogawa, D., Gizard, F., Zhao, Y., Heywood, E.B., Jones, K.L., Kawamori, R., Cassis, L.A., Tschop, M.H., and Bruemmer, D. (2007). Osteopontin mediates obesity-induced adipose tissue macrophage infiltration and insulin resistance in mice. The Journal of clinical investigation *117*, 2877-2888.

Norseen, J., Hosooka, T., Hammarstedt, A., Yore, M.M., Kant, S., Aryal, P., Kiernan, U.A., Phillips, D.A., Maruyama, H., Kraus, B.J.*, et al.* (2012). Retinol-binding protein 4 inhibits insulin signaling in adipocytes by inducing proinflammatory cytokines in macrophages through a c-Jun N-terminal kinase- and toll-like receptor 4-dependent and retinol-independent mechanism. Molecular and cellular biology *32*, 2010-2019.

Nussbaum, J.C., Van Dyken, S.J., von Moltke, J., Cheng, L.E., Mohapatra, A., Molofsky, A.B., Thornton, E.E., Krummel, M.F., Chawla, A., Liang, H.E., and Locksley, R.M. (2013). Type 2 innate lymphoid cells control eosinophil homeostasis. Nature *502*, 245-248.

Odegaard, J.I., and Chawla, A. (2011). Alternative macrophage activation and metabolism. Annual review of pathology *6*, 275-297.

Odegaard, J.I., and Chawla, A. (2013a). The immune system as a sensor of the metabolic state. Immunity *38*, 644-654.

Odegaard, J.I., and Chawla, A. (2013b). Pleiotropic actions of insulin resistance and inflammation in metabolic homeostasis. Science *339*, 172-177.

Odegaard, J.I., Ricardo-Gonzalez, R.R., Goforth, M.H., Morel, C.R., Subramanian, V., Mukundan, L., Red Eagle, A., Vats, D., Brombacher, F., Ferrante, A.W., and Chawla, A. (2007). Macrophage-specific PPARgamma controls alternative activation and improves insulin resistance. Nature *447*, 1116-1120.

Odegaard, J.I., Ricardo-Gonzalez, R.R., Red Eagle, A., Vats, D., Morel, C.R., Goforth, M.H., Subramanian, V., Mukundan, L., Ferrante, A.W., and Chawla, A. (2008). Alternative M2 activation of Kupffer cells by PPARdelta ameliorates obesity-induced insulin resistance. Cell metabolism *7*, 496-507.

Ogden, C.L., Carroll, M.D., Kit, B.K., and Flegal, K.M. (2012). Prevalence of obesity and trends in body mass index among US children and adolescents, 1999-2010. Jama *307*, 483-490.

Ogden, C.L., Carroll, M.D., Kit, B.K., and Flegal, K.M. (2014). Prevalence of childhood and adult obesity in the United States, 2011-2012. Jama *311*, 806-814.

Oh, D.Y., Morinaga, H., Talukdar, S., Bae, E.J., and Olefsky, J.M. (2012). Increased macrophage migration into adipose tissue in obese mice. Diabetes *61*, 346-354.

Olefsky, J.M., and Glass, C.K. (2010). Macrophages, inflammation, and insulin resistance. Annual review of physiology *72*, 219-246.

Oliphant, C.J., Hwang, Y.Y., Walker, J.A., Salimi, M., Wong, S.H., Brewer, J.M., Englezakis, A., Barlow, J.L., Hams, E., Scanlon, S.T.*, et al.* (2014). MHCII-mediated dialog between group 2 innate lymphoid cells and CD4(+) T cells potentiates type 2 immunity and promotes parasitic helminth expulsion. Immunity *41*, 283-295.

Oliveros, H., and Villamor, E. (2008). Obesity and mortality in critically ill adults: a systematic review and meta-analysis. Obesity *16*, 515-521.

Orr, J.S., Kennedy, A., Anderson-Baucum, E.K., Webb, C.D., Fordahl, S.C., Erikson, K.M., Zhang, Y., Etzerodt, A., Moestrup, S.K., and Hasty, A.H. (2014). Obesity alters adipose tissue macrophage iron content and tissue iron distribution. Diabetes *63*, 421-432.

Osborn, O., and Olefsky, J.M. (2012). The cellular and signaling networks linking the immune system and metabolism in disease. Nature medicine *18*, 363-374.

Osborne, L.C., Monticelli, L.A., Nice, T.J., Sutherland, T.E., Siracusa, M.C., Hepworth, M.R., Tomov, V.T., Kobuley, D., Tran, S.V., Bittinger, K.*, et al.* (2014). Coinfection. Virus-helminth coinfection reveals a microbiota-independent mechanism of immunomodulation. Science *345*, 578-582.

Ouchi, N., Parker, J.L., Lugus, J.J., and Walsh, K. (2011). Adipokines in inflammation and metabolic disease. Nature reviews. Immunology *11*, 85-97.
Pasarica, M., Sereda, O.R., Redman, L.M., Albarado, D.C., Hymel, D.T., Roan, L.E., Rood, J.C., Burk, D.H., and Smith, S.R. (2009). Reduced adipose tissue oxygenation in human obesity: evidence for rarefaction, macrophage chemotaxis, and inflammation without an angiogenic response. Diabetes *58*, 718-725.

Peirce, V., Carobbio, S., and Vidal-Puig, A. (2014). The different shades of fat. Nature *510*, 76-83.

Pfeifer, A., and Hoffmann, L.S. (2014). Brown, Beige, and White: The New Color Code of Fat and Its Pharmacological Implications. Annual review of pharmacology and toxicology. [Epub ahead of print].

Pi-Sunyer, F.X. (1999). Comorbidities of overweight and obesity: current evidence and research issues. Medicine and science in sports and exercise *31*, S602-608.

Poehlman, E.T., and Horton, E.S. (1989). The impact of food intake and exercise on energy expenditure. Nutrition reviews *47*, 129-137.

Pontiroli, A.E., and Morabito, A. (2011). Long-term prevention of mortality in morbid obesity through bariatric surgery. a systematic review and meta-analysis of trials performed with gastric banding and gastric bypass. Annals of surgery *253*, 484-487.

Price, A.E., Liang, H.E., Sullivan, B.M., Reinhardt, R.L., Eisley, C.J., Erle, D.J., and Locksley, R.M. (2010). Systemically dispersed innate IL-13-expressing cells in type 2 immunity. Proceedings of the National Academy of Sciences of the United States of America *107*, 11489-11494.

Qian, S.W., Tang, Y., Li, X., Liu, Y., Zhang, Y.Y., Huang, H.Y., Xue, R.D., Yu, H.Y., Guo, L., Gao, H.D.*, et al.* (2013). BMP4-mediated brown fat-like changes in white adipose tissue alter glucose and energy homeostasis. Proceedings of the National Academy of Sciences of the United States of America *110*, E798-807.

Qiu, Y., Nguyen, K.D., Odegaard, J.I., Cui, X., Tian, X., Locksley, R.M., Palmiter, R.D., and Chawla, A. (2014). Eosinophils and type 2 cytokine signaling in macrophages orchestrate development of functional beige fat. Cell *157*, 1292-1308.

Rao, R.R., Long, J.Z., White, J.P., Svensson, K.J., Lou, J., Lokurkar, I., Jedrychowski, M.P., Ruas, J.L., Wrann, C.D., Lo, J.C.*, et al.* (2014). Meteorin-like is a hormone that regulates immune-adipose interactions to increase beige fat thermogenesis. Cell *157*, 1279-1291.

Rausch, M.E., Weisberg, S., Vardhana, P., and Tortoriello, D.V. (2008). Obesity in C57BL/6J mice is characterized by adipose tissue hypoxia and cytotoxic T-cell infiltration. International journal of obesity *32*, 451-463.

Reese, T.A., Wakeman, B.S., Choi, H.S., Hufford, M.M., Huang, S.C., Zhang, X., Buck, M.D., Jezewski, A., Kambal, A., Liu, C.Y.*, et al.* (2014). Coinfection. Helminth infection reactivates latent gamma-herpesvirus via cytokine competition at a viral promoter. Science *345*, 573-577.

Reilly, J.J., and Kelly, J. (2011). Long-term impact of overweight and obesity in childhood and adolescence on morbidity and premature mortality in adulthood: systematic review. International journal of obesity *35*, 891-898.

Revelo, X.S., Tsai, S., Lei, H., Luck, H., Ghazarian, M., Tsui, H., Shi, S.Y., Schroer, S., Luk, C., Lin, G.H.*, et al.* (2014). Perforin is a Novel Immune Regulator of Obesity Related Insulin Resistance. Diabetes.

Ricardo-Gonzalez, R.R., Red Eagle, A., Odegaard, J.I., Jouihan, H., Morel, C.R., Heredia, J.E., Mukundan, L., Wu, D., Locksley, R.M., and Chawla, A. (2010). IL-4/STAT6 immune axis regulates peripheral nutrient metabolism and insulin sensitivity. Proceedings of the National Academy of Sciences of the United States of America *107*, 22617-22622.

Roberts, L.D., Bostrom, P., O'Sullivan, J.F., Schinzel, R.T., Lewis, G.D., Dejam, A., Lee, Y.K., Palma, M.J., Calhoun, S., Georgiadi, A.*, et al.* (2014). beta-Aminoisobutyric acid induces browning of white fat and hepatic beta-oxidation and is inversely correlated with cardiometabolic risk factors. Cell metabolism *19*, 96-108.

Rodriguez, C., Patel, A.V., Calle, E.E., Jacobs, E.J., Chao, A., and Thun, M.J. (2001). Body mass index, height, and prostate cancer mortality in two large cohorts of adult men in the United States. Cancer epidemiology, biomarkers & prevention : a publication of the American Association for Cancer Research, cosponsored by the American Society of Preventive Oncology *10*, 345-353.

Roediger, B., Kyle, R., Yip, K.H., Sumaria, N., Guy, T.V., Kim, B.S., Mitchell, A.J., Tay, S.S., Jain, R., Forbes-Blom, E.*, et al.* (2013). Cutaneous immunosurveillance and regulation of inflammation by group 2 innate lymphoid cells. Nature immunology *14*, 564-573.

Rosen, E.D., and Spiegelman, B.M. (2014). What we talk about when we talk about fat. Cell *156*, 20-44.

Rosenberg, H.F., Dyer, K.D., and Foster, P.S. (2013). Eosinophils: changing perspectives in health and disease. Nature reviews. Immunology *13*, 9-22.

Rosenwald, M., Perdikari, A., Rulicke, T., and Wolfrum, C. (2013). Bi-directional interconversion of brite and white adipocytes. Nature cell biology *15*, 659-667.
Rothenberg, M.E., and Hogan, S.P. (2006). The eosinophil. Annual review of immunology *24*, 147-174.

Saenz, S.A., Siracusa, M.C., Monticelli, L.A., Ziegler, C.G., Kim, B.S., Brestoff, J.R., Peterson, L.W., Wherry, E.J., Goldrath, A.W., Bhandoola, A., and Artis, D.

(2013). IL-25 simultaneously elicits distinct populations of innate lymphoid cells and multipotent progenitor type 2 (MPPtype2) cells. The Journal of experimental medicine *210*, 1823-1837.

Saito, M., Okamatsu-Ogura, Y., Matsushita, M., Watanabe, K., Yoneshiro, T., Nio-Kobayashi, J., Iwanaga, T., Miyagawa, M., Kameya, T., Nakada, K.*, et al.* (2009). High incidence of metabolically active brown adipose tissue in healthy adult humans: effects of cold exposure and adiposity. Diabetes *58*, 1526-1531.

Sanchez-Gurmaches, J., and Guertin, D.A. (2014). Adipocyte lineages: tracing back the origins of fat. Biochimica et biophysica acta *1842*, 340-351.

Schiering, C., Krausgruber, T., Chomka, A., Frohlich, A., Adelmann, K., Wohlfert, E.A., Pott, J., Griseri, T., Bollrath, J., Hegazy, A.N.*, et al.* (2014). The alarmin IL-33 promotes regulatory T-cell function in the intestine. Nature *513*, 564-568.

Schroder, K., Hertzog, P.J., Ravasi, T., and Hume, D.A. (2004). Interferon-gamma: an overview of signals, mechanisms and functions. Journal of leukocyte biology *75*, 163-189.

Schulz, T.J., Huang, T.L., Tran, T.T., Zhang, H., Townsend, K.L., Shadrach, J.L., Cerletti, M., McDougall, L.E., Giorgadze, N., Tchkonia, T.*, et al.* (2011). Identification of inducible brown adipocyte progenitors residing in skeletal muscle and white fat. Proceedings of the National Academy of Sciences of the United States of America *108*, 143-148.

Seale, P., Bjork, B., Yang, W., Kajimura, S., Chin, S., Kuang, S., Scime, A., Devarakonda, S., Conroe, H.M., Erdjument-Bromage, H.*, et al.* (2008). PRDM16 controls a brown fat/skeletal muscle switch. Nature *454*, 961-967.

Seale, P., Conroe, H.M., Estall, J., Kajimura, S., Frontini, A., Ishibashi, J., Cohen, P., Cinti, S., and Spiegelman, B.M. (2011). Prdm16 determines the thermogenic program of subcutaneous white adipose tissue in mice. The Journal of clinical investigation *121*, 96-105.

Seidah, N.G. (2011). The proprotein convertases, 20 years later. Methods in molecular biology *768*, 23-57.

Seidah, N.G., Sadr, M.S., Chretien, M., and Mbikay, M. (2013). The multifaceted proprotein convertases: their unique, redundant, complementary, and opposite functions. The Journal of biological chemistry *288*, 21473-21481.

Shabalina, I.G., Petrovic, N., de Jong, J.M., Kalinovich, A.V., Cannon, B., and Nedergaard, J. (2013). UCP1 in brite/beige adipose tissue mitochondria is functionally thermogenic. Cell reports *5*, 1196-1203.

Sharp, L.Z., Shinoda, K., Ohno, H., Scheel, D.W., Tomoda, E., Ruiz, L., Hu, H., Wang, L., Pavlova, Z., Gilsanz, V., and Kajimura, S. (2012). Human BAT possesses molecular signatures that resemble beige/brite cells. PloS one *7*, e49452.

Song, H., Shojima, N., Sakoda, H., Ogihara, T., Fujishiro, M., Katagiri, H., Anai, M., Onishi, Y., Ono, H., Inukai, K.*, et al.* (2002). Resistin is regulated by C/EBPs, PPARs, and signal-transducing molecules. Biochemical and biophysical research communications *299*, 291-298.

Sonnenberg, G.F., Mjosberg, J., Spits, H., and Artis, D. (2013). SnapShot: innate lymphoid cells. Immunity *39*, 622-622 e621.

Spalding, K.L., Arner, E., Westermark, P.O., Bernard, S., Buchholz, B.A., Bergmann, O., Blomqvist, L., Hoffstedt, J., Naslund, E., Britton, T.*, et al.* (2008). Dynamics of fat cell turnover in humans. Nature *453*, 783-787.

Spits, H., Artis, D., Colonna, M., Diefenbach, A., Di Santo, J.P., Eberl, G., Koyasu, S., Locksley, R.M., McKenzie, A.N., Mebius, R.E.*, et al.* (2013). Innate lymphoid cells--a proposal for uniform nomenclature. Nature reviews. Immunology *13*, 145-149.

Spits, H., and Cupedo, T. (2012). Innate lymphoid cells: emerging insights in development, lineage relationships, and function. Annual review of immunology *30*, 647-675.

Steppan, C.M., Bailey, S.T., Bhat, S., Brown, E.J., Banerjee, R.R., Wright, C.M., Patel, H.R., Ahima, R.S., and Lazar, M.A. (2001). The hormone resistin links obesity to diabetes. Nature *409*, 307-312.

Stolarczyk, E., Vong, C.T., Perucha, E., Jackson, I., Cawthorne, M.A., Wargent, E.T., Powell, N., Canavan, J.B., Lord, G.M., and Howard, J.K. (2013). Improved insulin sensitivity despite increased visceral adiposity in mice deficient for the immune cell transcription factor T-bet. Cell metabolism *17*, 520-533.

Sun, K., Kusminski, C.M., and Scherer, P.E. (2011). Adipose tissue remodeling and obesity. The Journal of clinical investigation *121*, 2094-2101.

Tajima, S., Ikeda, Y., Sawada, K., Yamano, N., Horinouchi, Y., Kihira, Y., Ishizawa, K., Izawa-Ishizawa, Y., Kawazoe, K., Tomita, S.*, et al.* (2012). Iron

reduction by deferoxamine leads to amelioration of adiposity via the regulation of oxidative stress and inflammation in obese and type 2 diabetes KKAy mice. American journal of physiology. Endocrinology and metabolism *302*, E77-86.

Thorrez, L., Van Deun, K., Tranchevent, L.C., Van Lommel, L., Engelen, K., Marchal, K., Moreau, Y., Van Mechelen, I., and Schuit, F. (2008). Using ribosomal protein genes as reference: a tale of caution. PloS one *3*, e1854.
Tseng, A., Nguyen, K., Hamid, A., Garg, M., Marquez, P., and Lutfy, K. (2013). The role of endogenous beta-endorphin and enkephalins in ethanol reward. Neuropharmacology *73*, 290-300.

van Marken Lichtenbelt, W.D., Vanhommerig, J.W., Smulders, N.M., Drossaerts, J.M., Kemerink, G.J., Bouvy, N.D., Schrauwen, P., and Teule, G.J. (2009). Cold-activated brown adipose tissue in healthy men. The New England journal of medicine *360*, 1500-1508.

Virtanen, K.A., Lidell, M.E., Orava, J., Heglind, M., Westergren, R., Niemi, T., Taittonen, M., Laine, J., Savisto, N.J., Enerback, S., and Nuutila, P. (2009). Functional brown adipose tissue in healthy adults. The New England journal of medicine *360*, 1518-1525.

Wagner, N.M., Brandhorst, G., Czepluch, F., Lankeit, M., Eberle, C., Herzberg, S., Faustin, V., Riggert, J., Oellerich, M., Hasenfuss, G*., et al.* (2013). Circulating regulatory T cells are reduced in obesity and may identify subjects at increased metabolic and cardiovascular risk. Obesity *21*, 461-468.

Walley, A.J., Asher, J.E., and Froguel, P. (2009). The genetic contribution to non-syndromic human obesity. Nature reviews. Genetics *10*, 431-442.

Wang, J., Liu, R., Wang, F., Hong, J., Li, X., Chen, M., Ke, Y., Zhang, X., Ma, Q., Wang, R*., et al.* (2013a). Ablation of LGR4 promotes energy expenditure by driving white-to-brown fat switch. Nature cell biology *15*, 1455-1463.

Wang, Q.A., Tao, C., Gupta, R.K., and Scherer, P.E. (2013b). Tracking adipogenesis during white adipose tissue development, expansion and regeneration. Nature medicine *19*, 1338-1344.

Weisberg, S.P., McCann, D., Desai, M., Rosenbaum, M., Leibel, R.L., and Ferrante, A.W., Jr. (2003). Obesity is associated with macrophage accumulation in adipose tissue. The Journal of clinical investigation *112*, 1796-1808.

Withrow, D., and Alter, D.A. (2011). The economic burden of obesity worldwide: a systematic review of the direct costs of obesity. Obesity reviews : an official journal of the International Association for the Study of Obesity *12*, 131-141.

Wu, D., Molofsky, A.B., Liang, H.E., Ricardo-Gonzalez, R.R., Jouihan, H.A., Bando, J.K., Chawla, A., and Locksley, R.M. (2011). Eosinophils sustain adipose alternatively activated macrophages associated with glucose homeostasis. Science *332*, 243-247.

Wu, J., Bostrom, P., Sparks, L.M., Ye, L., Choi, J.H., Giang, A.H., Khandekar, M., Virtanen, K.A., Nuutila, P., Schaart, G.*, et al.* (2012). Beige adipocytes are a distinct type of thermogenic fat cell in mouse and human. Cell *150*, 366-376.

Wu, J., Cohen, P., and Spiegelman, B.M. (2013). Adaptive thermogenesis in adipocytes: is beige the new brown? Genes & development *27*, 234-250.

Xu, X., Grijalva, A., Skowronski, A., van Eijk, M., Serlie, M.J., and Ferrante, A.W., Jr. (2013). Obesity activates a program of lysosomal-dependent lipid metabolism in adipose tissue macrophages independently of classic activation. Cell metabolism *18*, 816-830.

Xue, L., Salimi, M., Panse, I., Mjosberg, J.M., McKenzie, A.N., Spits, H., Klenerman, P., and Ogg, G. (2014). Prostaglandin D2 activates group 2 innate lymphoid cells through chemoattractant receptor-homologous molecule expressed on TH2 cells. The Journal of allergy and clinical immunology *133*, 1184-1194.

Yang, Q., Graham, T.E., Mody, N., Preitner, F., Peroni, O.D., Zabolotny, J.M., Kotani, K., Quadro, L., and Kahn, B.B. (2005). Serum retinol binding protein 4 contributes to insulin resistance in obesity and type 2 diabetes. Nature *436*, 356-362.

Yang, Q., Monticelli, L.A., Saenz, S.A., Chi, A.W., Sonnenberg, G.F., Tang, J., De Obaldia, M.E., Bailis, W., Bryson, J.L., Toscano, K.*, et al.* (2013a). T cell factor 1 is required for group 2 innate lymphoid cell generation. Immunity *38*, 694-704.

Yang, Z., Grinchuk, V., Smith, A., Qin, B., Bohl, J.A., Sun, R., Notari, L., Zhang, Z., Sesaki, H., Urban, J.F., Jr.*, et al.* (2013b). Parasitic nematode-induced modulation of body weight and associated metabolic dysfunction in mouse models of obesity. Infection and immunity *81*, 1905-1914.

Yoneshiro, T., Aita, S., Matsushita, M., Kameya, T., Nakada, K., Kawai, Y., and Saito, M. (2011). Brown adipose tissue, whole-body energy expenditure, and thermogenesis in healthy adult men. Obesity *19*, 13-16.

Zagon, I.S., Rahn, K.A., Bonneau, R.H., Turel, A.P., and McLaughlin, P.J. (2010). Opioid growth factor suppresses expression of experimental autoimmune encephalomyelitis. Brain research *1310*, 154-161.

Zeyda, M., Gollinger, K., Kriehuber, E., Kiefer, F.W., Neuhofer, A., and Stulnig, T.M. (2010). Newly identified adipose tissue macrophage populations in obesity with distinct chemokine and chemokine receptor expression. International journal of obesity *34*, 1684-1694.

Zeyda, M., Wernly, B., Demyanets, S., Kaun, C., Hammerle, M., Hantusch, B., Schranz, M., Neuhofer, A., Itariu, B.K., Keck, M.*, et al.* (2013). Severe obesity increases adipose tissue expression of interleukin-33 and its receptor ST2, both predominantly detectable in endothelial cells of human adipose tissue. International journal of obesity *37*, 658-665.

Zhong, J., Rao, X., Braunstein, Z., Taylor, A., Narula, V., Hazey, J., Mikami, D., Needleman, B., Rutsky, J., Sun, Q.*, et al.* (2014). T-cell costimulation protects obesity-induced adipose inflammation and insulin resistance. Diabetes *63*, 1289-1302.

[Epub ahead of print].